UNIVERSIDADE FEDERAL DE SANTA CATARINA
CENTRO DE CIÊNCIAS BIOLÓGICAS
PROGRAMA DE PÓS-GRADUAÇÃO BIOTECNOLOGIA E BIOCIÊNCIAS

Laryssa Vanessa de Liz

A comparative study of the CIF1 and FLA1BP proteins from different trypanosomatids

[Florianópolis]
[2020]

Laryssa Vanessa de Liz

A comparative study of the CIF1 and FLA1BP proteins from different trypanosomatids

Dissertation submitted to the Programa de Pós-Graduação em Biotecnologia e Biociências of the Universidade Federal de Santa Catarina in fullfilment of the requirements for the degree of Masters in Biotechnology and Biosciences.
Supervisors: Professor Edmundo C. Grisard and Dra. Patrícia Hermes Stoco.

[Florianópolis]
[2020]

Ficha de identificação da obra elaborada pelo autor,
através do Programa de Geração Automática da Biblioteca Universitária da UFSC.

de Liz, Laryssa Vanessa
A comparative study of the CIF1 and FLA1BP proteins from different trypanosomatids / Laryssa Vanessa de Liz ; orientador, Edmundo Carlos Grisard, 2020.
89 p.

Dissertação (mestrado) - Universidade Federal de Santa Catarina, Centro de Ciências Biológicas, Programa de Pós Graduação em Biotecnologia e Biociências, Florianópolis, 2020.

Inclui referências.

1. Biotecnologia e Biociências. 2. Citocinese. 3. Zona de adesão flagelar. 4. FLA3. 5. TOEFAZ1. I. Grisard, Edmundo Carlos. II. Universidade Federal de Santa Catarina. Programa de Pós-Graduação em Biotecnologia e Biociências. III. Título.

Laryssa Vanessa de Liz

A comparative study of the CIF1 and FLA1BP proteins from different trypanosomatids

O presente trabalho em nível de mestrado foi avaliado e aprovado por banca examinadora composta pelos seguintes membros:

Profª. Drª. Gislaine Fongaro
Universidade Federal de Santa Catarina

Prof. Dr. Jack Sunter,
Oxford Brookes University

Profª. Drª. Patrícia Flavia Quaresma
Universidade Federal de Santa Catarina

Prof. Dr. José Henrique Maia Campos de Oliveira
Universidade Federal de Santa Catarina

Certificamos que esta é a **versão original e final** do trabalho de conclusão que foi julgado adequado para obtenção do título de mestre em Biotecnologia e Biociências.

Documento assinado digitalmente
Glauber Wagner
Data: 07/07/2020 13:52:44-0300
CPF: 007.019.139-59

Prof. Dr. Glauber Wagner
Coordenador(a) do Programa

Documento assinado digitalmente
Edmundo Carlos Grisard
Data: 07/07/2020 14:19:08-0300
CPF: 573.319.019-15

Prof. Dr. Edmundo Carlos Grisard
Orientador

[Florianópolis], [2020].

This study is dedicated to my mother, Francisca Izanete Bueno de Morais.

ACKNOWLEDGMENTS

First, I would like to thank my parents, Francisca and Silvio for all always doing impossible things to provide opportunities for me. You have sacrificed many stuffs in order to give me conditions to pursue my dreams.

Second, I am completely grateful for my advisors, Professor Edmundo and Professor Patrícia, whom allowed me to study a subject that fascinates me. I cannot write how much you have helped me to grow as a scientist and how much you inspire me.

I am thankful to be surrounded by incredible people and I appreciate every help given by Laboratório de Protozoologia team, specially Carime, Nati, Adriana, Beatriz, Ana, and Abadio. I also thank the Laboratório de Bioinformática, Laboratório de Virologia Aplicada, Laboratório de Imunologia Aplicada À Aquicultura, and Laboratório Multiusurário de Estudos em Biologia from UFSC.

I also would like to thank my brothers, William, Maria Valentina and Pedro. William, you have been my partner since we were child and now, I cannot say how much proud I am of you and I cannot thank you enough for all the support. Despite Maria Valentina and Pedro being only babies now, you inspire me to be a better professional and an example to you. I hope you see how happiness I have from choosing this profession. I also thank other people from my family, specially my grandparents and my grandmother, Emílio, Dolores, Vitor and Marcolina.

This work would not be possible without all the help from the best friends in the world: Nati, Edu, Moni, Thaís, Kelly, Caibe, Michele, Fernanda, and Jéssica. I love you guys and you know that I would be always grateful for you being by my side during the most difficult time of my life.

In addition, I cannot forget to thank public education in Brazil. I have studied in public schools since always and I am the first in the family to graduate. Every aspect of this study is only possible due to social policies in Brazil, including free access to college and Science Without Borders program. So, I thank to all people who fight for a more inclusive world.

Finally, I would like to thank to my evaluators, whom accepted to read this study and help me to improve it.

RESUMO

Os tripanosomatídeos possuem uma estrutura celular particular, possuindo um único flagelo que emerge da bolsa flagelar sendo aderido ao corpo celular através da zona de adesão flagelar (FAZ). Esta região define o sítio de início da fenda de clivagem durante o processo de divisão celular e, dentre as proteínas envolvidas nestes processos, a FLA1BP e a CIF1 foram descritas em *Trypanosoma brucei*, sendo essenciais para a adesão flagelar (FLA1BP) e regulação da citocinese (CIF1). Como são escassos estudos comparando essas proteínas em outras espécies, o presente trabalho buscou investigar a diversificação destas proteínas em tripanosomatídeos, especialmente no gênero *Trypanosoma*. A análise de genômica comparativa de diferentes espécies revelou a ausência de conservação de sequências de CIF1, incluindo a ausência de domínios proteicos, assim como uma diversificação das proteínas que interagem com CIF1, podendo indicar que *T. brucei* passou por adaptações na via de ativação da citocinese. Em *Trypanosoma rangeli*, CIF1 não possui os domínios *coiled-coil* e *zinc finger*, sendo 28% idêntica à *Tb*CIF1 e possuindo menos sítios de fosforilação quanto comparada à esta. Além disso, os níveis de transcrição e de expressão da *Tr*CIF1 não são alterados durante a divisão celular, podendo sugerir uma função distinta desta proteína em *T. rangeli*. Quanto à FLA1BP, observou-se que os genes encontrados em *T. rangeli* e *Trypanosoma cruzi* estão presentes em cópia única no genoma e são sintênicos à *Tb*FLA1BP e, apesar de divergências nas sequências, a localização e a função desta proteína parecem ser conservadas dentro do gênero *Trypanosoma*. Uma análise comparativa de sequências de FLA1BP de diferentes espécies, revelou uma sequência conservada de 12 aminoácidos polares e hidrofóbicos, os quais podem constituir um domínio de endereçamento ou ancoramento de FLA1BP na FAZ. Nossos resultados sugerem que a ativação da citocinese em *T. brucei* pode não ser conservada em relação aos demais tripanosomatídeos, porém a adesão flagelar dependente de FLA1BP é conservada.

Palavras-chave: Trypanosomatidae. Citocinese. Zona de adesão flagelar. FLA3. TOEFAZ1.

RESUMO EXPANDIDO

Introdução

Parasitos do gênero *Trypanosoma* possuem um único flagelo que emerge da bolsa flagelar e é aderido ao corpo celular através da zona de adesão flagelar (FAZ). Esta região é importante para a motilidade, infectividade e divisão celular destes parasitos. Diversas proteínas compõem a região da FAZ, incluindo FLA1BP e CIF1, sendo que ambas foram caracterizadas molecularmente apenas na espécie *Trypanosoma brucei*. A proteína FLA1BP de *T. brucei* está localizada na membrana do flagelo do parasito e possui uma longa região extracelular que interage com a proteína FLA1, localizada na membrana do corpo celular, garantindo a adesão do flagelo. Além da porção extracelular, FLA1BP possui uma região transmembrana e uma curta porção intracelular. A deleção deste gene em *T. brucei* resulta no descolamento do flagelo e problemas na motilidade do parasito. Por outro lado, CIF1 de *T. brucei* interage com diversas proteínas envolvidas na ativação da citocinese deste parasito. Estre processo é dependente da fosforilação sofrida por CIF1 e dos domínios proteicos zinc-finger e coiled-coil. A ausência de CIF1, bem como a deleção dos domínios, impede a divisão celular.

Objetivos

O objetivo deste trabalho foi investigar a conservação das proteínas CIF1 e FLA1BP em diferentes tripanosomatídeos.

Material e Métodos

Para investigar a conservação de CIF1, a conservação de cada domínio e dos sítios de fosforilação desta proteína foram comparados entre as espécies *T. brucei* e *Trypanosoma rangeli*. As proteínas conhecidas por interagirem diretamente com CIF1 foram utilizadas para a busca de ortólogos em diferentes tripanosomatídeos. Os genes encontrados foram classificados quanto a possibilidade de possuírem função conservada. Ademais, a localização e os níveis de transcrição e expressão de CIF1 foram investigados através de imunofluorescência, qPCR e western blot, respectivamente. Foi realizada a sincronização do ciclo celular de *T. rangeli* com hidroxiureia e os níveis de transcritos e proteicos foram avaliados durante as diferentes fases do ciclo celular. Por fim, foi utilizada a metodogia CRISPR-Cas9 no intuito de substituir o gene CIF1 de *T. rangeli* por genes de resistência a antibióticos.

Quanto a FLA1BP, a sintenia entre o gene de *T. brucei* foi comparada as sequências ortólogas de *T. brucei* e *Trypanosoma cruzi*. Diferenças de transcrição, expressão e citolocalização nas diferentes formas de *T. cruzi* (epimastigota, amastigota e tripomastigota) e *T. rangeli* (epimastigota e tripomastigota) foram investigadas. A sequência intracelular de FLA1BP de diversos tripanosomatídeos foi alinhada a fim de se identificar resíduos de aminoácidos conservados. Para averiguar a conservação de função de FLA1BP em *T. cruzi* e *T. rangeli*, o gene de FLA1BP das duas espécies foi alvo de deleção gênica pela metodologia CRISPR-Cas9.

Resultados e Discussão

A proteína CIF1 de *T. rangeli* não possui conservados os domínios e sítios de fosforilação descritos na *Tb*CIF1 como importantes para sua função. Apesar de não dividirem, as formas tripomastigotas de T. *rangeli* possuem nível de transcrição de CIF1 mais elevado quando comparadas às formas epimastigotas. Entretanto, não foram observadas diferenças na expressão entre as duas formas. Além disso, não existe diferença entre os níveis de transcrição e expressão de CIF1 de *T. rangeli* durante o ciclo celular. A localização da proteína, essencial para sua função em *T. brucei*, difere na espécie *T. rangeli*. Após a tentativa de deleção da CIF1 de *T. rangeli*, não foram observadas diferenças na divisão celular destes parasitos. Ademais, observa-se que as proteínas que interagem com CIF1 podem ter perdido sua função não apenas em *T. rangeli*, mas também em outros tripanosomatídeos.

Quanto à FLA1BP, análises de sintenia indicam que *T. cruzi* e *T. rangeli* possuem ortólogos sintênicos à FLA1BP de *T. brucei*. Entretanto, *T. brucei* parece ter sofrido diversas duplicações gênicas de FLA1 e FLA1BP durante sua história evolutiva. Apesar da sequência de FLA1BP não ser conservada entre as espécies de tripanosomatídeos, observa-se uma sequência de 12 resíduos de aminoácidos extremamente conservada entre todas as espécies analisadas. Esta sequência se encontra na região intracelular de FLA1BP e corresponde a resíduos de aminoácidos polares e hidrofóbicos. Acredita-se que esta sequência seja a responsável pelo endereçamento de FLA1BP para a zona de adesão flagelar. Além disso, não foram observadas diferenças de expressão de FLA1BP entre as diferentes formas de *T. cruzi* e *T. rangeli*. Por

outro lado, observa-se que enquanto formas epimastigotas possuem FLA1BP dispersa pelo citoplasma, as formas tripomastigotas possuem a proteína concentrada na FAZ e localizada na forma de pontos, assim como o descrito para *T. brucei*. Por fim, a redução nos níveis de expressão de FLA1BP resultou no descolamento do flagelo em *T. rangeli*, sugerindo a conservação de função desta proteína na espécie.

Considerações Finais

Os resultados obtidos neste trabalho indicam que a função de CIF1 e consequentemente a ativação desta via de citocinese, é diferente em *T. brucei* quando comparado aos demais tripanosomatídeos. Por outro lado, apesar da diferença de sequências, a função de FLA1BP é conservada no gênero *Trypanosoma*.

ABSTRACT

Trypanosomatids possess a unique cell structure, containing a single flagellum emerging from the flagellar pocket which is attached along the cell body through the flagellar attachment zone (FAZ). The distal end of the FAZ defines the site for initiation of the cleavage furrow during cell division. Among several proteins involved in such processes, FLA1BP and CIF1 were described in *Trypanosoma brucei* and are essential for flagellar adhesion (FLA1BP) and cytokinesis regulation (CIF1). Due to the lack of comparative studies of these proteins in other trypanosomatids species, we aimed to investigate the presence and the variability of FLA1BP and CIF1 within the *Trypanosoma* genus. Comparative genome analysis shows the absence of domains and sequence conservation of *T. brucei* CIF1 and CIF1-interacting proteins in other species, suggesting adaptations of the cytokinesis activation in this taxon. The *Trypanosoma rangeli* CIF1 is 28% identical to *Tb*CIF1, lacks the coiled-coil and zinc finger domains and contains fewer phosphorylation sites when compared to *Tb*CIF1. Also, *Tr*CIF1 transcription and expression levels are not related to cell division, might be indicating a distinct role of CIF1 in this species. The *T. rangeli* and *Trypanosoma cruzi* FLA1BP genes are single-copy genes syntenic to *Tb*FLA1BP and, despite sequence divergencies, the localization and function of FLA1BP appear to be conserved within the *Trypanosoma* genus. Alignment of the FLA1BP sequence from different species revealed a conserved 12 amino acid sequence composed by polar and hydrophobic residues that may constitute the addressing or anchoring domain of FLA1BP on the FAZ. Our results indicate a conserved FLA1BP role in flagellar attachment among *Trypanosomes* and suggest that cytokinesis activation in *T. brucei* has diverged from other trypanosomatids.

Keywords: Trypanosomatidae. Cytokinesis. Flagellar attachment zone. FLA3. TOEFAZ1.

LIST OF FIGURES

LIST OF TABLES

LIST OF SUPPLEMENTARY MATERIAL

LIST OF ABREVIATIONS

μg – microgram
μL – microliter
BB – basal body
BLAST – Basic Local Alignment Search Tool
°C – degree Celsius
DMEM – Dulbecco's Modified Eagle Medium
EDTA – ethylenediamine tetra acetic acid
FAZ – *Flagellar Attachment Zone*
FLA3[1]
FLA3[2]
FP – flagellar pocket
g – standard gravity
h – hours
IPTG – isopropyl β-d-1-thiogalactopyranoside
K - kinetoplast
kDa – kilodalton
LB – Luria Bertani medium
LIT – Liver Infusion Tryptose
min – minutes
ml – milliliter
mM – millimolar
MtQ – microtubule quartet
N - nucleus
NCBI – National Center for Biotechnology Information
ng – nanogram
ORF – Open Reading Frame
bp – base pairs
PBS – Phosphate Buffered Saline
PCR – Polymerase Chain Reaction
pH – potential of hydrogen
BFS – bovine fetal serum
S - synthesis
SDS – sodium dodecyl sulfate
SDS-PAGE – sodium dodecyl sulfate - polyacrylamide gel electrophoresis
U – unit
X-gal – 5-bromo-4-chloro-3-indolyl-β-D-galactopyranoside

CONTENTS

1 INTRODUCTION

1.1 THE TRYPANOSOMATIDAE FAMILY

The Kinetoplastea clade comprises single-cell protists that possess a unique structure named the kinetoplast that is a complex mitochondrial DNA network composed of thousands of catenated circular DNA molecules (DESCHAMPS et al., 2010; LUKES et al., 2002). Within this clade, the family Trypanosomatidae contains a number of parasitic species that are either monoxenous, i.e., have a single host during the entire life cycle; or dixenous, alternating between insect vectors and hosts during their life cycle (KAUFER et al., 2017). Trypanosomatids are well known for their medical and economic importance, but also for their unusual biology and genome organization (SIMPSON et al., 2004).

Although being a diverse family, the most studied species are those causing impact on human or animal health and economy. Notably, *Trypanosoma cruzi*, the etiological agent of Chagas disease; *Trypanosoma brucei*, which causes Human African Trypanosomiasis and Animal Trypanosomiasis (in cattle and horses); and the *Leishmania* genus, that causes different types of leishmaniasis are by far the most studied species (KAUFER et al., 2017). Along with other animal trypanosomes of veterinary importance in Latin America such as *Trypanosoma vivax* and *Trypanosoma evansi* (OSÓRIO et al., 2018), the non-virulent *Trypanosoma rangeli* is also well studied due the relevance for Chagas disease serodiagnosis as well as for its intriguing biology (GRISARD; STEINDEL, 2016; GUHL; VALLEJO, 2003).

1.1.1 *Trypanosoma cruzi*

T. cruzi is the etiological agent of Chagas disease, also known as Human American Trypanosomiasis, affecting around 6-8 million people worldwide and causing approximately 10,000 deaths each year. As a major health problem for most Latin American countries, Chagas disease mainly affects people under socioeconomic vulnerability. It is noteworthy to mention that Chagas disease is no longer restricted to endemic countries were vectorial transmission occurs. Human migration and blood transfusion have spread the disease to other non-endemic countries (PÉREZ-MOLINA; MOLINA, 2018).

Once established the infection, the disease progression can be divided into an acute and a chronic phase. The acute phase is characterized by a detectable parasitemia and several clinical symptoms like fever, inflammatory response at the area of the bite, Romaña sign

(unilateral edema at the eyelid), lymphadenopathy, and hepatosplenomegaly, but patients can often be asymptomatic. There are no markers for disease progression and chronically infected patients might never develop any symptoms or pathologies or develop classical chronic phase pathologies leading to neurological, cardiac and/or digestive complications (PÉREZ-MOLINA; MOLINA, 2018).

T. cruzi alternates between triatomine vectors and mammalian hosts requiring adaptative answers to distinct environments, including the differentiation into distinct life-stages that differ in their morphology, metabolism, and ability to multiply and infect. *T. cruzi* has three main forms: the epimastigotes (proliferative forms found within triatomine vectors gut), the amastigotes (proliferative forms found inside infected mammalian host cells), and the infective but non-proliferative trypomastigotes that differentiate within the rectal ampulla of triatomines (metacyclic trypomastigotes) or are found on the infected mammal bloodstream (blood trypomastigotes) (LIDANI et al., 2019).

During the *T. cruzi* life cycle (Figure 1), infection of the triatomine occurs by ingestion of trypomastigotes during the bloodmeal on infected hosts. Once in the midgut, parasites differentiate into epimastigotes that attach to the perimicrovillar membrane of the insect and multiply by binary fission. After reaching the hindgut, *T. cruzi* differentiates into infective metacyclic trypomastigotes that are eliminated along with the triatomine bug feces (DE LANA; TAFURI, 2002).

Figure 1 – Life cycle of *Trypanosoma cruzi*. From Centers for Disease Control and Prevention (CDC).

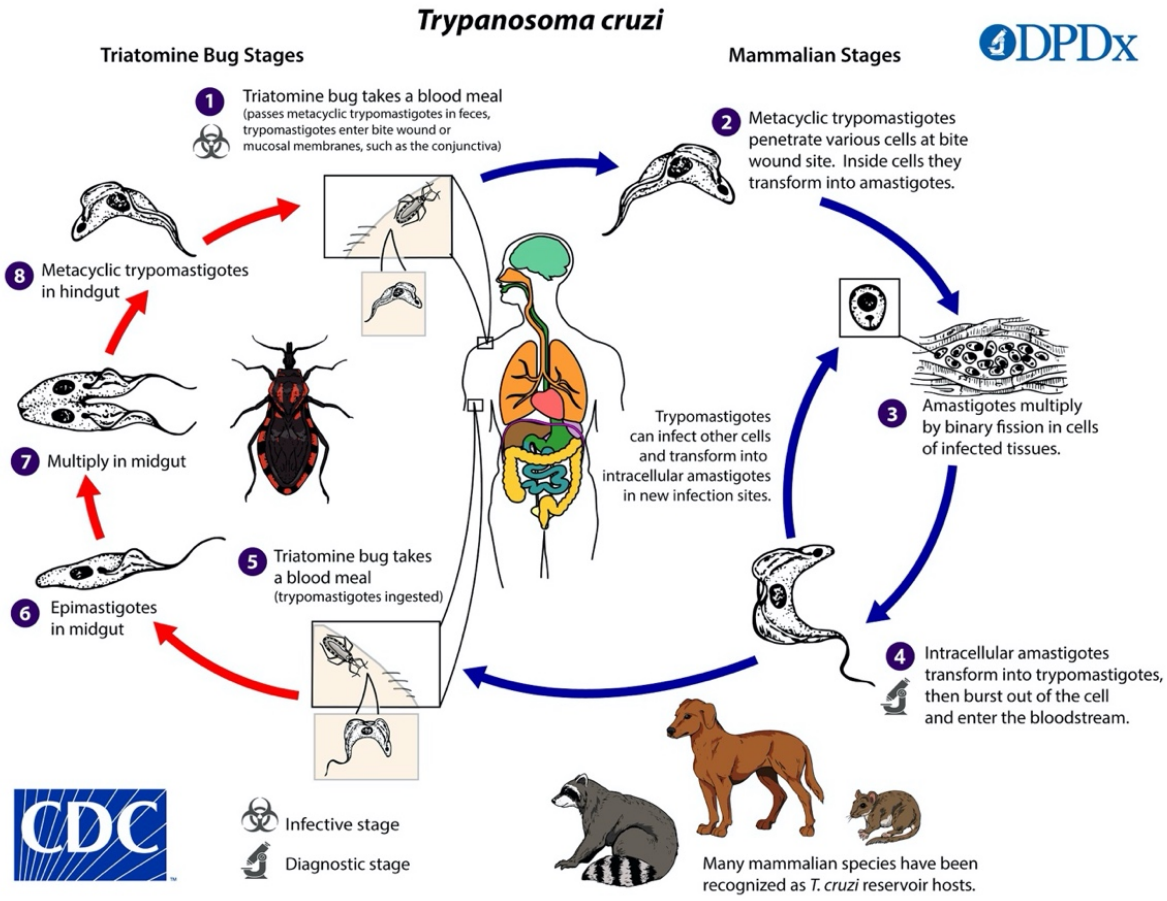

Infection of the mammalian host by metacyclic trypomastigotes occurs via penetration on mucosal membranes or via discontinuity in epidermis. Upon such contaminative infection, *T. cruzi* interacts with host cells, being able to penetrate and differentiate into proliferative amastigotes. These forms multiply intracellularly and ultimately lead to the host cell death, when the parasites differentiate to blood trypomastigotes and can infect other cells or are ingested by a triatomine bug (DE LANA; TAFURI, 2002).

1.1.2 *Trypanosoma rangeli*

T. rangeli is a non-virulent parasite of humans and other mammals, occurring in a wide, superimposed geographical area with *T. cruzi*, with whom they share triatomine vectors and several host species (Figure 2). Differently from *T. cruzi*, this parasite is primarily transmitted via the bite of triatomine vectors (inoculative or anterior transmission), particularly from *Rhodnius* genus, to whom *T. rangeli* is considered pathogenic due to the

infection of the hemolymph and salivary glands, causing deficiencies in moulting (GULL; VALLEJO, 2003). Additionally, both species are phylogenetically related and share a large number of genes, including some common epitopes recognized by the host immune system. It is thus well established that *T. rangeli* induces a humoral immune response that cross-reacts with *T. cruzi* antigens. As a result, infections by *T. rangeli* can lead to false-positive results on serological assays for Chagas disease (AFCHAIN et al., 1979; MORAES et al., 2008).

Figure 2 – Overlapped occurrence of *Trypanosoma cruzi* and *Trypanosoma rangeli*. Map from Central and South Americas representing areas with Chagas Disease (black) and confirmed *T. rangeli* infections in triatomines, humans and other wild animals (asterisks). From: Stoco et al. (2016).

Two distinct forms of *T. rangeli* are known to date: the epimastigotes, which are proliferative forms found in the gut and hemocoel of the triatomine vectors, and the infective but non-proliferative trypomastigotes that differentiate within the salivary glands of triatomines (metacyclic trypomastigotes) or are found on the infected mammal bloodstream (blood trypomastigotes) (GULL; VALLEJO, 2003).

Despite sharing hosts and vectors with *T. cruzi*, *T. rangeli* has a distinct life cycle within triatomines (Figure 3). During the blood meal, infection of the triatomine occurs via ingestion of bloodstream trypomastigotes that differentiate into epimastigotes and multiply in the gut vector. *T. rangeli* epimastigotes also interact with the gut epithelium but, distinctively from *T. cruzi*, the parasites are able to escape the intestinal tract and reach the insect's hemocoel, where they also divide and then migrate to the salivary glands. Once within the salivary glands, *T. rangeli* differentiate to metacyclic trypomastigotes that are directly inoculated along with the saliva of the triatomine in the bloodstream of the mammal during the blood meal (GRISARD; STEINDEL, 2016).

Curiously, the *T. rangeli* life cycle within the mammalian hosts remains controversial since the *T. rangeli* capability to multiply in this host is not understood. *T. rangeli* parasitemia is usually sub-patent and short term, reaching its peak around the fourth day of infection and being detectable for two weeks (AÑEZ, 1981; AÑEZ, 1985). Although undetectable after the acute phase in the bloodstream by light microscopy, the parasite can be detected several months later by hemoculture in experimentally infected mice (STEINDEL, 1993; PAREDES; PAREDES, 1949). Experimental infections in mice reveal an increased number of parasites in the bloodstream if compared to the original inoculum, suggesting that *T. rangeli* is able to multiply within mammals (URDANETA-MORALES; TEJERO, 1985).

Another hypothesis postulates that *T. rangeli* might have the ability to survive in the bloodstream for long periods without multiplying, until being eventually ingested by a triatomine. Former studies have shown that *in vitro* differentiated trypomastigotes cultivated with fibroblasts have survived up to three weeks but showing no signs of cell division (TANOURA et al., 1999). Evidences of low and long-term parasitemia of *T. rangeli* infection in humans (ZELEDÓN, 1954) and opossums (AÑEZ, 1981) has also been described. Nevertheless, such morphological studies have shown trypomastigotes with a rod-shaped kinetoplast similar to *T. cruzi* trypomastigotes, which do not divide. Due to the lack of proper

characterization of these few *T. rangeli* strains showing signs of long-lasting *in vitro* and *in vivo* infections, a cross-contamination with *T. cruzi* cannot be ruled out.

Figure 3 – Life cycle of *Trypanosoma rangeli*. A) Triatomine ingests bloodstream trypomastigotes within infected blood. B) Epimastigotes in the gut. C) After reaching the hemocoel, epimastigotes multiply in it. D) Few parasites invade hemocytes. E) Parasites penetrate the salivary glands and differentiate in metacyclic trypomastigotes. F) Metacyclic trypomastigotes are inoculated during bloodmeal. From: Stoco et al. (2016).

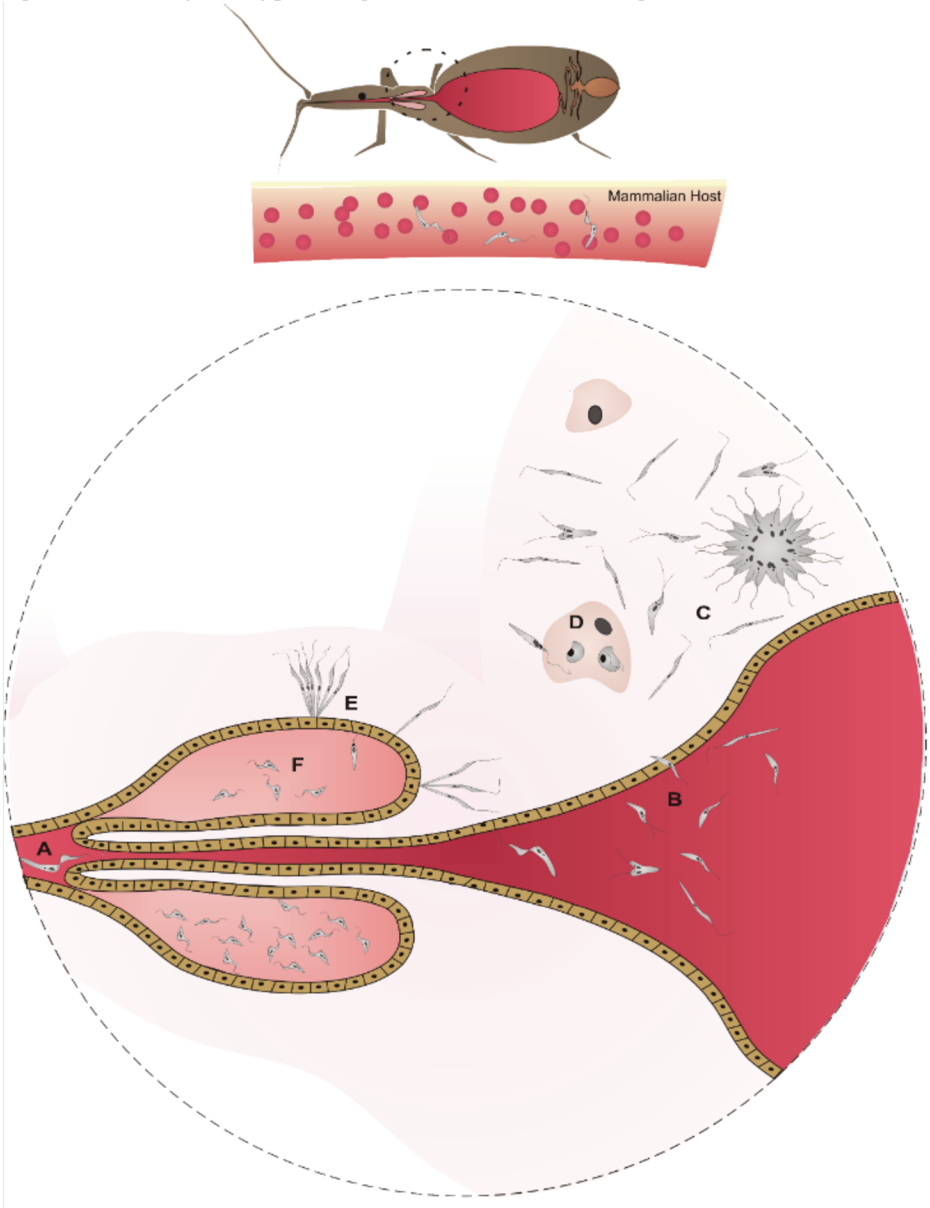

Assuming the reports that *T. rangeli* undergoes cell division within its mammalian hosts, conflicting data supporting hypothesis that this parasite multiplication could either occur intracellularly or extracellularly are observed in the literature. Morphological studies of bloodstream trypomastigotes based on stained smears described parasites showing two nuclei and two kinetoplasts, hence apparently performing cell division, were described by Grewal

(1956) and Molyneux (1973). Later, Añez proposed that such forms were not trypomastigotes in division, but abnormal parasites with altered morphology, probably due transition between morphotypes or forms recently inoculated by the insect vector (AÑEZ, 1981).

The study performed by Herbig-Sandreuter (1957) using serial sections of over 100 experimentally infected baby mice neither detected any evidence of intracellular forms nor signs of pathological changes. On the other hand, Urdaneta-Morales and Tejero (1986) reported *T. rangeli* nests containing amastigote-like parasites in the heart, liver, and spleen of experimentally infected mice, some presenting nuclei and kinetoplast that resembled the morphology observed during division. These authors also report that no bloodstream forms were seen performing cell division. Until now, this has been the only *in vivo* description of *T. rangeli* intracellular forms, achieved using a single strain and leading to inflammatory foci in the in brain, skeletal muscle (ZUÑIGA et al., 1997) and liver (MORALES, 2012), as usually observed during *T. cruzi* infections. Thus, we might speculate the possibility of a misidentified *T. rangeli* strain or a laboratory contamination with *T. cruzi*.

In vitro approaches to visualize *T. rangeli* intracellular multiplication also have shown discrepant results. The interaction of *T. rangeli* (Gorgas Memorial Laboratory Strain N°. $16[3026]_5$) with HeLa cells (derived from cervical cancer cells) and dog sarcoma cells, did not result in invasion or development of intracellular forms (MOLYNEUX, 1973). Later, Osorio et al. (1995) showed that *T. rangeli* (San Agustín strain and Ub66-5b clone), in interaction with U937 cells isolated from histiocytic lymphoma, were able to infect the cells and intracellularly differentiate in an amastigote-like shape, and then infect *Rhodnius prolixus*.

Interaction of Vero (phagocytic, isolated from monkey epithelial cells) and J774 (non-phagocytic, derived from murine reticulum cell sarcoma) cells with the C23 Colombian *T. rangeli* strain resulted in the observation of intracellular amastigote-like forms whose number increased overtime, implying intracellular multiplication was occurring (ZUÑIGA et al., 1997).

Studies of interactions using different strains of *T. rangeli* (Choachí, Macias, and SC-58) with Vero and J774 cells carried out by our group have shown low infection rates, a reduced number of intracellular parasites per cell and no signs of intracellular multiplication (EGER-MANGRICH et al., 2001).

It is thus clear that the evidence of the ability of *T. rangeli* to multiply within the mammalian host are quite interesting but still inconclusive. New studies or approaches are

scarce and the divergence of results in past studies do not provide sufficient evidence for a consensus, therefore requiring new approaches to address this uncertainty.

1.1.3 *Trypanosoma brucei*

T. brucei is the etiological agent of Human African Trypanosomiasis, known as sleeping sickness, a deadly disease if not properly diagnosed and treated. It is caused by two subspecies of *T. brucei*, *Trypanosoma brucei gambiense* and *Trypanosoma brucei rhodesiense*, which are transmitted by Tsetse flies (*Glossina* spp.). These *T. brucei* subspecies differ in their clinical manifestations and epidemiology. *T. brucei gambiense* infections are by far the most prevalent (95-97 %) and long-lasting if compared to *T. brucei rhodesiense* infections (RADWANSKA et al., 2018; KENNEDY, 2019).

In humans, *T. brucei* disseminates from the infective bite site to the bloodstream and lymphatic system, eventually reaching other organs. Due to the response of the host immune system to the parasite, the disease leads to fever, headache, dull pain in joint and muscle and inflated lymph nodes. Upon chronicity of the infection, *T. brucei* crosses the blood-brain barrier and affect the central nervous system, leading to sleeping disturbance and disorientation (BÜSCHER et al., 2017; BOTTIEAU; CLERINX, 2019). Major efforts from the World Health Organization have resulted in the reduction of the prevalence, and it is believed that disease will no longer be considered a neglected disease in the next few years (AKAZUE et al., 2019).

T. brucei faces two main environments during its life cycle, requiring the parasite to perform morphological and physiological adaptations (Figure 4). Infection of tsetse flies by *T. brucei* occurs by the ingestion of bloodstream trypomastigotes during the bloodmeal from an infected mammal. The parasite then differentiates to procyclic trypomastigotes in the vector midgut, multiply by binary fission and then migrates to the salivary glands' lumen. Once in the salivary glands, *T. brucei* transforms into replicative epimastigotes, multiply and then perform metacyclogenesis, differentiating to the infective metacyclic trypomastigotes that are inoculated along with the saliva during a new blood meal (AKAZUE et al., 2019).

Figure 4 – Life cycle of *Trypanosoma brucei*. From Centers for Disease Control and Prevention (CDC).

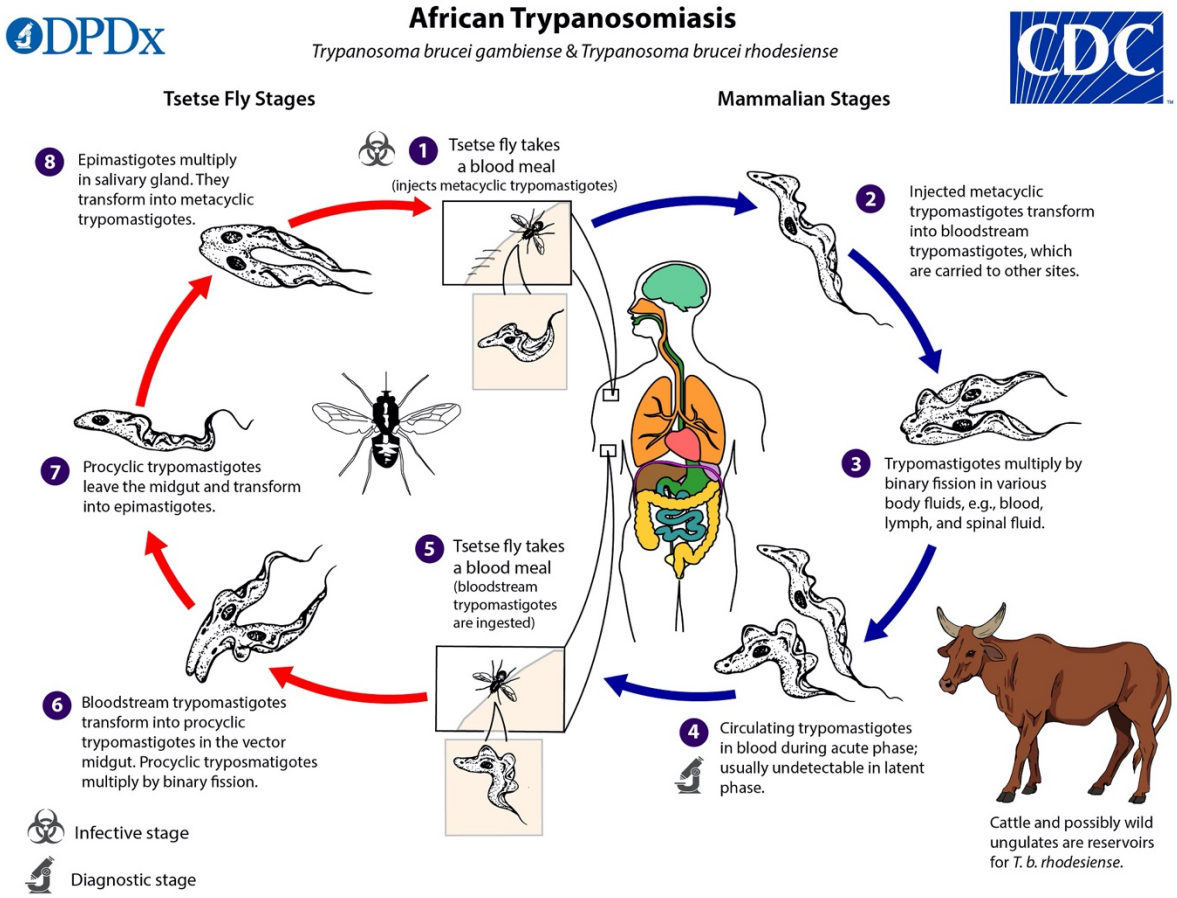

Once in the mammalian host, the parasite is exposed to a distinct environment that induce the transformation from metacyclic trypomastigotes to long slender bloodstream forms. Differently from the American Trypanosomiasis, where *T. cruzi* divide exclusively within a cell, these *T. brucei* forms multiply as extracellular parasites in the blood and tissue fluids of the host. As an adaptation to avoid the host immune system, *T. brucei* bloodstream forms express a repertoire of variant surface glycoproteins (VSGs) that vary during the infection. After reaching a peak of parasitemia, the long and slender parasites transform in short stumpy forms that eventually can be ingested by a new fly during the bloodmeal (AKAZUE et al., 2019).

1.2 THE *TRYPANOSOMA* CELL BODY

The cell shape of a given unicellular organism is ultimately a result of evolutionary history and, therefore, strongly related to responses or adaptations to the environment. Besides

the interchanges from mammalian hosts to insect vectors, species of the genus *Trypanosoma* may also face different habitats within the vectors (e.g. gut, hemocoel, and salivary glands) and within the mammals (e.g. bloodstream, and inside distinct types of cells). Such diversity of environments is reflected in the different cell morphologies such as epimastigotes, trypomastigotes (metacyclic, bloodstream, slender, stumpy) and amastigotes (Figure 5) (WHEELER, GLUENZ, GULL, 2013).

Figure 5 – Different cell morphologies of *Trypanosoma* genus. The kinetoplast from trypomastigotes is posterior to the nucleus, different from the anterior kinetoplast from epimastigotes and amastigotes. Blue = Nucleus and kinetoplast. Adapted from Sunter and Gull (2016).

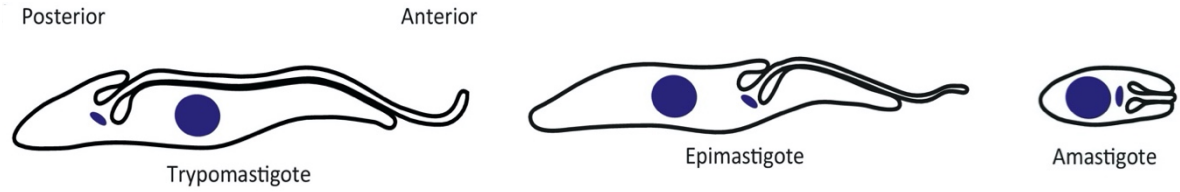

The *Trypanosoma* cell, therefore, can assume distinct shapes, but key features are preserved in all biological forms: a subpellicular array of microtubules that form the cell cytoskeleton, the kinetoplast, the basal body, the flagellar pocket and a single flagellum. The kinetoplast is linked to the basal body, which is positioned at the base of the flagellar pocket. From the flagellar pocket exits the flagellum, which is attached to the cell body through the Flagellar Attachment Zone (FAZ) (LACOMBLE et al., 2009; SUNTER; GULL, 2016).

1.3 THE FLAGELAR ATTACHMENT ZONE (FAZ)

The FAZ is a complex structure composed of many proteins, which connects the flagellum to the cell body. Studies in which different components of FAZ have been depleted have caused the detachment of the flagellum from the cell body, affecting the parasite morphology and its ability to swim, to infect vectors and hosts, to differentiate, and to multiply (BASOMBRÍO et al., 2002; SUNTER, 2016).

Generated by the interaction of different cellular components, FAZ can be divided into different regions and domains (Figure 6). This complexity demands from the cell the precise localization of several proteins, which must be correctly addressed during the assembling of a new FAZ during division. In addition, the formation of the new FAZ upon cell multiplication has to be synchronized with elongation of the new flagellum. Once the new

FAZ and the new flagellum have been assembled, the cell progresses to mitosis and then cytokinesis (SUNTER; GULL, 2016).

Figure 6 – Flagellar attachment zone of *Trypanosoma brucei*. (A) Schematic representation of a trypomastigote cell from *T. brucei*. Dashed line indicates the plane of transverse section picture (B). Regions from FAZ were indicated in (B). Adapted from: Sunter and Gull (2016).

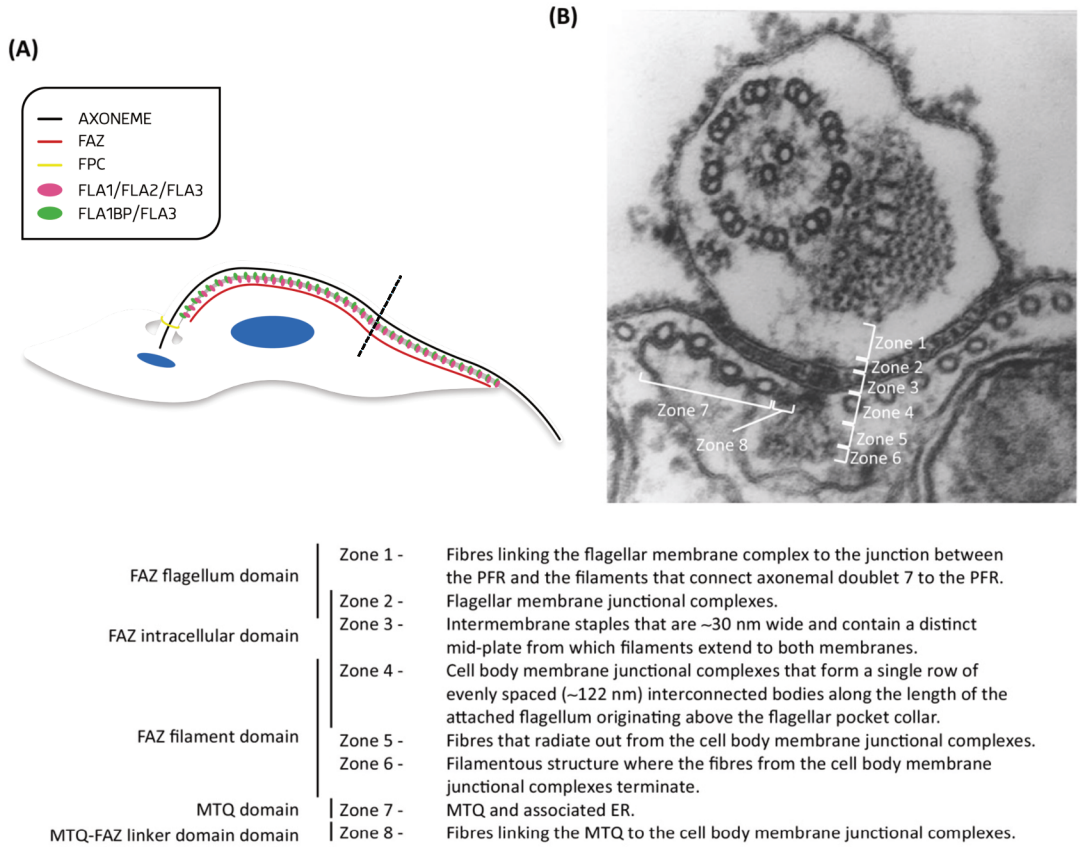

1.3.1 The Flagellar-Adhesion Glycoprotein 1 (FLA1)

The first FAZ protein described was a highly N-glycosylated 72 kDa glycoprotein (Gp72) from *T. cruzi* identified at the FAZ using the monoclonal antibody WIC 29.26. Functional studies of the Gp72 have shown that deletion of this gene resulted in errors of flagellar adhesion to the cell body (COOPER et al., 1991). Further studies using Gp72 knockout parasites have shown that this protein is also important for the parasite infectivity in both mice and vectors due to its role in flagellar attachment (COOPER; DE JESUS; CROSS, 1993; ROCHA et al., 2006; BASOMBRÍO et al., 2002).

The antibody WIC 29.26 only recognizes Gp72 from *T. cruzi* epimastigotes, not recognizing any protein on amastigotes and trypomastigotes, thus Gp72 has been described as a *T. cruzi* stage-specific protein (SNARY et al., 1981). However, further studies have concluded that this antibody was, in fact, specific for the Gp72 glycosylations and, since this protein is differently glycosylated during the *T. cruzi* life cycle, such post-translational modifications were not detected on amastigotes and trypomastigotes although Gp72 is indeed expressed in these stages (HAYNES; CROSS, 1996).

Despite being widely used as a classic and easily identified phenotype (flagellar detachment) on deletion studies, little is known about other *T. cruzi* Gp72 characteristics such as structure or interaction with other proteins (LANDER; CHIURILLUO, 2019).

In *T. brucei*, the Gp72 ortholog was named Flagellar-Adhesion Glycoprotein 1 (FLA1) (Tb927.8.4010) due to its role in flagellar attachment and glycosylation profile. Despite having similar function and localization when compared to Gp72, FLA1 is essential for *T. brucei* since deletion of both FLA1 alleles is not possible (NOZAKI; HAYNES; CROSS, 1996). In addition, RNAi studies have confirmed FLA1 function in *T. brucei* (LACOUNT; BARRETT; DONELSON, 2002). Later, two other genes very similar to FLA1 and almost identical to each other were discovered and named FLA2 (Tb927.8.4060) and FLA3 (Tb927.8.4110). In this study, FLA3 described by Sun et al. (2013) will be termed as FLA3-A. While FLA1 is expressed in both bloodstream and procyclic forms, FLA2/FLA3-A are bloodstream-specific proteins (SUN et al., 2013).

FLA1/FLA2/FLA3-A/Gp72 proteins share canonical elements that include a N-terminal peptide-signal, an extracellular region containing several N-glycosylation sites and an NHL domain, a transmembrane region and a short intracellular C-terminal tail. Despite being found in the cellular membrane and flagellar pocket, FLA1 is concentrated at the FAZ, where its transmembrane region crosses the membrane of the cell body (Figure 6) (SUN et al., 2013).

1.3.2 The Fla1-Binding Protein (FLA1BP)

Immunoprecipitation assays used to assess the FLA1 role in flagellar attachment in *T. brucei* identified a new FLA-related protein named FLA1-Bindind Protein (FLA1BP), that is encoded by two identical genes, FLA1BP-1 (Tb927.8.4100) and FLA1BP-2 (Tb927.8.4050). The interaction of FLA1 with FLA1BP at the FAZ promotes the connection

between the flagellum membrane to the cell membrane, and these two proteins likely act as a protein zipper (Figure 6) (SUN et al., 2013).

In the same year, Woods et al. described another FAZ protein similar to FLA1BP, called as FLA3. However, FLA3 is also the name of another protein described by Sun et al. (2013) (FLA3-A, similar to FLA1). Therefore, the FLA3 described by Woods et al. (2013) will be referred as FLA3-B in our study, a protein exclusively expressed in bloodstream forms of *T. brucei* (SUN et al., 2013; WOODS et al., 2013).

As observed for FLA1, FLA1BP and FLA3-B also possess the canonical elements described for FLA1 (peptide signal, NHL domain, transmembrane region, C-terminal tail), being also post-transcriptionally glycosylated on their extracellular portion. However, while FLA1 is localized at the cell body membrane of the FAZ region, FLA1BP is on the flagellar membrane. Although the FLA1BP extracellular region is required for FLA1-FLA1BP interaction, it is probable that the intracellular C-terminal tail is important for FLA1BP localization at the FAZ (SUN et al., 2013; WOODS et al., 2013).

Except for the studies on the *T. cruzi* Gp72, little is known about FLA1BP in *T. cruzi* and *T. rangeli*. Preliminary studies carried out by our group have shown the presence of single copy genes coding for FLA1BP and FLA3-B in these taxa. *T. rangeli* FLA1BP/FLA3-B is 35.82 % identical to *Tb*FLA1BP and 36.36 % identical to *Tb*FLA3-B, while for *T. cruzi* the identities were 37.42 % and 37.71 %, respectively (DE LIZ, 2017).

1.4 THE CELL DIVISION OF TRYPANOSOMATIDS

During the cell cycle, the trypanosomatids undergo a number of critical steps that includes the division and segregation of the nucleus, the kinetoplast and cytoskeletal components. These three events have several steps that happen simultaneously but whose co-ordination it is not conserved among trypanosomatids (Figure 7) (WHEELER; GULL; SUNTER, 2019).

During mitosis, trypanosomatids must segregate megabase-sized chromosomes and mini-chromosomes. The segregation for both types of chromosomes is distinct, but no condensation is observed, and the nucleolus is preserved (ZHOU; HU; LI, 2014; WHEELER; GULL; SUNTER, 2019).

To multiply the catenated DNA of the kinetoplast, minicircles are disconnected from the network during S phase, replicated and carried to the antipodal sites, where they are

attached again to the network. Little is known concerning the maxicircles replication, but before completing full kDNA multiplication, the new kinetoplast is segregated being carried by the basal body (ZHOU; HU; LI, 2014; WHEELER; GULL; SUNTER, 2019).

Figure 7 – Major steps in *Trypanosoma brucei* procyclic form cell cycle. Schematic representation of cell division process in *T. brucei* procyclic form (A) and approximate timing of nucleus (B), cytoskeleton (C) and kinetoplast (D) multiplication. From: Wheeler, Gull and Sunter (2019).

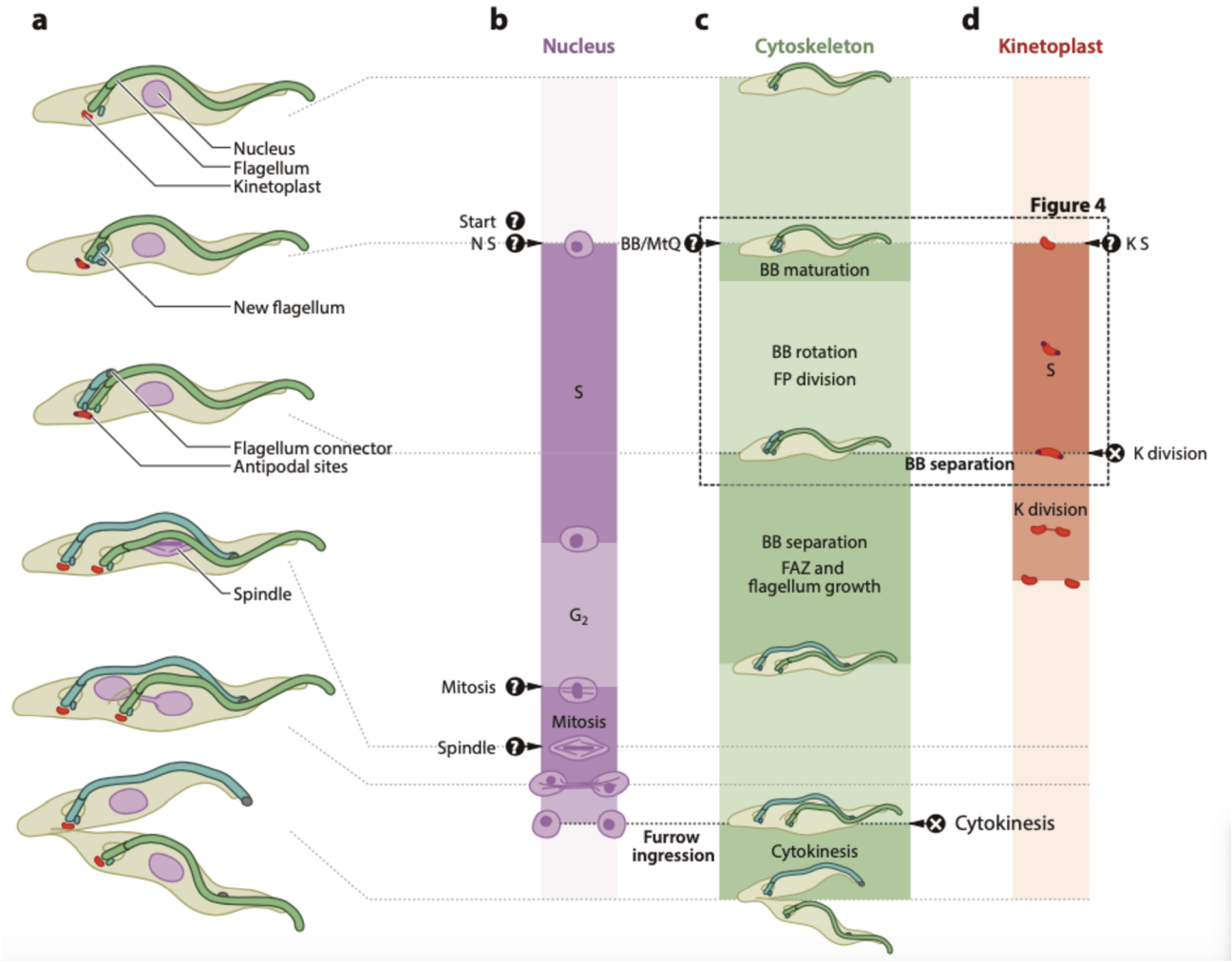

The ordering of some cell division events may vary within the *Trypanosoma* genus, which may have influence on their different duplication times. Mitosis can happen after kinetoplast division as observed for *T. brucei*, *T. cruzi* and *T. rangeli*, or at variable times, as in *Trypanosoma abeli*, a fish trypanosome. In *Leishmania* sp., mitosis simultaneously occurs with the kinetoplast division (HAMMARTON, 2019; PRESTES et al., 2019; WHEELER; GULL; SUNTER, 2019).

During cell division, trypanosomatids duplicate the flagellum and the FAZ assembling them alongside the existing flagellum and FAZ. After the duplication of the new FAZ and flagellum, the remodeling of the cytoskeleton around the furrow site at the distal end of the FAZ is followed by the invagination of the plasma membrane between the recently duplicated flagella and FAZs (HAMMARTON, 2019). Finally, cytokinesis occurs when the cleavage furrow starts from the anterior end of the new FAZ towards the posterior end of the cell (ROBINSON et al., 1995; KOHL et al., 2003; ZHOU et al., 2011).

The initiation of the cytokinesis process has been extensively studied in *T. brucei*, yet it is not fully understood. At the centrin arm or hook, the *T. brucei* Polo-like kinase (*Tb*PLK) phosphorylates the Cytokinesis Initiation Factor 1 (*Tb*CIF1) that is recruited to the new FAZ tip. There, *Tb*CIF1 interacts with the Aurora kinase 1 (*Tb*AUK1) leading to the initiation of furrow ingression (Figure 8) (ZHOU; LI, 2016).

Figure 8 – Cytokinesis initiation in *Trypanosoma brucei*. From: Zhou and Li (2016).

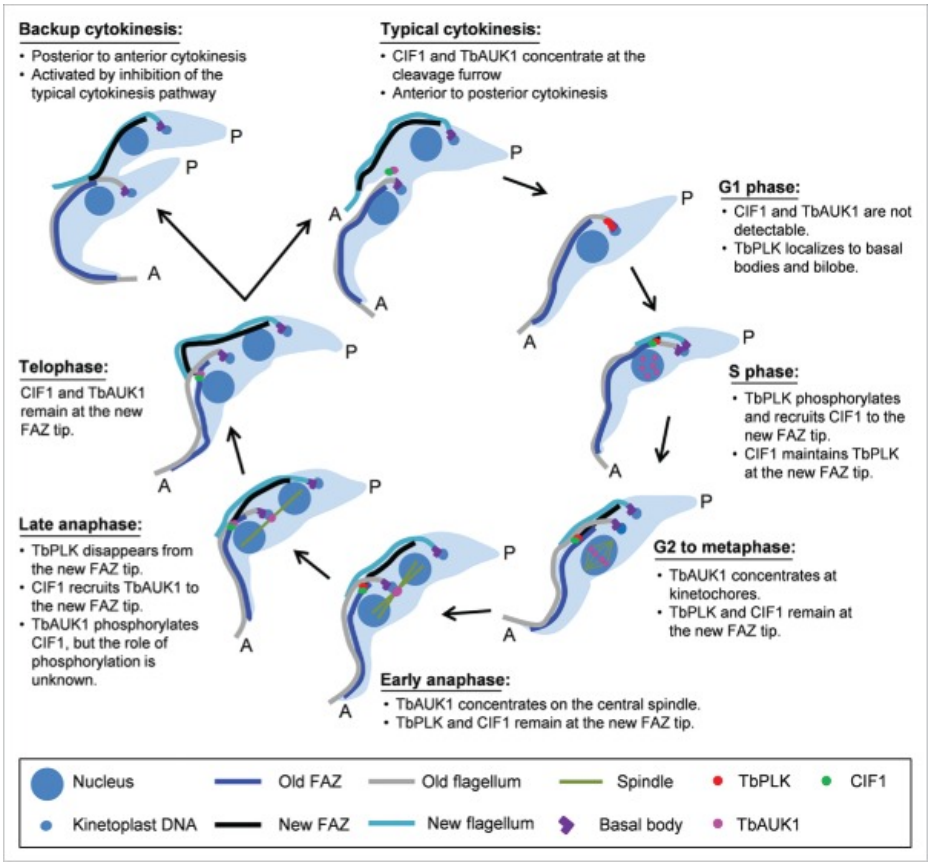

1.4.1 The Cytokinesis Initiation Factor 1

While both PLK and AUK1 are conserved among eukaryotes, CIF1 is exclusive to the trypanosomatids. Initially described as "Tip of the Expanding FAZ Filament 1" (TOEFAZ1) due to its localization (McALLASTER et al., 2015), the protein was then renamed as CIF1 due to its function as a crucial factor for cytokinesis initiation. CIF1 knockdown resulted in an abnormal cell division from posterior to anterior cell end, resulting in a slower process with more aberrant cells than those observed during normal cytokinesis performed by wild-type cells (ZHOU et al., 2016).

Thus, CIF1 plays a central role in *T. brucei* cytokinesis regulation. Besides interacting with PLK and AUK1, it has been demonstrated that *Tb*CIF1 interacts with several proteins, including CIF2, CIF3, CIF4, KAT80, KLIF, FRW1, FAZ29, FPRC and KPP1. Two domains have major impact on CIF1 interactions with such proteins: the coiled-coil and the zinc-finger domains (ZHOU et al., 2018; HU et al., 2019). In our preliminary studies we have observed a reduced similarity of *T. cruzi* and *T. rangeli* CIF1 to the *T. brucei* ortholog, potentially indicating a loss or an alternative function (DE LIZ, 2017).

1.5 AIMS AND OBJECTIVES

Since most studies about the flagellar adhesion zone (FAZ) and cytokinesis have used *T. brucei* as a biological model, little is known concerning FLA1 and FLA1BP proteins as well as cytokinesis factors in the other trypanosomatid species. As a consequence, it is not known if such processes are conserved across species of this family. Therefore, the overall aim of this study is to examine and compare the CIF1 and the FLA1BP proteins from different trypanosomatid species and to investigate the divergence and similarity in conservation of FAZ and cytokinesis-related proteins in trypanosomatids.

1.5.1 Aims of chapter one

Investigate the role of CIF1 in *T. rangeli* cytokinesis and in other trypanosomatid species.

1.5.1.1 Specific objectives

- Compare CIF1 and CIF1-interacting proteins conservation in the Trypanosomatidae family;

- Characterize the transcription and the expression levels and define the cytolocalization of the CIF1 protein from *T. rangeli* (*Tr*CIF1);
- Investigate the *Tr*CIF1 role in *T. rangeli* cytokinesis through functional studies using CIF1-knockout parasites.

1.5.2 Aims of chapter two

Analyze FLA1BP conservation within the *Trypanosoma* genus.

1.5.2.1 Specific objectives

- Evaluate and discuss FLA1BP and FLA1 gene evolution in trypanosomes;
- Characterize the transcription and the expression levels and define the cytolocalization of the FLA1BP protein from *T. rangeli* (*Tr*FLA1BP) and *T. cruzi* (*Tc*FLA1BP);
- Investigate the role of FLA1BP in the *T. rangeli* FAZ via functional studies using FLA1BP-knockout parasites.

2 MATERIALS AND METHODS

2.1 ETHICAL AND BIOSAFETY ASPECTS

This work used female BALB/c mice from the Department of Microbiology, Immunology and Parasitology (MIP/UFSC) animal facility. The animals have been used to obtain *T. rangeli* blood trypomastigotes and to generate anti-r*Tr*CIF1 polyclonal anti-serum.

Animals were maintained at controlled temperature in mini isolators containing sterile pine shavings as bedding, having water and animal food *ad libitum*. Procedures evolving animal experiments were previously approved by the UFSC Ethics Commission for Animal Use – CEUA (Process: 9923170516/2016) and were performed according to the Ethical Principles for Laboratory Animal Use, established by the Brazilian College of Animal Experimentation - COBEA (from Portuguese *Colégio Brasileiro de Experimentação Animal*).

Our laboratory is certified by the National Biosafety Committee – CTNBio (from Portuguese *Comissão Técnica Nacional de Biossegurança*) to perform experiments involving genetically modified pathogenic organisms (NB2) as stated on the UFSC certificate 101/99.

2.2 *IN SILICO* ANALYSIS

2.2.1 Conservancy of CIF1 and CIF1-interacting proteins

To investigate the presence of orthologous FLA1BP, CIF1 and CIF1-interacting proteins among trypanosomatids (Supplementary Material A), the sequence of the described proteins for *T. brucei* (Strain TREU927) were used as query in *tBLASTn* searches using the GenBank (https://www.ncbi.nlm.nih.gov/genbank/) and the TriTrypDB (http://tritrypdb.org/tritrypdb/) databases, as well as the updated version of the *T. rangeli* genome generated by our group. Searches were carried out using the genomes from the following parasite species and strains: *T. rangeli* (SC58), *Trypanosoma vivax* (Y486), *Trypanosoma evansi* (STIB 805), *Leishmania braziliensis* (MHOM/BR/75/M2904), *Leishmania major* (LV39c5), *Leishmania infantum* (JPCM5), *Trypanosoma cruzi* (DM28c), *Endotrypanum monterogeii* (LV88), *Trypanosoma grayi* (ANR4), *Leishmania tarentolae* (Parrot-TarII), *Crithidia fasciculata* (strain Cf-Cl), *Leptomonas seymouri* (ATCC 30220), *Paratrypanosoma confusum* (CUL13), *Phytomonas* sp., *Blechomonas ayalai* (B08-376) and *Bodo saltans* (strain Lake Konstanz).

All positive results from the *tBLASTn* analysis were retrieved and had their amino acid sequences predicted using the ExPASy Translate tool (https://web.expasy.org/translate/). The predicted protein sequences were analyzed for their expected molecular weight

(https://web.expasy.org/protparam/), presence of domains (https://www.ncbi.nlm.nih.gov/Structure/cdd/wrpsb.cgi and http://www.ebi.ac.uk/interpro/), presence of coiled-coils signatures (https://embnet.vital-it.ch/software/COILS_form.html), and phosphorylation sites (http://www.cbs.dtu.dk/services/NetPhos/). The sequence conservancy was analyzed using the SkyLign tool (http://skylign.org/).

2.2.2 Synteny analysis of CIF1 and FLA1BP

Initially, the *T. brucei Tb*CIF1 (accession number Tb927.11.15800) and *Tb*FLA1BP-2 (accession number Tb927.8.4050) genes were retrieved from the public databases described in 2.2.1 and used as query in BLAST analysis to verify the presence of orthologous genes in *T. cruzi* and *T. rangeli*.

Analysis of the genomic organization of CIF1 and FLA1BP genes from *T. brucei*, *T. cruzi* and *T. rangeli* was carried out by comparing the upstream and downstream regions of their genomes flanking the target genes in order to assess synteny. For that, chromosomal or scaffold regions from the *T. brucei* (strain TREU927), *T. cruzi* (strain DM28c) and *T. rangeli* (SC58) genomes containing CIF1 or FLA1BP genes, as well as their respective 5' and 3'end genes, was drawn for each species using the Illustrator for Biological Sciences (IBS) software and then visually compared.

2.2.3 Analysis of the FLA1BP transcription levels in *Trypanosoma rangeli* and *Trypanosoma cruzi*

To assess the FLA1BP transcription in *T. rangeli*, RNAseq data generated by our group (unpublished data) using total RNA obtained from *T. rangeli* bloodstream trypomastigotes obtained from experimentally infected mice, metacyclic trypomastigotes obtained from salivary glands of *Rhodnius prolixus* and epimastigotes obtained from *R. prolixus* hemolymph was used. A total of nine cDNA libraries (three for each parasite form) were generated and sequenced using an Illumina HiSeq 2500 equipment at Science for Life Laboratories from the Karolinska Institute (Stockholm). The obtained transcriptome was assembled using the Trinity v2.2.0 software (GRABHERR et al., 2011) and the transcripts levels were measured using the Kallisto software. Analysis of FLA1BP transcription in *T. cruzi* used transcriptomic data obtained by Illumina platform from the NCBI database (SRA

project SRP072022), which include epimastigote, amastigote and trypomastigote data (BERNÁ et al., 2017).

FLA1BP nucleotide sequence from *T. rangeli* and *T. cruzi* (DE LIZ, 2017) was used to search for FLA1BP transcription in both databases. For *T. rangeli*, mRNA levels were analyzed by software START (https://kcvi.shinyapps.io/START), while for *T. cruzi* normalized nCounts data was used to generate transcription graph at Prism 6.0 Software (item 2.7).

2.3 PARASITE CULTURE

2.3.1 *Trypanosoma rangeli*

T. rangeli epimastigotes from Choachí strain, originally isolated from salivary glands from *Rhodnius prolixus* captured in Colombia (SCHOTTELIUS, 1987), were cultivated by weekly passages in LIT medium (*Liver Infusion Tryptose*) supplemented with 10% of fetal bovine serum (FBS, Gibco), 100 U/mL of penicillium and 100 µg of streptomycin (Cultilab) at 27.5 ºC.

To obtain *in vitro* differentiated trypomastigotes, epimastigotes were harvested from LIT medium and incubated in DMEM (*Dulbecco's Modified Eagle Medium*, Himedia), pH 8.0, supplemented with 5 % of FBS at 27.5 ºC in tissue culture flasks of 25 cm^2. On the seventh day of culture, the percentage of trypomastigotes was determined by counting 200 randomly chosen cells in Giemsa-stained (Merck) smears (KOERICH et al., 2002). Only the cultures that revealed percentages over 97 % were considered for the experiments.

2.3.2 *Trypanosoma cruzi*

T. cruzi epimastigotes (Y strain), originally isolated from a human case in Brazil (SILVA; NUSSENZWEIG, 1953), were cultivated by weekly passages in LIT medium (10% of FBS, 100 U/mL of penicillium and 100 µg of streptomycin) at 27.5 ºC. Trypomastigotes were obtained by infection of L929 cultivated at 37 ºC in DMEM containing 5 % of FBS and 5 % of CO_2 in a humidified atmosphere. Three days after cells infection, trypomastigotes were collected from the culture supernatant.

2.3.3 *Trypanosoma brucei* and *Leishmania infantum*

Procyclic forms from *T. brucei*, strain 29.13, were grown in SDM-79 medium supplemented with 10 % FBS, 25 µg/mL of G418 and 25 µg/mL of hygromycin (SCH

ÖNENBERGER, 1979). The culture was diluted when cell density reached approximately 5 x 10^6/mL.

For *L. infantum*, promastigotes of the PP75 strain were cultured by weekly passages in *Schneider´s Insect medium* (Sigma) supplemented with 10 % FBS, 5 % human male sterile urine, 100 U/mL of penicillium and 100 µg/mL of streptomycin at 27.5 ºC (HENDRICKS; WRIGHT, 1979).

2.4 *Trypanosoma rangeli* CELL CYCLE SYNCHRONIZATION

2.4.1 Cell cycle synchronization and sample processing

The synchronization of the *in vitro* cell cycle of *T. rangeli* was performed as described by Prestes et al. (2019). Briefly, a total of 3 X 10^7 epimastigotes were resuspended in 9 mL of complete LIT medium and incubated with 20 mM of hydroxyurea (HU) for 24 h at 27.5 ºC. Parasites were then washed twice with PBS (pH 7.4) and resuspended in 9 mL of fresh LIT. Aiming to obtain parasites in different stages of the cell cycle, triplicates were kept in HU-free LIT for 0 h, 5 h, 10 h, 15 h, and 20 h. After each time-point, parasites were washed three times in PBS (pH 7.4) by centrifugation (3,000 x *g* for 10 min), resuspended in 3 mL of PBS (pH 7.4) and each sample was divided into three tubes for further analysis of the cell cycle and for mRNA and protein extraction.

2.4.2 Flow cytometry

To determine the phase of the cell cycle, samples (2.4.1) were fixed in cold methanol 50 % in PBS (pH 7.4), on ice, for 10 min. Parasites were then resuspended in PBS (pH 7.4), incubated with 50 µg/mL of RNase A for 20 min at 37 ˚C, centrifuged for 3.000 x *g* for 5 min and resuspended in PBS (pH 7.4). Before data acquisition, 4 ng/µL of propidium iodide was added to each tube.

Measurements were performed using the BD FACSCanto II flow cytometer from the UFSC Multiuser Laboratory of Biological Studies (LAMEB). To select the population for analysis, first, the equipment was calibrated with non-labelled live epimastigotes and with methanol-fixed epimastigotes. Measurements were carried out using the PerCP-Cy5.5 channel, using channel FITC as negative control. In average, 30.000 events were obtained for each sample and the obtained results were analyzed using the Flowing software to generate

the histograms. Proportions based on the number of parasites in each cell cycle were defined using the automated analysis of the Flowing software.

2.5 CYTOLOCALIZATION AND EXPRESSION LEVELS ANALYSIS

Assessment of FLA1BP and CIF1 expression levels and localization was carried out through western blot and indirect immunofluorescence assays. For that, polyclonal antiserum anti-r*Tr*CIF1 generated as described on item 2.5.3 and anti-r*Tc*FLA1BP and r*Tr*FLA1BP that were previously generated by our group (DE LIZ, 2017) were used.

2.5.1 Primers design and cloning of a fragment from *Tr*CIF1

Aiming to optimize heterologous protein expression of CIF1 from *T. rangeli*, for the generation of an anti-r*Tr*CIF1 polyclonal antiserum, different software was used to select a fragment from *Tr*CIF1 (*Tr*CIF1_frag) avoiding regions with rare codons (https://people.mbi.ucla.edu/sumchan/caltor.html) and highly hydrophobic amino acids (https://web.expasy.org/protscale/). After such analyzes, a 12.62 kDa fragment corresponding to the C-terminal portion of *Tr*CIF1 was selected and PCR amplified using primers *Tr*CIF_frag_F 5′- **CATATGAA**GTATAGGCGAACTGTGGAAC - 3′ and *Tr*CIF_frag_R 5′- **GGATCC**CACGCTCCGACAAAATACC - 3′, that were designed using the DNASTAR software. Restriction sites for *Nde*I and *Bam*HI (bold/underlined) were added at the 5′end of these primers to enable downstream cloning into an expression vector.

The *Tr*CIF1_frag was PCR amplified using 20 ng of total DNA extracted from the *T. rangeli* (Choachí Strain), 1 pmol of each primer, and 1 U GoTaq DNA polymerase (Promega) on proper buffer. The reaction was performed with a first step at 95 ºC for 5 min, 35 cycles of 1 min at 95 ºC, 1 min at 60 ºC and 1 min at 72 ºC, and a final step of 10 min at 72 ºC. Amplification was confirmed by resolving the PCR products on 1 % agarose gel electrophoresis stained with ethidium bromide (1 µg/mL). The amplicons were then gel-purified using the GFX PCR DNA and Gel Band Purification kit (GE Healthcare), digested with *Nde*I and *Bam*HI, precipitated with isopropanol and cloned onto the pET14b plasmid, (previously digested with the same enzymes and conditions) using a DNA T4-ligase.

The ligation product was then used to transform *Escherichia coli* DH5α calcium-competent cell following standard laboratory protocols. Briefly, the ligation product was incubated with *E. coli* DH5α competent cells for 30 min in ice. The mixture was then incubated at 42 ºC for 45 s and then in ice for 2 min. After adding 300 µL of SOC medium (2

g/L of tryptone, 0.5 g/L of yeast extract, 1 mM NaCl, 0.25 mM KCl, 2 mM $Mg2^{+}$ and 2 mM glucose), cells were incubated at 37 ºC under shaking and then spread in LB-agar plates (10 g/L of tryptone, 5 g/L of yeast extract, 0.17 mM NaCl, 15 g/L of agar) containing 100 µg/mL of ampicillin.

After incubation overnight at 37 ˚C, identification of positive colonies was performed by PCR using primers targeting both plasmid (T7_F 5′- TAATACGACTCACTATAGGG - 3′ and T7_R 5′- GCTAGTTATTGCTCAGCGG - 3′) and *Tr*CIF1_frag sequences (*Tr*CIF_frag_F and *Tr*CIF_frag_R) to verify the presence and the correct orientation of the insert. After resolution of the amplicons on 1 % agarose gel electrophoresis stained with ethidium bromide, positive colonies were selected to grow in 10 mL of LB medium (10 g/L tryptone, 5 g/L yeast extract, 0.17 mM NaCl) containing ampicillin 100 µg/mL for 16 h, under shaking, at 37 ºC. Plasmid extraction was carried out using standard alkaline lysis (miniprep) as described by Sambrook and Russell (2001), following resolution of the extracted plasmids in 1 % agarose gel electrophoresis stained with ethidium bromide for integrity check.

The identity of the inserts was further confirmed by DNA sequencing as described above, using primers targeting the plasmidial (T7_F and T7_R) and the *Tr*CIF1_frag sequences (*Tr*CIF_frag_F and *Tr*CIF_frag_R). The obtained sequences for each clone were then clustered and evaluated for their quality using the Phred/Phrap/Consed (http://www.phrap.org). Sequences with Phred>20 were used to perform *BLASTn* against *T. rangeli* genome to confirm their identity.

2.5.2 Heterologous expression and purification of *Tr*CIF1_Frag

The pET14b-*Tr*CIF1_frag were used to transform *E. coli* Rosetta-gami (DE3) pLysS (Novagen) calcium-competent cells as described above. Selected colonies were then grown overnight at 37 ºC under shaking in LB medium containing 200 µg/mL of ampicillin, 15 µg/mL of kanamycin, 34 µg/mL of chloramphenicol and 1 % glucose and then used as pre-inoculum to a new culture that was grown under the same conditions until reaching the optic density of 0.5. Cells were then harvested and washed twice in LB medium w/o glucose by centrifugation for 10 min at 2,000 x *g*. The pellet was resuspended in LB medium w/o glucose and heterologous expression of the *Tr*CIF1_frag was induced by adding 0.1 mM of Isopropyl β-d-1-thiogalactopyranoside (IPTG) following incubation at 37 ºC for 3 h under shaking.

Purification of the recombinant *Tr*CIF1_frag (r*Tr*CIF1_frag) was carried out by harvesting the culture by centrifugation at 2.000 x *g* for 15 min at room temperature following cell lysis by addition of 10 mL of B buffer pH 8 (8 M urea, 100 mM NaH_2PO_4, 100 mM Tris HCl pH 8.0) for one hour at 60 ˚C. Total bacteria extract was then treated with RNAse A (10 µg/mL) at room temperature for five minutes and then centrifuged at 12.000 x *g* for 30 min at 4 ˚C. A fraction of the supernatant was kept for further analysis by 12 % SDS-PAGE (item 2.5.4).

The insoluble fraction was then submitted to an affinity chromatography using Ni-NTA Agarose resin (Qiagen) columns. The lysate was mixed to 1 mL of resin previously equilibrated with B buffer and incubated under agitation for 1 h at 4 ˚C. After collecting the flow through fraction, the resin was washed five times with 10 mL of washing buffer pH 6.3 (8 M urea, 100 mM NaH_2PO_4, 100 mM Tris HCl pH 8.0) following elution of the recombinant protein with 600 µL of elution buffer pH 4.5 (8 M urea, 100 mM NaH_2PO_4, 100 mM Tris HCl pH 8.0) for seven times. Each elution wash was carried out for three minutes and the eluates were stored at 4 ˚C for further dialysis.

After purification, each elution sample was dialyzed for 12 h in dialysis buffer 1 (0.5 mM EDTA, 500 mM NaCl, 100 mM Tris HCl pH 8.5, 20 % glycerol, pH 8.5) following a new round of dialysis for 12 h in dialysis buffer 2 (0.5 mM EDTA, 500 mM NaCl, 100 mM Tris HCl pH 8.5, 40 % glycerol, pH 8.5). The dialyzed eluates were then quantified using the Bradford method (BRADFORD, 1976) and resolved by SDS-PAGE (item 2.5.4).

2.5.3 Generation of an anti-r*Tr*CIF1 polyclonal antiserum

To generate the anti-r*Tr*CIF1 polyclonal antiserum, pre-immune serum was collected from four mice prior to the first immunization. Each animal received four subcutaneous immunizations, ten days apart, containing 50 µg of the purified recombinant fragment (section 2.5.2) along Freund's incomplete adjuvant (v/v) (Sigma-Aldrich) on the first immunization and Alu-Gel S (1:5) (aluminum hydroxide 1,3 %) (Serva) on the following injections. Ten days after the fourth immunization, animals were deeply sedated with ketamine (100 mg/kg) and xylazine (10 mg/kg), and bleed by heart puncture. Total blood was centrifuged for 10 min at 2,000 x *g* for 5 min at 4 ºC for serum collection and storage at -20 ºC.

2.5.4 SDS-PAGE and Western blot

To verify protein expression by western blot, protein extracts from CIF1 purification steps (15 µL of each sample) and parasites (100 µg) were used. Protein extracts were resuspended in sample buffer for SDS-PAGE (20% glycerol, 0.5% bromophenol blue, 0.5 M Tris-HCl pH 6.8, 4.4 % SDS and 2 % 2-mercaptoethanol) and boiled for five minutes. Samples and protein ladder (Precision Plus Protein^{TM} Dual Color Standards, Bio-Rad) were resolved in 10 % or 12 % SDS-PAGE stained with Coomassie Blue for 12 h, under agitation, at room temperature.

The resolved proteins were transferred to nitrocellulose Hybond-ECL (GE Healthcare) membranes as described by Towbin et al. (1979). Transfer was confirmed by staining the membrane with Ponceau S 1 % in acetic acid 10 % for five minutes, and then counterstained with ultrapure water for five minutes at room temperature. The membrane was then blocked with blocking solution (5% nonfat milk, 150 mM NaCl, 25 mM Tris-HCl pH 7.4, 1 % Tween 20, 5 % NaCl, 25 mM Tris-HCl pH 7.4, 1 % Tween 20). Excess blocking solution was washed out by washing the membrane for five times of five minutes with blotting buffer (150 mM NaCl, 25 mM Tris-HCl pH 7.4, 1 % Tween 20, 5 % NaCl, 25 mM Tris-HCl pH 7.4, 1 % Tween 20).

Next, membrane was incubated with primary antibodies anti-r*Tr*CIF1, anti-r*Tr*FLA1BP, anti-r*Tc*FLA1BP, or anti-ß Tubulin (Table 1) diluted in blotting buffer with 2 % of nonfat milk for 90 min at room temperature. After washing five times with blotting buffer, the membrane was incubated with the secondary antibody anti-Mouse HRP or anti-Rabbit HRP (Table 2) for 60 min. The membrane was washed five times, incubated with the ECL reagent (Pierce) for five minutes and exposed to radiographic films at room temperature. The films were then developed using a SRX101A (Konica-Minolta) equipment and results were digitally recorded.

2.6.5 Immunofluorescence assays

To investigate the expression sites of CIF1 and FLA1BP in *T. rangeli and T. cruzi* epimastigotes and trypomastigotes, parasites were washed twice with PBS (pH 7.4) and deposited on glass slides and incubated for 20 min at room temperature for adhesion to the glass. For *T. cruzi* trypomastigotes, slides were previously treated with poly-lysine 0.1% (Sigma) for five minutes following manufacturer's instructions. After removing non-adherent

parasites, cells were fixed with 4 % paraformaldehyde in PBS (pH 7.4) for five minutes and washed three times with PBS (pH 7.4) for five minutes each wash. Parasites were then permeabilized with Triton X-100 (0.05 %) solution for five minutes, washed with PBS (pH 7.4) and slides were blocked overnight with blocking solution (5% non-fat milk in PBS (pH 7.4) at 4 ˚C.

Once blocked, slides were individually incubated with primary antibodies (anti-r*Tr*CIF1, anti-r*Tr*Fla1B, anti-r*Tc*Fla1BP, or anti-FCaBP) (Table 1) for one hour at room temperature. After washed with PBS (pH 7.4), slides were incubated with secondary antibodies (Alexa Fluor 488 or 594) (Table 1) for 15 min and then incubated with DAPI (1 mg/mL) for 5 min at room temperature. After washing three times with PBS (pH 7.4) and a final wash with ultra-pure water, slides were dried and covered with coverslips using Hydromount (National Diagnostics). Results were observed in Olympus – Bx40–FL (Olympus) fluorescent microscope or Leica DMI6000 B Microscope and the results were digitally recorded.

Table 1 – Antibodies used for detection of CIF1 and FLA1BP. MP = Mouse polyclonal. MM = Mouse monoclonal. GM = Goat monoclonal. RM = Rabbit monoclonal. WB = Western blot. IFA = Immunofluorescence assay.

Name	Antigen	Type	Dilution WB	Dilution IFA	Origin/Manufacturer
Anti-*Tr*CIF1	*Tr*CIF1	MP	1:100	1:20	This study
Anti-*Tr*FLA1BP	*Tr*FLA1BP	MP	1:100	1:20	DE LIZ, 2017
Anti-*Tc*FLA1BP	*Tc*FLA1BP	MP	1:100	1:20	DE LIZ, 2017
Anti-FCaBP	FCaBP	MM	NU	1:100	Dr. Sergio Schenkman, Unifesp, Brazil
Anti-ß Tubulin	ß Tubulin	MP	1:2,000	NU	Cell Signalling
Anti-His Tag	6X His Tag	MM	1:2,000	NU	Thermo Fisher Scientific
Anti-Mouse HRP	Mouse IgG	GM	1:5,000	NU	Invitrogen
Anti-Rabbit HRP	Rabbit IgG	GM	1:20,000	NU	Santa Cruz Biotechnology
Anti-Mouse Alexa 488	Mouse IgG	GM	NU	1:1,000	Invitrogen
Anti-Mouse Alexa 594	Mouse IgG	RM	NU	1:1,000	Invitrogen

2.6 Evaluation of *Tr*CIF1 transcription levels

2.6.1 Primers design

To evaluate the *Tr*CIF1 transcription levels, specific primers *Tr*CIF1_qPCR_F: 5′ - CCG GAG CGT GAA GGA GTC - 3′ and *Tr*CIF1_qPCR_R: 5′ - TCG CGC TT G AAT GTA GAC TG - 3′ were designed using the DNASTAR software. In order to validate the specificity of the primers, a PCR was performed with 20 ng of genomic DNA from *T. rangeli*,

0.8 pmol of *Tr*CIF1_qPCR_F and *Tr*CIF1_qPCR_R, and 1 U of GoTaq DNA polymerase (Promega). The reaction was performed with a first step at 95 ºC for 5 min, 35 cycles of 1 min at 95 ºC, 1 min at 58 ºC and 1 min at 72 ºC, and a final step of 10 min at 72 ºC. The identity of the fragment was confirmed by sequencing and polyacrylamide gel 8% stained with ethidium bromide.

2.6.2 qPCR

2.6.2.1 RNA extraction

A total of 1 X 10^8 epimastigotes, trypomastigotes, and synchronized parasites (item 2.4.1), washed two times with PBS (pH 7.4) and stored in -80 ˚C, were used to extract total RNA was performed with Trizol. Samples were incubated for five minutes at room temperature after adding 200 µL of chloroform and mixing for 15 s. Samples were harvested by centrifugation at 12.000 x *g* for 15 min at 4 ˚C and top layer, containing RNA, was separated into a new tube. Isopropanol was added to reach 60 % of total sample volume and samples were harvested for 20 min. Supernatant was discarded and after washing pellet for five minutes with cold ethanol 75 %, RNA was eluted in water RNA-free. After extraction, RNA was kept at -80 ˚C, quantified and evaluated for their integrity in spectrophotometer and agarose gel stained with ethidium bromide (1 µg/mL).

2.6.2.2 cDNA generation

1 µg of extracted RNA from each sample was treated with DNase I (Thermo Scientific) for DNA contaminants elimination. After DNase inactivation, samples were incubated with OligodT-Anchor and incubated at 70 ˚C for five minutes. Then, samples were used to generate cDNA with MM-MLV (Invitrogen, Carlsbad) following kit procedures.

2.6.2.3 Quantitative polymerase chain reaction (qPCR)

cDNA was diluted eight times to be used for qPCR with *Maxima SYBR Green/ROX qPCR Master Mix* (Thermo Scientific). Primers targeting a fragment from CIF1 (item 2.6.1) and reference genes GAPDH, RN60S and HGPRT were used and qPCR was performed and analyzed as described by Prestes et al., where raw quantification cycle results were normalized to an average value obtained for two reference genes and used to obtain relative quantification of transcription levels (PRESTES et al., 2019).

2.7 DATA ANALYSIS

Statistical analysis was performed using the Prism 6.0 Software (GraphPad) that also generated the graphs. To compare two samples, unpaired Student`s *t*-test was used, while comparisons between more than two samples were carried out with one-way ANOVA. *p* values < 0.01 were considered statistically significant.

2.8 DELETION OF ENDOGENOUS GENES

To investigate CIF1 and FLA1BP function conservation in *T. rangeli*, endogenous genes were deleted using CRISPR Cas9 deletion. Protocol developed by Costa et al. (2018) and adapted to *T. rangeli* by Carime Lessa Mansur Pontes MSc (unpublished data) was followed, in which epimastigotes from *T. rangeli* were transfected with transcription templates for sgRNAs (containing T7 polymerase promoter), donor sequences containing resistance genes for antibiotics blasticidin and puromycin (flanked by homology arms) and pLEWCas9 plasmid. If successful, endogenous genes should be replaced by resistance genes for blasticidin and puromycin (Figure 9).

Figure 9 – Schematic representation of CRISPR-Cas9 strategy adopted to delete CIF1 and FLA1BP from *Trypanosoma rangeli* genome. Scissors and dashed lines indicate sgRNA targets. Grey = 30 nt homology arm.

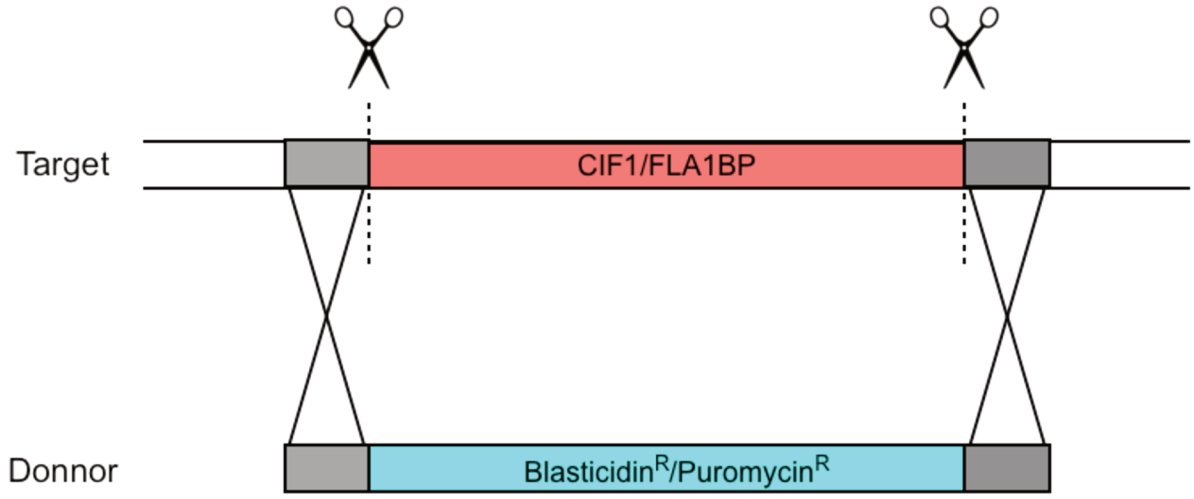

Identification of targets for sgRNAs and donor sequences as well as primers design were carried out using the Eukaryotic Pathogen CRISPR guide RNA/DNA Design Tool (http://grna.ctegd.uga.edu) software. PCR primers used for amplification of sgRNA template

and donor sequences are shown in Table 2, and reactions were carried out as proposed by Costa et al. (2018).

Next, 10^7 cells were transfected with amplification products, 400 ng/µL of pLEWCas9, and 200 µL of Tb-BSF buffer using program X-014 on a Nucleofector (Lonza). After transfection, parasites were transferred to 5 mL NNN-LIT and incubated at 27 ˚C. 24 h later, blasticidin (0.2 µg/mL) and puromycin (0.166 µg/mL) were added. Drug concentration was weekly increased up to 4 µg/mL of blasticidin and 2 µg/mL of puromycin.

Table 2 – Primers used for deletion of *Trypanosoma rangeli* CIF1 and FLA1BP genes.

Name	Sequence
*Tr*CIF1_Up Fw	ggcgtgtcgattgggcttggcgttgcctgggtataatgcagacctgctgc
*Tr*CIF1_5sgRNA	gaaattaatacgactcactataggacgtcgctgtcagtggacatggggttttagagctagaaatagc
*Tr*CIF1_Down Rev	tctaactctcgtaagatcacttattcgcgcccaatttgagagacctgtgc
*Tr*CIF1_3sgRNA	gaaattaatacgactcactataggaatgtagactgccacggcgacgggttttagagctagaaatagc
*Tr*Fla1BP_Up Fw	tttgcctctttctttttccttctctctgtggtataatgcagacctgctgc
*Tr*Fla1BP_5sgRNA	gaaattaatacgactcactataggggaggctgaacggatagggagggttttagagctagaaatagc
*Tr*Fla1BP_Down Rev	cggtgggaatgacctcttttgtcctcgttcccaatttgagagacctgtgc
*Tr*Fla1BP_3sgRNA	gaaattaatacgactcactataggaacctgccctccccatgcagcgggttttagagctagaaatagc

Finally, to confirm the replacement of endogenous genes by resistance genes, genomic DNA was extracted from parasites after drug selection and used to perform semi-quantiative PCR using specific primers for each endogenous gene. Reactions were performed using 50 ng of total DNA, 10 pmol of each primer, 100 µM dNTP and 1 U of GoTaq DNA polymersase. The amplification was performed with a first denaturing step of 3 min at 94 ˚C, followed by 20 cycles of denaturing (92 ˚C for 30 s), primers annealing (60 ˚C for 30 s) and DNA elongation (72 ˚C for 1-3 min).

2.9 MASS SPECTROMETRY

To confirm the identity of the *Tr*CIF1_frag, protein bands visualized by SDS-PAGE, the gel band was excised from gel and incubated for 30 min at 37 ˚C with destaining solution I (50 % methanol, 5 % acetic acid) following by incubation with destaining solution II (50 % acetonitrile, 5 mM NH_4HCO_3) for 30 min at 37 ˚C. Samples were then dehydrated by addition of 200 µL of acetonitrile following treatment with 10 mM dithiothreitol (DTT) for 1 h at 60 ˚C. After DTT removal, samples were incubated with iodoacetamide (IAA) for 30 min at room

temperature, following incubation with destaining solution II for 15 min at 37 ˚C and a new dehydration step with acetonitrile under the same conditions. Proteins were digested with 2 μg of trypsin (Promega) with digestion buffer (50 mM AmBic, 1 mM calcium chloride, pH 8.5) overnight at 37 ˚C. After sonication (40 kHz) for 5 min at room temperature, the protein-containing solution was transferred to a new tube. A further protein extraction step was then carried out with the excised gel by treatment for 1 h at 37 ˚C with 50 % acetonitrile/5 % trifluoroacetic acid. The extracted proteins were then dehydrated by vacuum centrifugation (SpeedVac, Eppendorf) and stored at -80 ˚C.

Mass spectrometry was performed at the Centers for Disease Control and Prevention (CDC) using a LC-ESI-MS/MS platform as described by Wagner et al. (2013). Raw data was processed with software MASCOT Distiller® (Matrix Science) and the identity of samples was obtained by comparison to the *T. rangeli* genome. To validate identified proteins, Scaffold software was used. Proteins having at least two peptides, with False Discovery Rate up to 1 %, and with probability of correct identification up to 95 %, were considered.

3 CHAPTER ONE: CIF1 AND CELL DIVISION OF *TRYPANOSOMA RANGELI*

3.1 RESULTS

3.1.1 Analysis of CIF1 from *Trypanosoma rangeli* and other trypanosomatids

Search for *Tb*CIF1 (Tb927.11.15800) orthologs in *T. rangeli* by *tBLASTn* revealed a single predicted protein of 643 aa (~69 kDa), which was 28.19% identical to *Tb*CIF1. Comparison of the genomic organization of *Tr*CIF1 and *Tb*CIF1 revealed that these genes are within a conserved syntenic block in these parasites genomes as shown on figure 10 (Table 3 & 4).

Figure 10 - Schematic representation of the CIF gene synteny between *Trypanosoma brucei* and *Trypanosoma rangeli*. Illustration of a fragment of chromosome 11 (from position 4,168,958 to 4,199,941) of *T. brucei*. Box numbers represent genes from *T. brucei* (Table 3) and *T. rangeli* (Table 4) genomes. The size of each box is proportional to real gene length. Dashed lines indicate orthologous genes between both species. CIF1 gene is highlighted in blue.

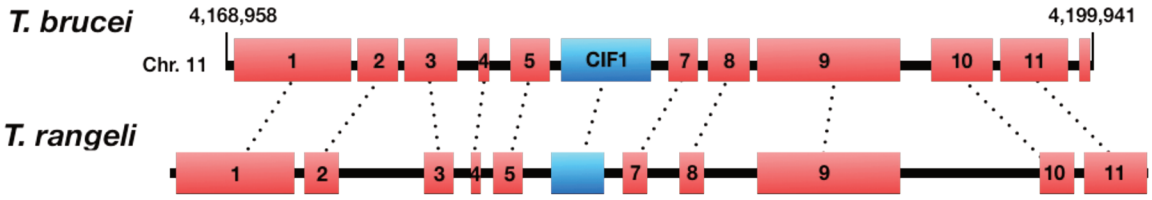

Table 3 – List of genes upstream and downstream CIF1 from *Trypanosoma brucei*. N° = Gene position within *T. brucei* chromosome fragment representation (Figure 10).

N°	Gene ID (Tritrypdb 4.2)	Name	Nº aa
1	Tb927.11.15750	AMP deaminase	1417
2	Tb927.11.15760	GPI transamidase subunit Tta1	377
3	Tb927.11.15770	Hypothetical protein	357
4	Tb927.11.15780	Hypothetical protein	98
5	Tb927.11.15790	Hypothetical protein	398
6	Tb927.11.15800	CIF1	793
7	Tb927.11.15810	NDUFB9	304
8	Tb927.11.15820	SODC	309
9	Tb927.11.15830	RNA methyltransferase, putative	1716
10	Tb927.11.15840	L-Lysine transport protein, putative	462
11	Tb927.11.15850	Kinteoplast poly(A) polymerase complex 1 subunit	754

Table 4 – List of genes upstream and downstream CIF1 from *Trypanosoma rangeli*. N° = Gene position within *T. rangeli* scaffold fragment representation (Figure 10).

N°	*T. brucei* ortholog (Tritrypdb 4.2)	Nº aa	Scaffold	Starting position	Ending position
1	Tb927.11.15750	1432	1	6084268	6088563
2	Tb927.11.15760	387	1	6088899	6090059

3	Tb927.11.15770	350	1	6093205	6094254
4	Tb927.11.15780	108	1	6094883	6095206
5	Tb927.11.15790	308	1	6095727	6096650
6	Tb927.11.15800	639	1	6097748	6099664
7	Tb927.11.15810	296	1	6100297	6101184
8	Tb927.11.15820	303	1	6102302	6103210
9	Tb927.11.15830	1718	1	6105084	6110237
10	Tb927.11.15840	437	1	6115191	6116501
11	Tb927.11.15850	755	1	6116812	6119076

According to the literature, *Tb*CIF1 protein contains the following domains: N-terminal domain (NTD, residues 1-121), coiled-coil domain (CC, residues 121-271), intrinsic-disordered domain (IDR, residues 271-667) and the zinc-finger domain (ZF, residues 667-804) (HU et al., 2019). Along with the size and sequence differences observed, the domain predictors used in our study pointed-out a reduced conservation of the *Tb*CIF1 domains in *Tr*CIF1, as we were unable to identify the zinc-finger and the CC domains in *Tr*CIF1 despite the sequence conservation (Figure 11).

Figure 11 - Schematic representation of *Tb*CIF1 regions and identity of each correspondent *Tr*CIF1 domain. NTD = N-terminal domain. CC = Coiled coil. IDR = Intrinsic disordered region. ZnF1&2 = Zinc-finger motif 1 and 2.

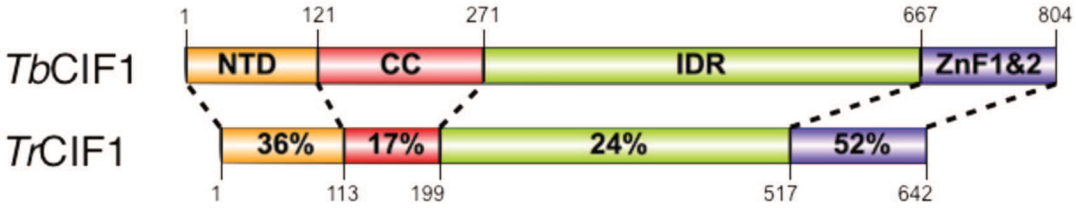

This observation was further confirmed by using coiled-coil predictors that were also unable to detect a coiled-coil domain in *Tr*CIF1 (Figure 12).

Figure 12 - Coiled-coil prediction of CIF1 from *Trypanosoma brucei* and *Trypanosoma rangeli*. Prediction of COILS program for coiled-coils conformation in *Tb*CIF1 (A) and *Tr*CIF1 (B). Y axis = Probability of coiled coil. X axis = Amino acidic residue position.

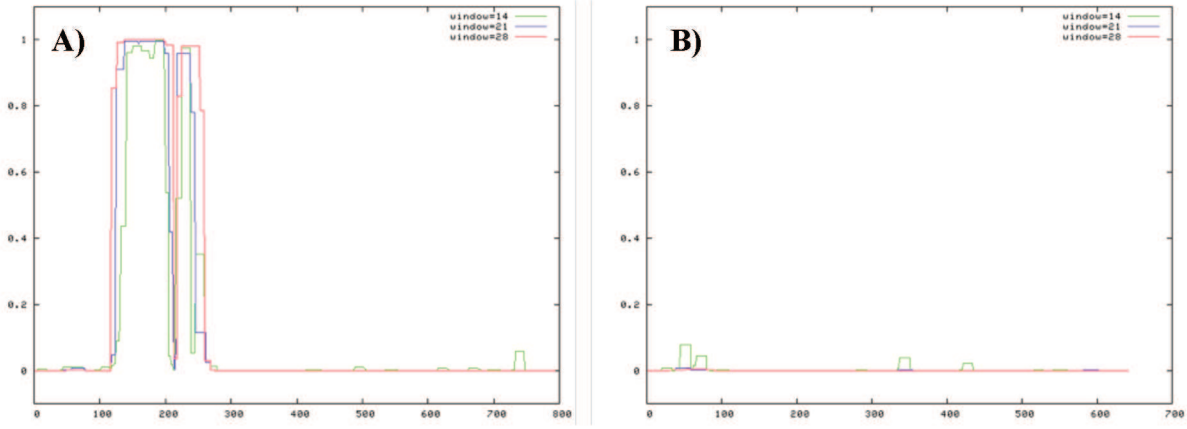

It has been reported that *Tb*CIF1 is phosphorylated at both the NTD and IDR domains, a post-translational modification required for CIF1 involvement in several biological processes (ZHOU et al., 2018). We thus performed a comparative search for potential phosphorylation sites in *Tr*CIF1 and *Tb*CIF1. Our results indicate that while *Tr*CIF1 contains less phosphorylation sites at the NTD and IDR regions when compared to *Tb*CIF1 (Figure 13, Table 5), threonine residues at the *Tb*CIF1zinc-finger region required for phosphorylation are almost absent in *Tr*CIF1.

Figure 13 – Predicted phosphorylation sites on *Trypanosoma brucei* and *Trypanosoma rangeli* CIF1. Prediction of phosphorylated sites in *Tb*CIF1 (A) and *Tr*CIF1 (B).

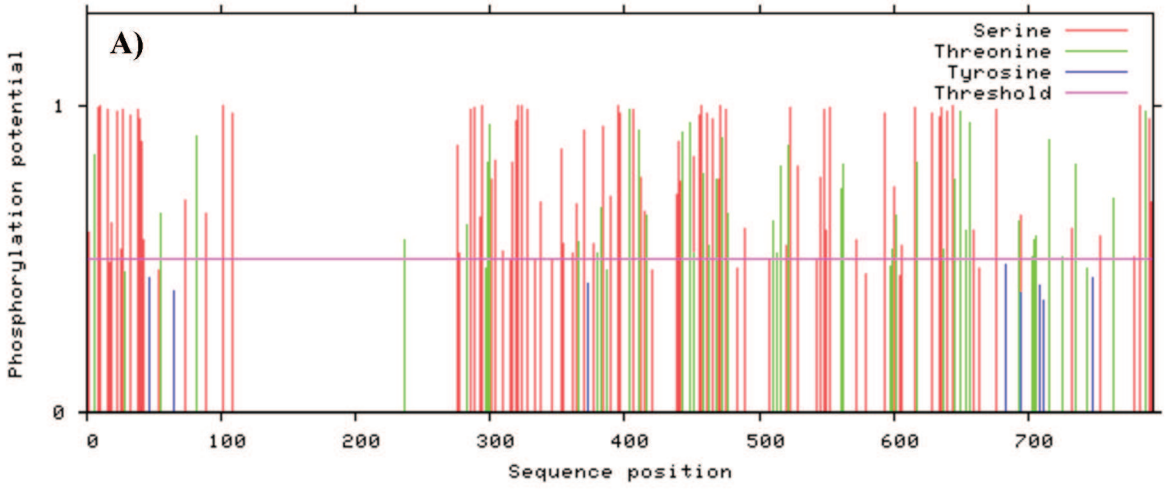

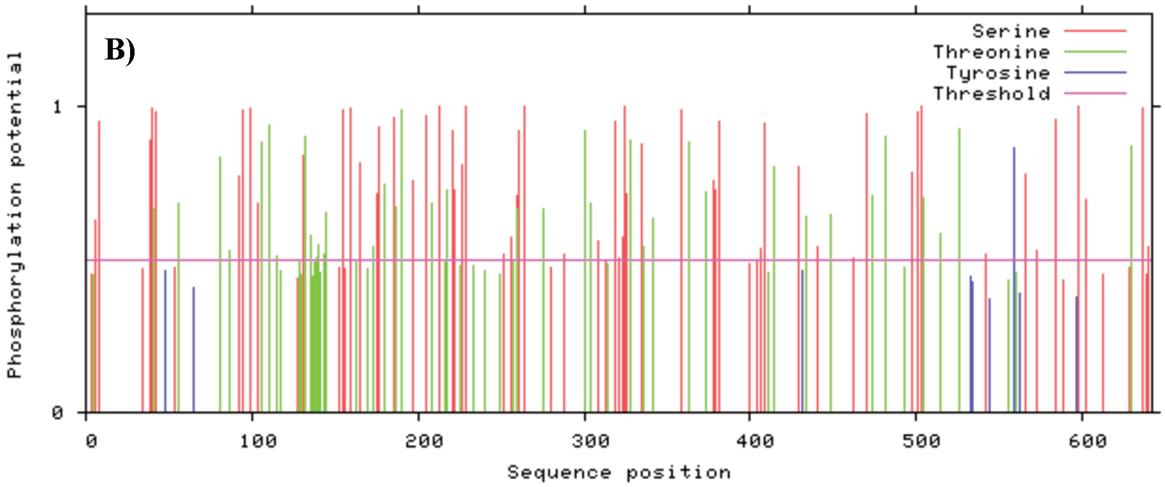

Table 5 – Predicted phosphorylated amino acid residues on *Trypanosoma brucei* and *Trypanosoma rangeli* CIF1. NTD = N-terminal domain. CC = Coiled coil. IDR = Intrinsic disordered region. ZnF = Zinc-finger motif 1 and 2.

Region	Residue	*Tb*CIF1	*Tr*CIF1
NTD	Serine	17	9
	Threonine	3	6
	Tyrosine	0	0
CC	Serine	0	8
	Threonine	1	11
	Tyrosine	0	0
IDR	Serine	66	32
	Threonine	31	19
	Tyrosine	0	0
ZnF	Serine	10	8
	Threonine	10	2
	Tyrosine	0	1

3.1.2 Analysis of CIF1-interacting proteins from *Trypanosoma rangeli* and other trypanosomatids

To compare the evolutionary divergence of genes coding for CIF1 and CIF1-interacting proteins among trypanosomatids, including monoxenic and heteroxenic species, CIF1 and CIF1-interacting proteins sequences described for *T. brucei* (Supplementary material A) were used as queries for searching for orthologous genes in different taxa. Using the *T. brucei* genes in *tBLASTn* analyzes, (i) sequence identities, (ii) predicted protein sizes, and (iii) the presence and conservation of canonical domains were assessed for orthologous genes (Table 6).

Table 6 – Comparison of the conservancy of CIF1 and CIF1-interacting proteins between *Trypanosoma brucei* and other trypanosomatids. Green = Conserved ortholog, with conserved domain and identity over 25% or identity over 50% and lacking conserved domains. Yellow = Conserved function is not clear and ortholog may have lost its function, with identity between 40-20 % and lacking conserved domain, or identity between 20-25% and conserving domains. Red = Absent genes or lacking conservation (above 20% identity). * = Sequences with variability in the number of coiled coils. ** = Sequences highly conserved, but lacking tropomyosin domain. ? = Division within mammal host is unknown.

Habit	Host	Division site within host	Species	CIF1 and CIF1-interacting proteins									
			Trypanosoma brucei	**CIF1**	**CIF2**	**CIF3**	**CIF4**	**FAZ20**	**KPP1**	**KAT80**	**KLIF**	**FRW1**	**FPRC**
Heteroxenic	**Insect/Mammal**	**Extracellular**	*Trypanosoma vivax*									*	*
			Trypanosoma evansi									*	
		?	*Trypanosoma rangeli*									*	*
		Intracelullar	*Trypanosoma cruzi marinkellei*								**	*	*
			Leishmania braziliensis									*	*
			Leishmania major									*	*
			Leishmania infantum									*	
			Endotrypanum monterogeii									*	*
	Insect/Reptile	**Intracelullar**	*Leishmania tarentolae*								**	*	*
		Extracellular	*Trypanosoma grayi*			*					**	*	
	Insect/Plant	**Extracellular**	*Phytomonas sp.*										*
Monoxenic	**Insect**		*Blechomonas ayalai*									*	*
			Crithidia fasciculata									*	*
			Leptomonas seymouri									*	*
			Paratrypanosoma confusum									*	*
Free-living			*Bodo saltans*										

While *T. evansi* has all CIF1 and CIF1-interacting proteins conserved when compared to *T. brucei*, the zinc-finger domain is absent in all CIF1 genes from the analyzed trypanosomatids as found for *Tr*CIF1. Also, the majority of the analyzed species also had CIF1 sequences lacking one or both coiled-coil domains. In our analysis, no CIF1 or CIF1-related genes orthologs were observed in the *B. saltans* and *P. confusum* genomes.

Other CIF1 or CIF1-related proteins also had distinct variability in their domains, yet were conserved overall like FRW1, FPRC and CIF3 that had a variable number of coiled-coils among species. Despite the high identity of KLIF between *T. cruzi*, *T. grayi* and *L. tarentolae* (> 50.01%) in comparison to *Tb*KLIF, the tropomyosin-like domain of KLIF was not identified. In addition, in several species such as *T. vivax*, *T. rangeli*, *L. infatum*, *C. fasciculata*, *P. confusum*, *B. saltans* and *B. ayalai*, although having identities ranging between 37-50% when compared to *Tb*KLIF, the tropomyosin-like domain was not found.

CIF3 is conserved exclusively in the genus *Trypanosoma* and except for *T. grayi*, all analyzed species from this genus had two coiled coils coding sequences predicted in their CIF3 gene, as observed in *Tb*CIF3.

3.1.3 Generation of anti-r*Tr*CIF1 polyclonal antiserum

In order to assess the expression levels and the possible cytolocalization of the *T. rangeli* CIF1 (*Tr*CIF1), a fragment of the protein was chosen to be heterologously expressed. Avoiding sequences with highly hydrophobic regions and presenting rare codons, a fragment of 112 aa corresponding to the C-terminus fragment was chosen, resulting in a predicted protein of ~12 kDa. The fragment named *Tr*CIF1_frag was then PCR amplified from the *T. rangeli* genome and sub-cloned onto pET14b expression vectors for the purification of the recombinant protein.

Although confirmation of the cloning by DNA sequencing, transformed bacteria failed to growth to a cell density that allows protein purification. Several strategies to increase the expression of the r*Tr*CIF1_frag such as addition of glucose or the use of disfferent bacterial strains as Rosetta-gami (DE3) pLysS were performed that allowed bacteria to grow before heterologous expression induction. Therefore, bacteria were grown in medium supplemented with glucose and then transferred to a glucose-free medium to induce sufficient levels of heterologous expression prior to purification (Figure 14).

Figure 14 - Purification of the recombinant fragment of *Tr*CIF1. Western blot (A) and equivalent denaturant polyacrylamide gel (B) analyses of the purification steps of *Tr*CIF1_frag expressed in the bacteria Rosetta-gami (DE3) pLysS. SDS-PAGE 12% was stained with Coomassie Blue and the western blot was performed with anti-His tag antibody. S = Supernatant. FT = Flow Through.

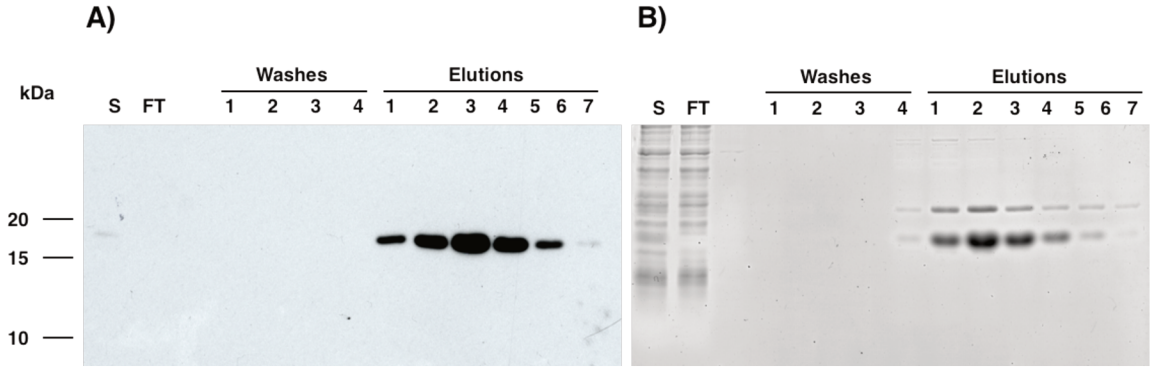

Along with the expected band of ~12 kDa, a second protein band of ~20 kDa was co-purified as shown on figure 14B, which was not recognized by the anti-His tag antibody (Figure 14A). Interestingly, both protein bands observed on figure 14B corresponded to CIF1 from *T. rangeli* as revealed by mass spectrometry analysis.

Elutions were then combined and used to generate an anti-r*Tr*CIF1_frag polyclonal antiserum in mice as described. The serum obtained from all immunized mice recognized the two protein bands of the purified fragment of r*Tr*CIF1 (Figure 15A).

However, western blot using total protein extracts from *T. rangeli* epimastigotes and the anti-r*Tr*CIF1_frag polyclonal antiserum showed distinct results (Figure 15B). While serum from mice #1, 2 and 4 have revealed a faint recognition of proteins over 250 kDa, serum from mouse #3 recognized a band of ~70 kDa that we considered to be CIF1, but also recognized other further proteins of high molecular weight (Figure 15B). All recognized bands were excised and sent of MS analysis and serum from mouse #3 was then used for downstream experiments.

Figure 15 – Evaluation of serum anti-r*Tr*CIF1. Western blot showing the recognition of purified recombinant *Tr*CIF1_frag (A) and *Tr*CIF1 in *T. rangeli* epimastigotes total proteins (B). Western blot performed with serum anti-r*Tr*CIF1 produced in mice.

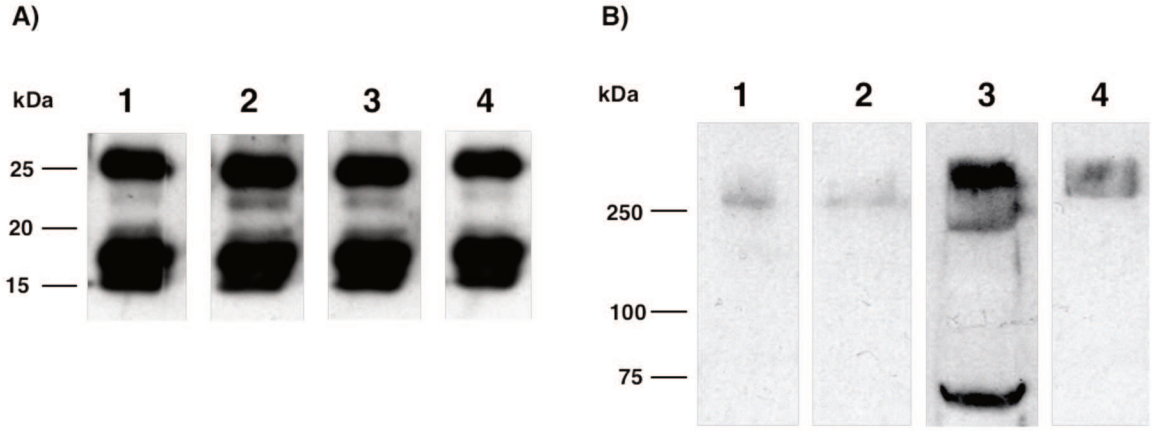

3.1.4 Analysis of CIF1 transcription, expression and localization in *Trypanosoma rangeli*

Aiming to characterize the *T. rangeli* CIF1, assessment of protein localization and levels of transcription and expression were carried out using culture-derived epimastigotes and *in vitro* differentiated trypomastigotes.

3.1.4.1 Transcription of CIF1 in Trypanosoma rangeli

Specific primers (*Tr*CIF1_qPCR_F and *Tr*CIF1_qPCR_R) were designed to investigate the *Tr*CIF1transcription levels by qPCR. Primers were initially used on a regular PCR assay to amplify the target sequence from the parasite genomic DNA, resulting in the single-specific amplification of a fragment of the expected size (Figure 16) whose identity was confirmed by DNA sequencing (data not shown).

Figure 16 – Amplification of a fragment of CIF1 from *Trypanosoma rangeli*. Electrophoresis in polyacrylamide gel 8% stained with ethidium bromide, showing the amplification product of a fragment of *Tr*CIF1 chosen for qPCR analysis (1). NC = PCR negative control (no DNA added).

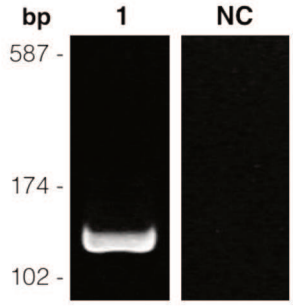

The primers were then validated for qPCR using serial dilutions of cDNA mixtures from epimastigotes and trypomastigotes, resulting in an efficiency mean of 100.92 %. As reference genes we used GAPDH, RNA 60S and HGPRT as reported previously (PRESTES, 2019).

T. rangeli mRNA obtained from biological triplicates was then assayed by qPCR targeting the CIF1 transcripts, revealing that *Tr*CIF1 is more transcribed by the *in vitro*-derived trypomastigotes (2.72 times) than epimastigotes (Figure 17).

Figure 17 – Transcription of CIF1 by *Trypanosoma rangeli* epimastigotes and trypomastigotes. Levels of CIF1 mRNA in epimastigotes (Epi) and trypomastigotes (Trypo). Unpaired Student's t-test was used for statistical analysis: * = $p < 0.01$. Relative quantification scores were obtained using the reference genes GAPDH and HGPRT. RQ = Relative Quantification by qPCR.

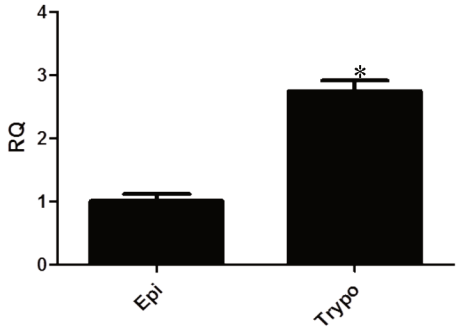

3.1.4.2 Expression of CIF1 in Trypanosoma rangeli

The anti-r*Tr*CIF1 serum obtained as reported above was used to investigate the *Tr*CIF1 protein expression in *T. rangeli* epimastigotes and trypomastigotes. Results of the Western blot assays showed that, although higher in trypomastigotes, no significant difference was observed for *Tr*CIF1 expression between *T. rangeli* forms (Figure 18).

Figure 18 – Expression of CIF1 by *Trypanosoma rangeli* epimastigotes and trypomastigotes. (A) Western blot revealing detection of *Tr*CIF1 (upper protein band) and tubulin (lower band) between trypomastigotes (Trypo) and epimastigotes (Epi). (B) Relative density optic quantification of *Tr*CIF1 expression, normalized with tubulin expression.

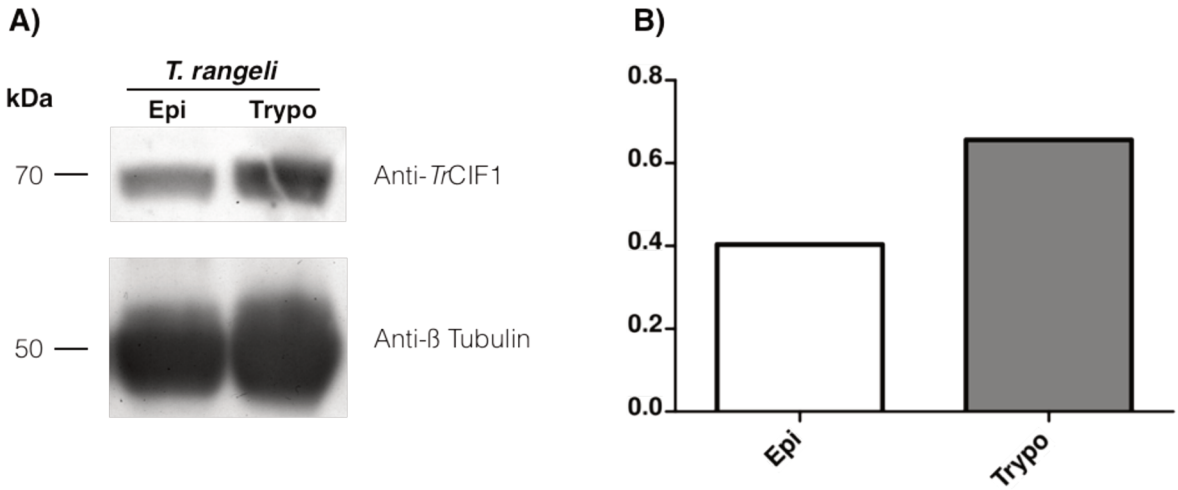

The specificity of the anti-r*Tr*CIF1 antiserum was tested using total *T. cruzi*, *T. brucei* and *L. infantum* protein extracts in western blot assays. While no recognition was observed for *L. infantum*, recognition of a ~70 kDa protein was observed for both *T. cruzi* and *T. brucei* extracts, which was stronger and unique for *T. brucei* and fainter for *T. cruzi*, where an additional band of smaller size was also observed (Figure 19). The *T. cruzi* and *T. brucei* protein bands recognized by the anti-r*Tr*CIF1 antiserum were also excised and sent for MS analysis.

Figure 19 – Recognition of CIF1 in *Trypanosoma cruzi*, *Trypanosoma brucei* and *Leishmania infantum* by anti-r*Tr*CIF1 antiserum. Western blot revealing detection by anti-*Tr*CIF1 serum (upper protein band) and tubulin by anti-ß Tubulin monoclonal antibody (lower band).

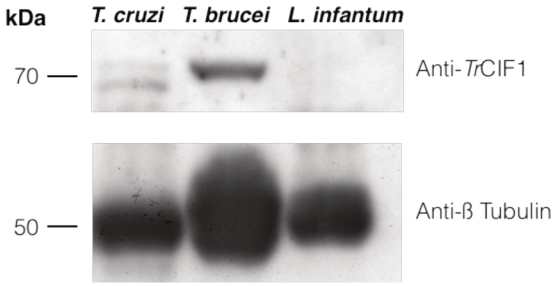

3.1.4.3 Localization of CIF1 in Trypanosoma rangeli

Cytolocalization assays of CIF1 in *T. rangeli* epimastigotes and trypomastigotes using the anti-r*Tr*CIF1 antiserum revealed interesting results (Figure 20). While epimastigotes

showed an irregular, diffuse and cytoplasmic-distributed labelling with a stronger labelling close to the flagellar pocket, *T. rangeli* trypomastigotes presented a clear and stronger labelling of the flagellar pocket and the entire flagellum, showing some CIF1 concentration at the flagellar tip.

Figure 20 – CIF1 localization in *Trypanosoma rangeli* epimastigotes and trypomastigotes. Immunofluorescence assay *revealing TrCIF1 localization in* epimastigotes and trypomastigotes. Detection of anti-*Tr*CIF1 antibodies by Alexa Fluor 488-labeled conjugate and detection of anti-FCaBP antibodies by Alexa Fluor 594-labeled conjugate. Bar - 10 µm.

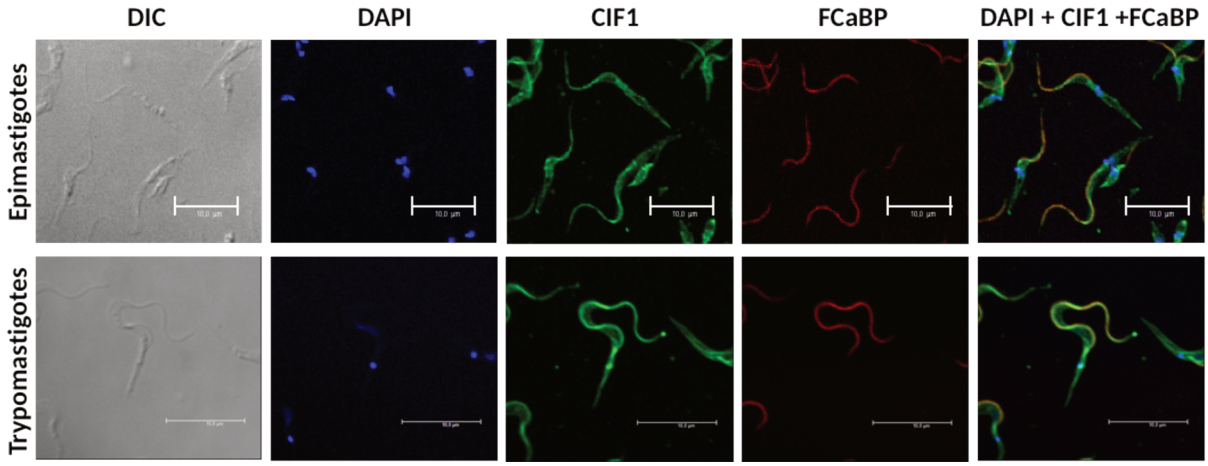

3.1.5 Impact of cell cycle in CIF1 transcription and expression

3.1.5.1 Cell cycle synchronization

To investigate *Tr*CIF1 transcription and expression during cell cycle, parasites were treated with HU to synchronize their cell cycle (Figure 21). After treating the cell culture for 24 h, an increase of parasites in G1 was observed. However, after 5 h of HU removal, the number of synchronized parasites in S phase increased. Later, the majority of parasites reached G2/M at 10 h, but the cell cycle did not return to normal proportions at times 15 h and 20 h, thus part of the population failed to complete cell cycle synchronously.

Figure 21 – Cell cycle progression in *Trypanosoma rangeli* treated with hydroxyurea. A) Histogram representing number of cells (Y axis) in relation to DNA content (X axis) in different times after the release of hydroxyurea from medium. I, II and III represent three replicates. Hydroxyurea was not added to controls. Blue = G1 phase. Green = S phase. Red = G2/M phase. GS = Gating strategy.

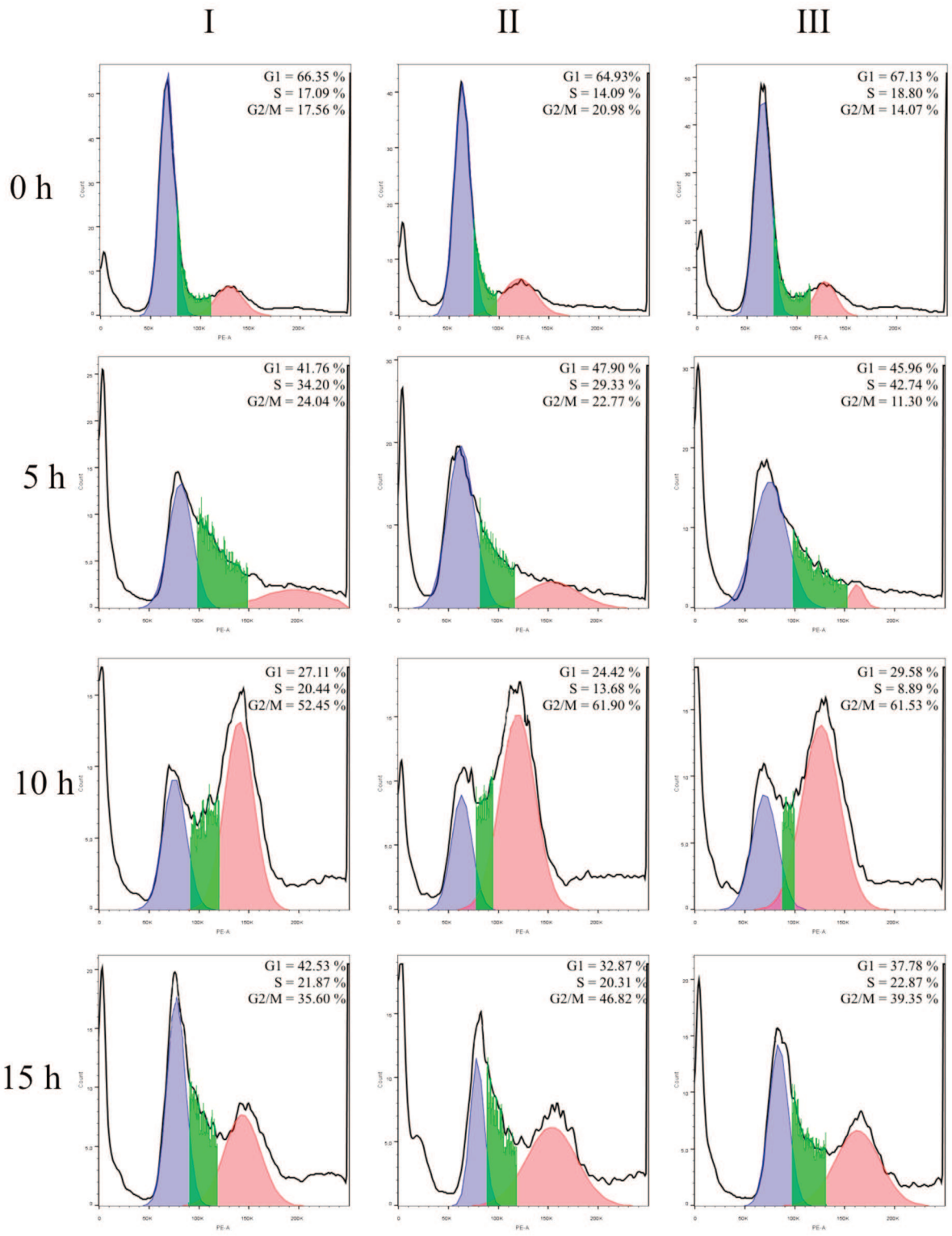

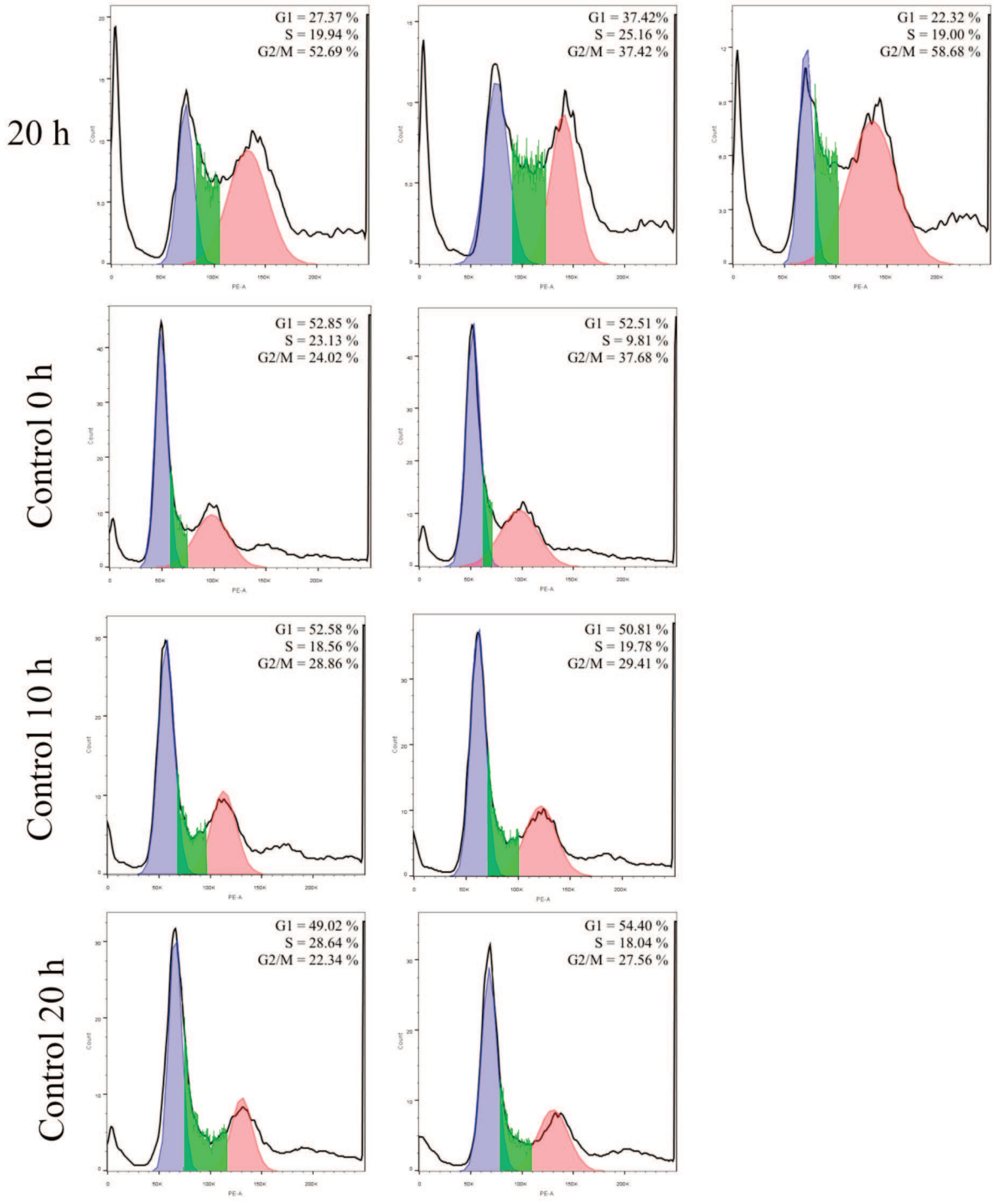
20 h
G1 = 27.37 %
S = 19.94 %
G2/M = 52.69 %
G1 = 37.42%
S = 25.16 %
G2/M = 37.42 %
G1 = 22.32 %
S = 19.00 %
G2/M = 58.68 %
Control 0 h
G1 = 52.85 %
S = 23.13 %
G2/M = 24.02 %
G1 = 52.51 %
S = 9.81 %
G2/M = 37.68 %
Control 10 h
G1 = 52.58 %
S = 18.56 %
G2/M = 28.86 %
G1 = 50.81 %
S = 19.78 %
G2/M = 29.41 %
Control 20 h
G1 = 49.02 %
S = 28.64 %
G2/M = 22.34 %
G1 = 54.40 %
S = 18.04 %
G2/M = 27.56 %

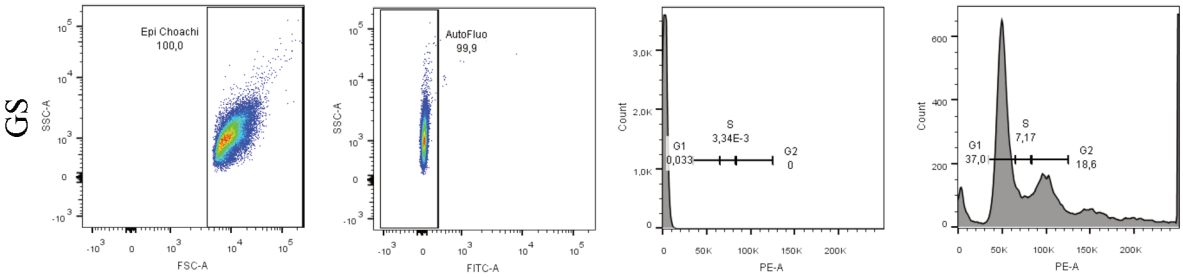

3.1.5.2 TrCIF1 transcription and expression in synchronized parasites

Likely due to the incomplete synchronization process, with parasites from each of the cell cycle phases observed, analysis of the mRNA levels of *Tr*CIF1 did not significantly differ overtime during the *T. rangeli* cell cycle among synchronized parasites, although higher transcription was observed on the G2/M phase (10 h) (Figure 22). Since trypanosomes possess post-transcriptional and post-translational regulation of gene expression, the expression of *Tr*CIF1 was assessed at the same timepoints and revealed no significant differences in protein expression during the parasite cell cycle (Figure 23).

Figure 22 – Transcription levels of CIF1 during the *Trypanosoma rangeli* cell cycle *in vitro*. Levels of *Tr*CIF1 mRNA after the removal of hydroxyurea from epimastigotes culture. Relative quantification scores were obtained using the reference genes GAPDH and RNA60S. RQ = Relative Quantification by qPCR.

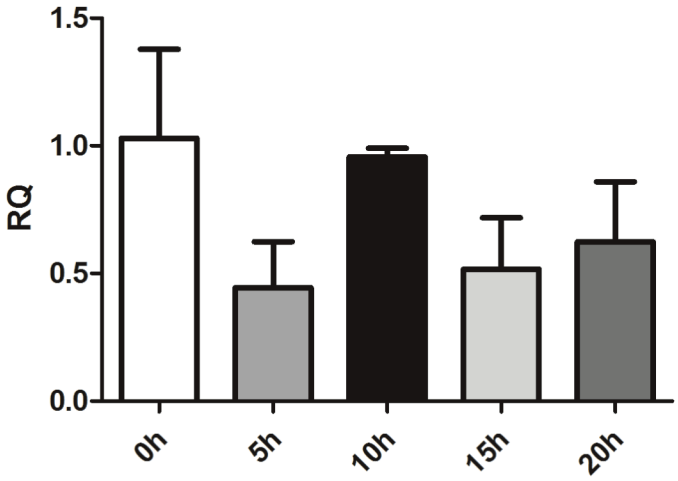

Figure 23 – Expression levels of CIF1 by *Trypanosoma rangeli* epimastigotes during the *in vitro* cell cycle. (A) Relative density optic quantification of *Tr*CIF1 expression (Y axis), normalized with tubulin expression, from *T. rangeli* culture of different times after release of HU from medium (X axis). Results represent triplicated experiments. (B) *Western blot* revealing detection of *Tr*CIF1 by anti-*Tr*CIF1

serum (upper protein band) and tubulin by anti-ß Tubulin monoclonal antibody (lower band).

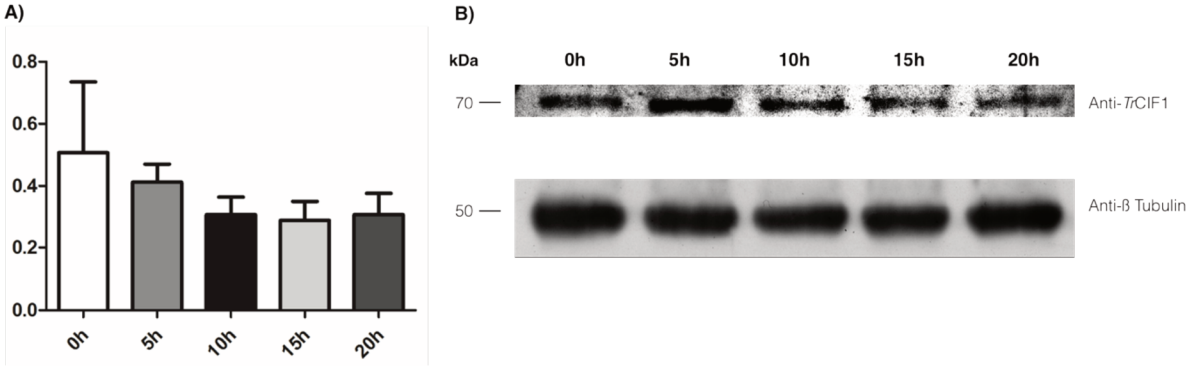

3.1.6 Analysis of CIF1 deletion from *Trypanosoma rangeli*

To investigate the effects of CIF1 gene deletion on *T. rangeli* we used CRISPR-Cas9 technology to replace both alleles of *Tr*CIF1 with resistance genes for blasticidin and puromycin. After transfection and selection with the addition of up to 4 µg/mL of blasticidin and 2 µg/mL of puromycin, parasites continued to multiply *in vitro* when compared to non-transfected control parasites and did not show any detectable morphological abnormalities.

*Tr*CIF1 deletion on selected parasites will be further assessed by PCR using *Tr*CIF1-specific primers for CIF1 to determine if the gene deletion was successful. In addition, transcription and expression levels of CIF1 will be analyzed by qPCR and western blot, respectively. Finally, the ability to perform cytokinesis will be addressed by comparing selected and wild type parasites growth curves.

3.2 DISCUSSION

3.2.1 Analysis of CIF1 and CIF1-interacting proteins from *Trypanosoma rangeli* and other trypanosomatids

Orthologous genes usually maintain a conserved function across closely related taxa, but such a statement is not necessarily true. Orthologous genes are two genes that have evolved from a speciation event. Therefore, orthologous genes in two given species have a common ancestral gene that remained conserved in their genomes after speciation. Duplication events of single genes or multiple genes might occur during evolution, leading to paralogous genes, i.e., duplicate copies of the same gene in a given genome. Duplication events allow the diversification of the duplicated gene, which can ultimately lead to different function, however, paralogous genes can also maintain the same function (JENSEN, 2018; TEKAIA, 2016; ALTENHOFF; GLOVER; DESSIMOZ, 2019).

Evolutionary analysis aiming to infer functionality relies on different strategies. Besides sequence similarity, analysis of synteny and domain conservancy are also relevant approaches to define orthology and putative function (TEKAIA, 2016). Therefore, comparative *in-silico* analysis of CIF1 and CIF1-interacting proteins would contribute to the understanding of the evolutionary history of the genes related to cytokinesis regulation in trypanosomatids.

*Tr*CIF1 protein sequence is shorter than *Tb*CIF1 and, despite the low identity of their amino acid sequences, *Tr*CIF1 is syntenic to *Tb*CIF1 and therefore it was considered an ortholog gene. However, due to the observed sequence differences, especially on some CIF1 canonical domains, it is still unclear if this protein has the same function in *T. rangeli* as it has in *T. brucei*.

Sinclair-Davis, McAllaster and Graffenried (2017) originally described and functionally characterized the CIF1/TOEFAZ1 domains. In that study, CIF1 was described as having three different domains: a N-terminal α-helical (from aa 1-319), intrinsically disordered protein or IDP (from aa 320-649) and, a C-terminal containing two zinc finger motifs (from aa 650-790).

Recently, a second, similar domain organization, was proposed by Hu et al. (2019), where the CIF1 N-terminal was further divided into a N-terminal domain (NTD, from aa 1-121) and a coiled-coil motif (CC, from aa 122-271) (Figure 10). In addition, in this same study the authors proposed to change the IDP motif name to Intrinsically Disordered Region (IDR). Since the major difference between both proposals is the subdivision of the N-terminal domain

into NTD and CC and considering that the recent work has separately assessed the role of both domains, in our study we have characterized the *Tr*CIF1 according to the Hu et al. (2019) model.

The NTD region of *Tr*CIF1 is 36% identical to the corresponding *Tb*CIF1 domain. Moreover, the low frequency of serine and threonine residues in the NTD and IDR regions of *Tr*CIF1 could significantly impact protein phosphorylation and, therefore, its function. In *T. brucei*, CIF1 phosphorylation is important for several functions. As an example, NTD phosphorylation is required for interaction with KPP1 (Hu et al., 2019), whereas CIF1 phosphorylation is essential for addressing the protein to the tip of the new FAZ (ZHOU et al., 2016).

In comparison to *Tb*CIF1, the coiled-coil motif of *Tr*CIF1 is shorter, has low sequence identity and no canonical coiled-coil motifs were identified. Based on such differences we might infer a distinct activity or function for *Tr*CIF1 in *T. rangeli*.

In *T. brucei*, the coiled-coil motif is essential for the CIF1 role in cytokinesis, as it is responsible for addressing CIF1 to the tip of the new filament FAZ (HU et al., 2017). The impact of such differences is difficult to predict but are likely to be significant. Absence or reduction in coiled coils numbers was also observed in CIF1 from other trypanosomatids.

The zinc-finger domain is required for cytokinesis initiation, CIF1 oligomerization (SINCLAIR-DAVIS, McALLASTER, GRAFFENRIED, 2017) and interaction with other proteins such as CIF2 (HU et al., 2017) and KPP1 (ZHOU et al., 2018). Interestingly, despite the 52% identity of the *Tr*CIF1 zinc-finger motif to a syntenic *Tb*CIF1 region, no zinc-finger domain was detected on the *Tr*CIF1 by the domain predicting software used.

It is well established that the *Tb*CIF1 zinc-finger region contains threonine residues that must be phosphorylated in order to allow the interaction with *Tb*KPP1 (ZHOU et al., 2018). However, since threonine residues are scarce in *Tr*CIF1 we might hypothesize that this protein ability to interact with KPP1 would be different from the *T. brucei* ortholog. *Tr*KPP1, however, is 83 % identical to the *Tb*KPP1.

The conservation of genes coding for CIF1 and CIF1-interacting proteins is consistent with the phylogenetic trees of trypanosomatids (SKALICKY, 2017). While *T. evansi*, a genetically closer species to *T. brucei* (MORENO; NAVA, 2015) maintained all CIF1 and CIF1-interacting genes, *B. saltans* and *P. confusum* were the most divergent species when compared to *T. brucei*. Although *B. saltans* is not a trypanosomatid, it is in the closest

clade to *P. confusum*, which is considered the most basal species among of trypanosomatids and the missing evolutionary link with bodonids (KAUFER et al., 2017; SKALICKY, et al, 2017). Therefore, it was expected that both species would differ the most from *T. brucei* CIF1 and CIF1-related genes having evolved differently from other trypanosomatids.

Except from *T. brucei* and *T. evansi* CIF1 genes, the zinc-finger domain was not predicted in any other trypanosomatid species included in this study. Even considering the bias that might be related to the different software's algorithm in predicting the presence/absence of domains, assuming that zinc-finger domains are exclusively present in the *T. brucei* and *T. evansi* CIF1 genes, it is tempting to speculate that CIF1 in other species may play a different role than described for *Tb*CIF1 since the zinc-finger domains are essential for CIF1 interaction with several other proteins (ZHOU et al., 2018).

Coiled-coils are formed by a pattern of hydrophobic and charged residues forming alpha-helices structures that acts as regulators of several proteins involved in *T. brucei* cytokinesis, including FPRC, CIF3, FRW1, BOH1 and CIF4 (HU et al., 2019). In our study, divergent numbers of predicted coiled-coil domains were found in orthologous FRW1, FPRC and CIF3 sequences from other trypanosomatids. In *T. brucei*, coiled-coil domains observed on FRW1 and FPRC are known to be relevant for complex protein formation at the FAZ tip (ZHOU et al., 2018). It is thus necessary to investigate if these differences in the number and on the sequence of coiled-coil domains would impact on protein activity and, consequently, in cytokinesis initiation in other species.

Along with the differences observed in the zinc-finger and coiled-coil domains, we noticed that the tropomyosin domain within KLIF was absent in most of the studies species. This domain was exclusively predicted for *L. braziliensis*, *T. evansi* and *L. seymouri* KLIF sequences, presenting high identity when compared to *Tb*KLIF. In yeast, a protein containing the tropomyosin-like domain is essential for cytokinesis (BALASUBRAMANIAN; HELFMAN; HEMMINGSEN, 1992). However, its role in KLIF has not been addressed. So, further experiments would be required to investigate the tropomyosin-like role in KLIF activity in trypanosomatids.

After description of CIF3 by Kurawasa et al. (2018), authors have noticed the absence of CIF3 gene orthologs in *Leishmania* sp., with this gene appearing to be restricted to *Trypanosoma*. Conservation of CIF1-interacting genes among species seems to point to the *Trypanosoma* genus having evolved some particularities in cytokinesis initiation. In this

sense, KLIF and FRW1 along with CIF1 are more conserved in *Trypanosoma* than other genera.

Selective pressures related to cell division in different environments may have molded many aspects of cytokinesis among trypanosomatids. It is well stablished that cytokinesis in this family does not require an actomyosin contractile ring, and instead involves many exclusive cytokinesis regulators (ZHOU; HU; LI, 2014). Nevertheless, since some regulators are stage-specific (ZHANG et al., 2019), some components of the cytokinesis pathway could have evolved differently in *T. brucei* and *T. evansi*, which multiply within mammal host as bloodstream forms that have a trypomastigote morphology.

3.2.2 Molecular characterization of CIF1 from *Trypanosoma rangeli*

Characterization of *Tr*CIF1 expression levels and cytolocalization using the anti-r*Tr*CIF1 antiserum generated in this present study revealed interesting results. Western blot assays using total *T. rangeli* extracts revealed a band of the expected size for *Tr*CIF1. If the protein recognized by anti-r*Tr*CIF1 antiserum is in fact CIF1, it would imply in differences in both species concerning CIF1 post-translational modifications, since the observed and expected molecular weight for *T. rangeli* CIF1 is the same, whereas in *T. brucei* CIF1 has a higher molecular weight due to post-translational modifications (Zhou et al., 2016). In addition, the serum also recognized proteins with similar molecular weight in *T. cruzi*, which also had an expected molecular weight of 70 kDa.

In *T. brucei*, CIF1 has a predicted molecular weight of 89 kDa, however, western blot analysis reveals a molecular weight of approximately 120 kDa (Zhou et al., 2016; Zhou et al., 2018). Using our anti-r*Tr*CIF1, a protein band of approximately 70 kDa, a similar size as was observed for *T. rangeli* and *T. cruzi*, was recognized in *T. brucei* extracts. Despite being lower than the described size of *Tb*CIF1, two independent western blot analyses of *Tb*CIF1 expression using different approaches (anti-*Tb*CIF1 to recognize native *Tb*CIF1 or anti-HA to *Tb*CIF1 fused to HA tag) also recognized a weak protein band of 75 kDa (Zhou et al., 2016; Zhou et al., 2018). Therefore, we believe that the protein recognized by anti-r*Tr*CIF1 is also recognizing the same protein considered as a non-specific band by Zhou et al. (2016).

Due to the reported role of CIF1 in cell division, we have expected to observe either higher levels of transcription or protein expression in *T. rangeli* epimastigotes than trypomastigotes since this later is considered as a non-proliferative form. However,

transcription and expression levels revealed no significant differences between both *T. rangeli* forms. Furthermore, no significant differences in transcription and expression of CIF1 was observed on synchronized parasites during the cell cycle *in vitro*, implying that *Tr*CIF1 is not cell-cycle regulated unlike *Tb*CIF1 (KURASAWA et al., 2018).

Considering the interaction of CIF1 with several proteins at the tip of the new FAZ filament, the observed cytolocalization suggests a different function for *Tr*CIF1. *T. rangeli* proliferative forms (epimastigotes) had a diffuse *Tr*CIF1 protein distribution throughout the cell body, whereas in trypomastigotes *Tr*CIF1 was concentrated at FAZ and tip of flagellum. Therefore, the misaddressing of CIF1 in *T. rangeli* could impact its function at promoting cleavage furrow and might be related to the differences observed in some of the *Tr*CIF1 domains.

The differential CIF1 localization in *T. rangeli* epimastigotes is perhaps difficult to compare with the reports for *T. brucei*, in which CIF1 was only described in procyclic and bloodstream forms that possess trypomastigotes cell shapes. While in *T. brucei* those forms are able to divide and CIF1 promotes the ingression of cleavage furrow, *T. rangeli* epimastigotes have a distinct morphology and possibly a particular mechanism of furrow ingression.

So far, *Tr*CIF1-/- mutants are under selection with growing concentrations of selective antibiotics and multiplying *in vitro* as compared to control parasites. Once selected, these populations will allow precise observations for phenotype changes.

Altogether, our results have characterized the *Tr*CIF1, pointing out differences between *T. rangeli* and *T. brucei* CIF1 which indicates that *Tr*CIF1 may have a distinct function in this species.

4 CHAPTER TWO: COMPARATIVE STUDY OF FLA1BP FROM *TRYPANOSOMA RANGELI*, *TRYPANOSOMA CRUZI* AND *TRYPANOSOMA BRUCEI*

4.1 RESULTS

4.1.1 Analysis of FLA1BP from *Trypanosoma rangeli*, *Trypanosoma cruzi*, and *Trypanosoma brucei*

Since FLA1/FLA2/FLA3-A and FLA1BP/FLA3-B are present as single-copy genes in the *T. cruzi* and *T. rangeli* genomes and due to their pivotal involvement in the cell division, we investigated the evolution of FLA1BP/FLA3 genes in the *Trypanosoma* genus. Following the identification of orthologous genes in these taxa by comparative analysis with the *T. brucei* FLA1BP, we have comparatively investigated the structural aspects of these genes. The genes located upstream and downstream of the FLA1BP gene were retrieved from the *T. brucei* (Supplementary Material B), *T. cruzi* (DM28c strain) (Supplementary Material C) and *T. rangeli* (SC58 strain) (Supplementary Material D) genomes. Based on the position of the *Tb*FLA1BP (Tb927.8.4050; Tb927.8.4100) and the genes located 5' and 3'end of this gene, the ordering of the orthologous genes in each species was drawn and presented in Figure 24.

Figure 24 - Schematic representation of synteny between FLA1 and FLA1BP genes from *Trypanosoma brucei*, *Trypanosoma cruzi*, and *Trypanosoma rangeli*. Illustration of a fragment of chromosome 8 (from position 1,217,959 to 1,194,665) of *T. brucei*. Boxes represent genes from *T. brucei*, *T. cruzi* and *T. rangeli* genomes. The size of each box is proportional to real gene length. Dashed lines indicate homologous genes between species. Genes represented with same color share significant protein sequence similarity.

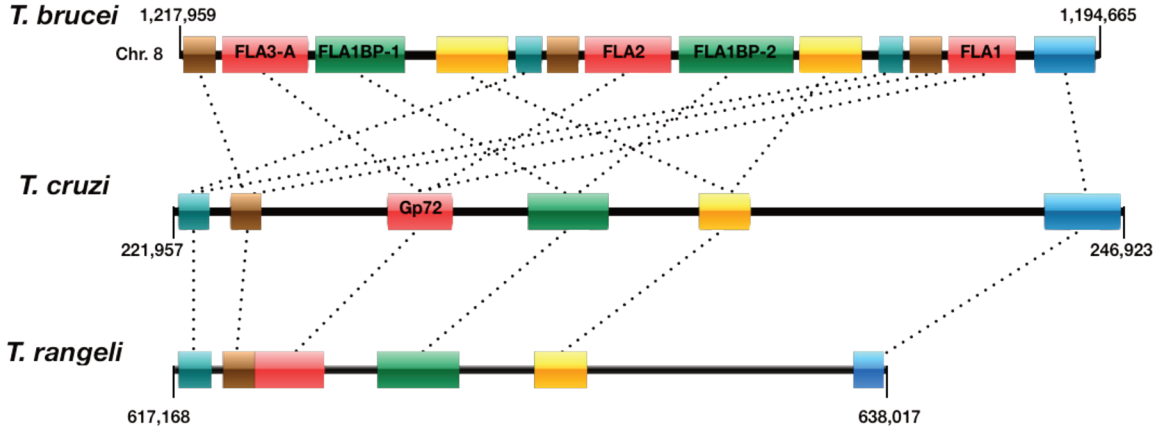

Our results thus indicate a maintenance of the synteny of *T. cruzi* and *T. rangeli* FLA1BP/FLA3-B with *T. brucei* FLA1BP. However, the genomic localization of FLA1BP/FLA3-B in *T. cruzi* and *T. rangeli* is not syntenic with the *T. brucei* FLA3-B

sequences (Tb927.5.4570; Tb927.5.4580). Therefore, in this study the *T. cruzi* and *T. rangeli* sequences will be referred as *Tc*FLA1BP and *Tr*FLA1BP, respectively.

We have also investigated the presence and the synteny of the hypothetical protein resembling the *T. brucei* FLA1-like protein (Tb927.10.6180) described by Sun et al. (2013) and have found syntenic orthologs in both the *T. cruzi* and *T. rangeli* genomes.

4.1.2 FLA1BP intracellular portion

Alignment of the FLA1BP sequences from *T. rangeli*, *T. cruzi* and *T. brucei* (Supplementary material E) revealed a low conservation of several amino acid residues as well as some domains, but there was a short C-terminal sequence conserved among these three species. This conserved sequence is within the intracellular region of *Tb*FLA1BP. Since it was proposed that the intracellular tail could be related to the FLA1BP dotted localization along the FAZ (SUN et al., 2013), it could be a domain responsible for FLA1BP localization to the FAZ.

To investigate if this sequence is conserved in other trypanosomatids, FLA1BP sequences from different species were obtained as described in 2.2.1 and their intracellular sequences were aligned (Figure 25). The first twelve amino acid residues following the transmembrane region were conserved. The sequence SKR(R/K)RLA(A/T)VV(A/V/T)P consists of four positively charged residues followed by five hydrophobic residues.

Figure 25 - FLA1BP from Trypanosomatids. A) Schematic representation of FLA1BP from *Trypanosoma brucei*, highlighting key elements in FLA1BP from Trypanosomatids. SP = Signal Peptide. ER = Extracellular region. TR = Transmembrane region. IR = Intracellular region. B) Alignment of the intracellular sequence of FLA1BP from different species, revealing the conservation of 12 amino acid residues (green square).

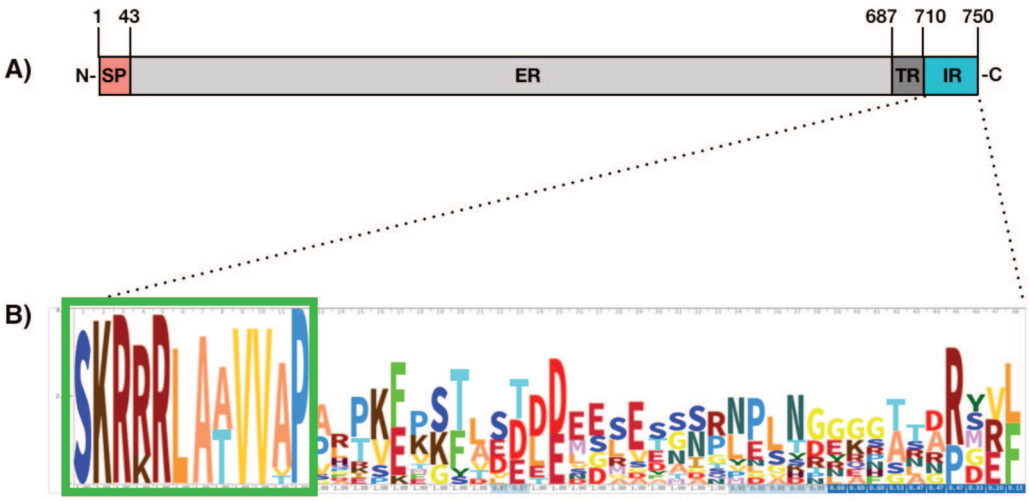

4.1.3 FLA1BP transcription, expression and localization in *Trypanosoma rangeli* and *Trypanosoma cruzi*

After FLA1BP transcription in *T. brucei*, which is upregulated in procyclic forms, FLA1BP is translated and then glycosylated. Then, it is directed to FAZ, where it localizes in dots along the flagellum membrane region (SUN et al., 2013). To initially characterize FLA1BP in *T. cruzi* and *T. rangeli*, we analyzed their transcription, expression and localization.

For mRNA levels, transcriptomic data from epimastigotes, bloodstream trypomastigotes, and metacyclic trypomastigotes from *T. rangeli* and epimastigotes, trypomastigotes and amastigotes from *T. cruzi* were analyzed. In *T. rangeli*, FLA1BP transcription is upregulated in epimastigotes in comparison to both metacyclic and bloodstream trypomastigotes (Figure 26). That differs from the observations in *T. cruzi*, which had a slightly higher level of mRNA in the trypomastigotes (Figure 27).

Figure 26 – Transcription levels of FLA1BP among trypomastigotes and epimastigotes from *Trypanosoma rangeli*. Box plot of log2 of counts per million (Y axis). Pink = Metacyclic trypomastigotes. Green = Epimastigotes. Blue = Bloodstream trypomastigotes. Counts are represented as means (rhombus) with quartiles.

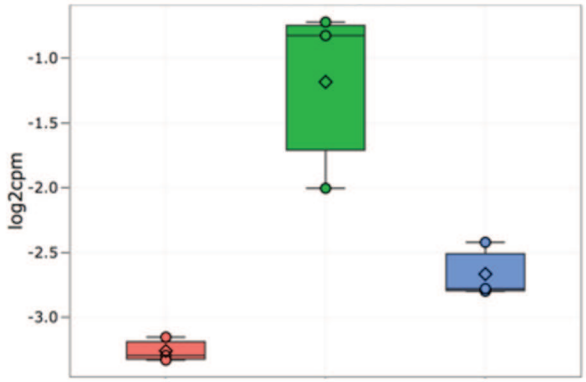

Figure 27 – Transcription levels of FLA1BP among trypomastigotes, epimastigotes, and amastigotes from *Trypanosoma cruzi*. Normalized nCounts of *Tc*FLA1BP in amastigotes (Ama), epimastigotes (Epi) and Trypomastigotes (Trypo).

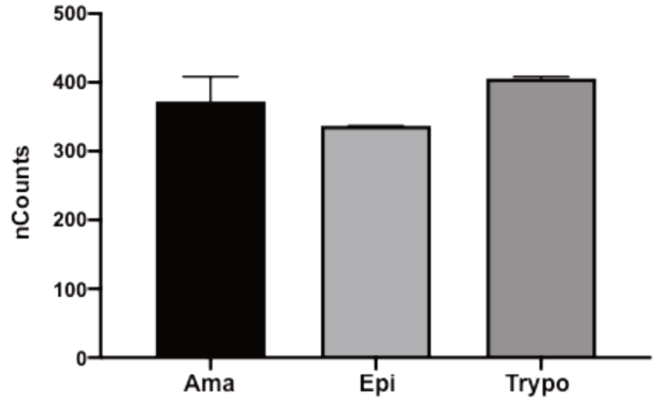

To investigate FLA1BP protein expression, polyclonal antibodies against *Tr*FLA1BP and *Tc*Fla1BP were used (DE LIZ, 2017). For both species, antibodies recognized two bands of approximately 100 and 250 kDa in both epimastigotes and trypomastigotes (Figure 28).

Figure 28 – Expression of FLA1B from *Trypanosoma rangeli* and *Trypanosoma cruzi* epimastigotes and trypomastigotes. Western blot revealing detection of *Tr*FLA1BP by anti-r*Tr*FLA1BP and *Tc*FLA1BP by anti-r*Tc*FLA1BP serum in epimastigotes (Epi) and trypomastigotes (Trypo).

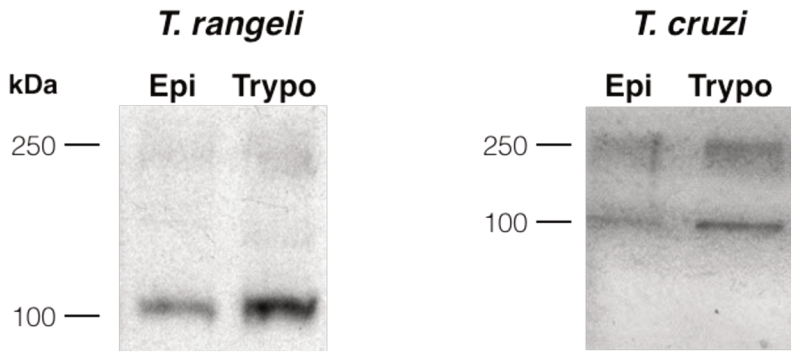

In addition, the antibodies were used to reveal FLA1BP localization in the different forms of *T. rangeli* and *T. cruzi*. Immunofluorescence assays showed that for both species have a similar FLA1BP localization (Figure 29 and 30). While FLA1BP had a disperse signal in the whole cell from epimastigotes, in trypomastigotes a dotted arrangement along the FAZ.

Figure 29 – Localization of FLA1BP in *Trypanosoma rangeli*. Immunofluorescence assay revealing *Tr*FLA1BP localization in epimastigotes and trypomastigotes. Detection of anti-r*Tr*FLA1BP antibodies by Alexa Fluor 488-labeled conjugate. Bar - 10 µm.

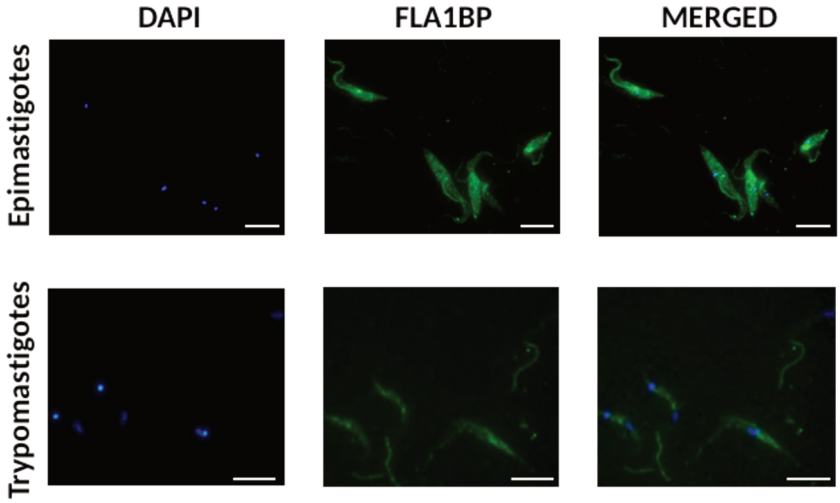

Figure 30 – Localization of FLA1BP in *Trypanosoma cruzi*. Immunofluorescence assay revealing *Tc*FLA1BP localization in epimastigotes, trypomastigotes, and amastigotes. Detection of anti-r*Tr*FLA1BP antibodies by Alexa Fluor 488-labeled conjugate. Bar - 10 µm.

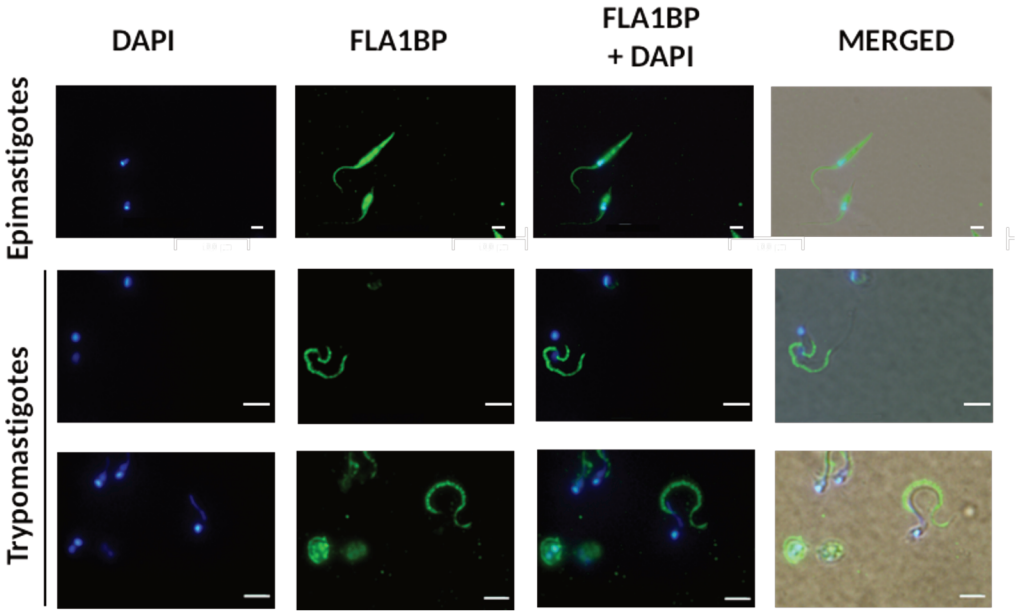

4.1.4 Deletion of FLA1BP from *Trypanosoma rangeli*

To investigate the effects of FLA1BP deletion in *T. rangeli*, both *Tr*FLA1BP alleles were replaced by resistance genes for blasticidin and puromycin. After months of selection, it was not possible to obtain a FLA1BP double knockout (Figure 31). However, a semi-quantitative PCR comparison of the gDNA from wild type and transfected parasites showed

a reduction in the amount of FLA1BP in the transfected parasites, indicating a possible deletion of one of the alleles.

Figure 31 - Evaluation of FLA1BP deletion from *Trypanosoma rangeli*. Electrophoresis in agarose gel 1% stained with ethidium bromide, revealing the amplification product of *Tr*FLA1BP by a semi-quantitative PCR. Mut = Mutants. WT = Wild type parasites = WT. NC = Negative control.

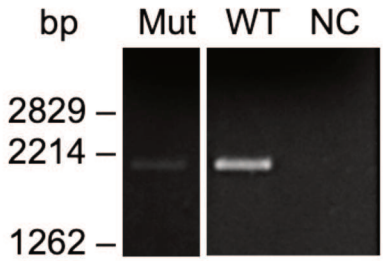

Deletion of both FLA1 and FLA1BP resulted in reduction of FLA1BP protein expression (Figure 32). In addition, selected parasites presented detachment of flagellum (Figure 33) and defects *in vitro* differentiation (data not shown).

Figure 32 - Expression of FLA1BP in *Trypanosoma rangeli* after deletion of FLA1 or FLA1BP. (A) *Western blot* revealing detection of *Tr*FLA1BP by anti-r*Tr*FLA1BP serum (upper protein band) and tubulin by anti-Tubulin monoclonal antibody (lower band). (B) Relative density optic quantification of *Tr*FLA1B expression (Y axis), normalized with tubulin expression, from *T. rangeli* after deletion of FLA1 or FLA1BP genes (X axis). WT = Wild type. + = 1 µg/mL of blasticidin and 0.5 µg/mL of puromycin. ++ = 2 µg/mL of blasticidin and 1 µg/mL of puromycin.

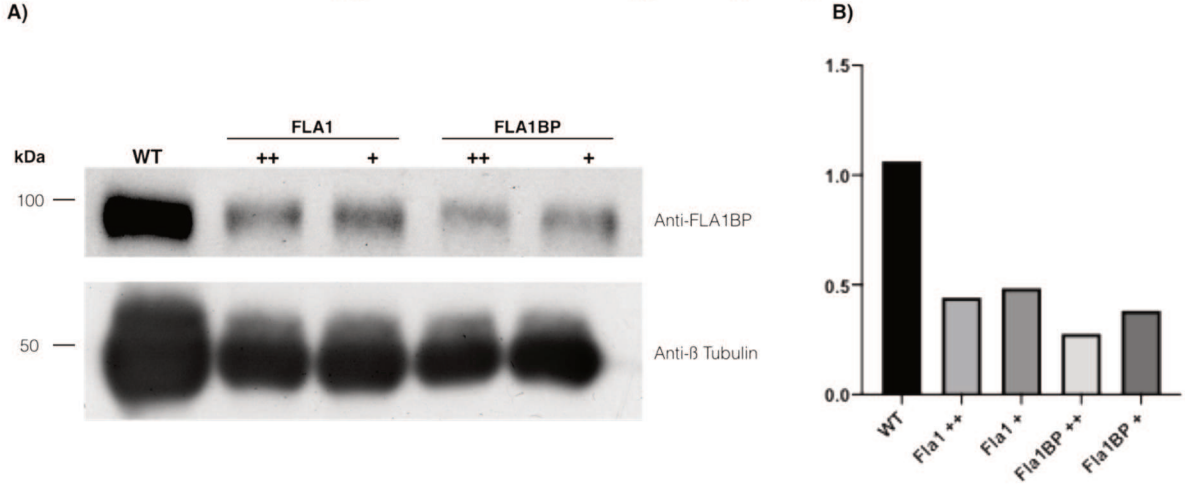

Figure 33 – Effects of FLA1 and FLA1BP deletion in *Trypanosoma rangeli* epimastigotes.
A) Wild type. B) Deletion of FLA1. C) Deletion of FLA1BP. Arrow = Detached flagellum.

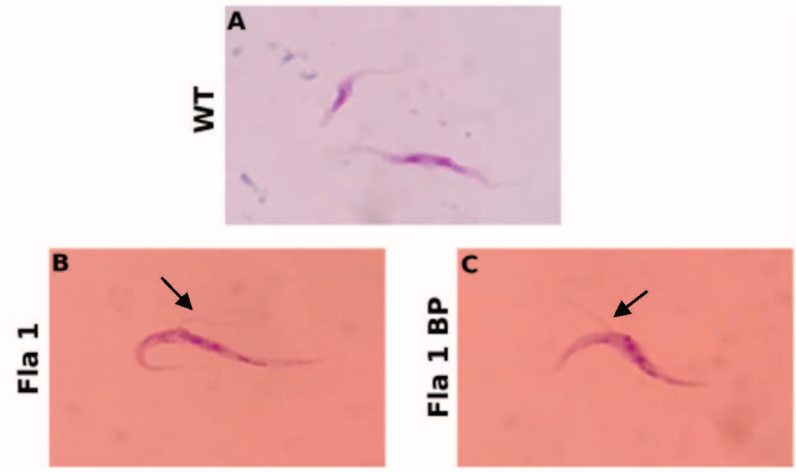

4.2 DISCUSSION

As described before, *T. cruzi* and *T. rangeli* have a single copy gene coding for FLA1BP/FLA3-B which has a signal peptide, an extracellular region and a transmembrane region followed by a C-terminal tail (DE LIZ, 2017). Despite structure conservation, it is not clear if this protein from both species are functionally conserved when compared to *T. brucei*.

Since *T. brucei* has numerous FLA1 and FLA1BP genes and *T. rangeli* and *T. cruzi* have single genes for each protein, we analyzed the synteny of these genes among species to understand their evolution. The region where FLA1BP is situated in the *T. brucei* genome consists of a block of FLA1/FLA1BP genes, and it seems to have suffered several gene duplications, resulting in paralogs of FLA1/FLA2/FLA3-A/FLA1-like and FLA1BP-1/FLA1BP-2/FLA3-B. Therefore, since the orthologous sequences from *T. rangeli* and *T. cruzi* are syntenic to *Tb*FLA1BP but not to *Tb*FLA3-B, we called them *Tr*FLA1BP and *Tc*FLA1BP.

Considering the occurrence of gene duplication of FLA genes and lack of orthologs of *Tb*FLA3-B in *T. cruzi* and *T. rangeli*, it is likely that an ancestral FLA1BP have been duplicated and originated this gene diversity in *T. brucei*. Same must have occurred and originated FLA1, FLA2, FLA3-A and the uncharacterized FLA1-like protein. However, since both *T. cruzi* and *T. rangeli* possess a single ortholog to FLA1-like protein, the common ancestor of *T. rangeli*, *T. cruzi* and *T. brucei* must have had two copies of FLA1-like genes.

Once it was assumed *Tr*FLA1BP and *Tc*FLA1BP ancestry to *Tb*FLA1BP, it was intended to characterize FLA1BP from *T. rangeli* and *T. cruzi.* To begin, transcription levels in both species were investigated to identify possible differences in transcription between biological forms. Since transcription data was obtained from different methods, mRNA levels between both species were not compared, only between biological forms from the same species. In *T. cruzi*, no difference was observed among amastigotes, trypomastigotes and epimastigotes. That differs from *T. rangeli*, which up-regulate FLA1BP transcription in epimastigotes. Increased transcription at this stage could be related to active cell division in epimastigotes. Since trypomastigotes from *T. rangeli* do not divide and therefore do not need to synthesize great amounts of FLA1BP to assemble a new FAZ, it would be expected to see a down-regulation of transcription in those forms. However, this is contradicted by the transcription data from *T. cruzi*.

Since trypanosomatids transcription is polycistronic, mRNA levels are not necessarily and indicative of protein levels since parasites do not differentially transcribe

individual genes. However, transcription levels can be regulated by post-transcriptional degradation of mRNA (ARCHER et al., 2011).

FLA1BP protein expression was investigated using the antibodies anti-r*Tr*FLA1BP and *Tc*FLA1BP, which recognized proteins from *T. rangeli* and *T. cruzi* with a higher molecular weight than expected. This has previously been observed for *Tb*FLA1BP, *Tb*FLA3[2] and *Tb*FLA[1]. This difference has been attributed to post-translation modifications, specifically glycosylation, which is required for flagellar attachment to cell body (SUN et al., 2013; WOODS et al, 2013). FLA1BP is expressed in both forms, although expression analysis will be required to check stage-specific particularities.

Localization of FLA1BP in *T. brucei* has only been studied in procyclic forms, which have a trypomastigotes-like cell shape. In those forms, FLA1BP is concentrated in dots along the FAZ region (SUN et al., 2013). Immunofluorescence assays show similar a localization in *T. cruzi* and *T. rangeli*, indicating conservation of localization among species. In addition, FLA1BP localization seems to be highly influenced by trypanosome biological form. In the IFA of *T. rangeli* using *in vitro* differentiated trypomastigotes, we observed that parasites with advanced transition to trypomastigotes had a clearer protein concentration at the FAZ. Studies on FLA1BP/FLA3-2 localization in *T. brucei* epimastigotes would help to understand FLA1BP localization differences among epimastigotes and trypomastigotes from the Trypanosoma genus.

Since FLA1BP localization in trypomastigotes is conserved, it is likely that these species have a conserved mechanism to address or to maintain FLA1BP within the FAZ. Sun et al. (2013) have suggested that intracellular sequence of FLA1BP could be related to its localization or interaction with the axoneme. Since these new results indicate that among these three species of trypanosomes this localization is conserved despite sequence divergences, we investigated the intracellular sequence of FLA1BP to identify residues.

The sequence SKR(R/K)RLA(A/T)VV(A/V/T)P is conserved in the intracellular region of FLA1BP of all analyzed species, and is characterized by several positive residues followed by hydrophobic residues. Sun et al. (2013) have suggested that the intracellular region of FLA1BP could have some implication in FLA1BP localization at FAZ. Since only the first 12 amino acid residues of the intracellular sequence are conserved, this sequence could be required for FLA1BP addressing or anchoring at the FAZ, thus SKR(R/K)RLA(A/T)VV(A/V/T)P is potentially a domain for FAZ localization preserved in

the Trypanosomatidae clade. Further analysis would be necessary to understand SKR(R/K)RLA(A/T)VV(A/V/T)P importance to the FLA1BPs.

Lastly, it was not possible to completely delete FLA1 or FLA1BP from *T. rangeli*. However, FLA1BP expression was disturbed in both mutants, and selected parasites showed a similar phenotype to that described for the Gp72 knock-out in *T. cruzi*, where the flagellum is detached from the cell body and *in vitro* differentiation failed, but parasites were able to survive in culture.

Therefore, we hypothesize that FLA1BP from *T. cruzi* and *T. rangeli* have an analogous function to *Tb*FLA1BP, and are required for flagellar attachment and possibly interact with FLA1/Gp72.

CONCLUSION

Cytokinesis initiation mediated by CIF1 seem to be a distinct process among trypanosomatids. We revealed that CIF1 as well as CIF1-related proteins have variable degrees of sequence conservation, especially in the domains related to localization and phosphorylation. These *in silico* observations are consistent with our results on the molecular characterization of *T. rangeli* CIF1, in which CIF1 appears to be not required for cell division.

Despite *T. brucei* having evolved FLA1/FLA1BP gene duplications, the FLA1BP proteins are conserved in *Trypanosoma* genus and possibly in others. Except for a short C-terminal sequence conserved in all analyzed species, which might play a role in the FLA1BP addressing and/or anchoring to the FAZ, the FLA1BP sequence is not highly conserved among the trypanosomatids species.

The obtained results allow us to infer a possibly distinct cytokinesis activation process in *T. brucei* when compared to other trypanosome species, yet basic elements for flagellar attachment may have been originated in the common ancestor of the Trypanosomatidae clade.

REFERENCES

AFCHAIN, D. et al. Antigenic make-up of *Trypanosoma cruzi* culture forms: identification of a specific component. **The Journal Of Parasitology**, Lawrence, v. 65, n. 4, p.507-514, ago. 1979.

AKAZUE, P. I. et al. Sustainable Elimination (Zero Cases) of Sleeping Sickness: How Far Are We from Achieving This Goal? **Pathogens**, [s.l.], v. 8, n. 3, p.1-18, 29 ago. 2019. MDPI AG. http://dx.doi.org/10.3390/pathogens8030135.

AÑEZ, N. Studies on *Trypanosoma rangeli* Tejera, 1920. I – Deposition, migration and growth of *T. rangeli* in two mammals. In: **Parasitological Topics**. Kansas: Allen Press, 1981. p. 19-26.

AÑEZ, N..; VELANDIA, J..; RODRIGUEZ, A. M. Estudios sobre *Trypanosoma rangeli* Tejera, 1920. VIII. Respuesta a las infecciones en dos mamiferos. **Mem Inst Oswaldo Cruz**, v. 80, n. 2, p. 149-53, 1985.

ARCHER, S. K. et al. The Cell Cycle Regulated Transcriptome of *Trypanosoma brucei*. **Plos One**, [s.l.], v. 6, n. 3, p.1-14, 31 mar. 2011. Public Library of Science (PLoS). http://dx.doi.org/10.1371/journal.pone.0018425.

BASOMBRÍO, M. A. et al. Targeted deletion of the GP72 gene decreases the infectivity of *Trypanosoma cruzi* for mice and insect vectors. **Journal Of Parasitology**, [s.l.], v. 88, n. 3, p.489-493, jun. 2002. American Society of Parasitologists. http://dx.doi.org/10.1645/0022-3395(2002)088[0489:tdotgg]2.0.co;2.

BERNÁ, L. et al. Transcriptomic analysis reveals metabolic switches and surface remodeling as key processes for stage transition in *Trypanosoma cruzi*. **Peerj**, [s.l.], v. 5, p.1-32, 8 mar. 2017. PeerJ. http://dx.doi.org/10.7717/peerj.3017.

BOTTIEAU, E.; CLERINX, J.. Human African Trypanosomiasis. **Infectious Disease Clinics Of North America**, [s.l.], v. 33, n. 1, p.61-77, mar. 2019. Elsevier BV. http://dx.doi.org/10.1016/j.idc.2018.10.003.

BÜSCHER, P. et al. Human African trypanosomiasis. **The Lancet**, [s.l.], v. 390, n. 10110, p.2397-2409, nov. 2017. Elsevier BV. http://dx.doi.org/10.1016/s0140-6736(17)31510-6.

COOPER, R. et al. Characterization of a candidate gene for Gp72, an insect stage-specific antigen of *Trypanosoma cruzi*. **Molecular and Biochemical Parasitology**, v. 49, n. 1, p. 45–59, nov. 1991.

COOPER, R.; DE JESUS, A. R.; CROSS, G. A. M. Deletion of an immunodominant *Trypanosoma cruzi* surface glycoprotein disrupts flagellum-cell adhesion. **Journal of Cell Biology**, v. 122, n. 1, p. 149–156, 1993.

DE LANA, M.; TAFURI, W. T. *Trypanosoma cruzi* e Doença de Chagas. In: **Parasitologia Humana**. [s.l.] Atheneu, 2002.

DE LIZ, L. V. **Análise in silico de proteínas da zona de adesão flagelar e caracterização molecular da glicoproteína de adesão flagelar 3 (Fla3) de Trypanosoma rangeli e de Trypanosoma cruzi**. 2017. Trabalho de conclusão de curso, Universidade Federal de Santa Catarina. Disponível em: <https://repositorio.ufsc.br/xmlui/handle/123456789/177817>. Acesso em: 10 jan. 2020.

DESCHAMPS, P. et al. Phylogenomic Analysis of Kinetoplastids Supports That Trypanosomatids Arose from within Bodonids. **Molecular Biology And Evolution**, [s.l.], v. 28, n. 1, p.53-58, 28 out. 2010. Oxford University Press (OUP). http://dx.doi.org/10.1093/molbev/msq289.

EGER-MANGRICH, I.; DE OLIVEIRA, M. A.; GRISARD, E. C.; DE SOUZA, W.; STEINDEL, M. Interaction of *Trypanosoma rangeli* Tejera, 1920 with different cell lines in vitro. **Parasitol Res**, v. 87, n. 6, p. 505-9, 2001.

GRABHERR, M. G.; HAAS, B. J.; YASSOUR, M. et al. Trinity: reconstructing a full-length transcriptome without a genome from RNA- Seq data. **Nat Biotechnol**, v 29, p. 644-652, 2011.

GREWAL, M. *Trypanosoma rangeli* Tejera, 1920, in its vertebrate and invertebrate hosts. **Trans R Soc Trop Med Hyg**, v. 50, n., p. 301-02, 1956.

GRISARD, E. C.; ROMANHA, A. J.; STEINDEL, M. *Trypanosoma (Herpetosoma) rangeli*. In: **Parasitologia Humana**. 13a Edição. ed. São Paulo: Atheneu, 2016.

GUHL, F.; VALLEJO, G. A.. *Trypanosoma* (*Herpetosoma*) *rangeli* Tejera, 1920: an updated review. **Memórias do Instituto Oswaldo Cruz**, [s.l.], v. 98, n. 4, p.435-442, jun. 2003. FapUNIFESP (SciELO). http://dx.doi.org/10.1590/s0074-02762003000400001.

HAMMARTON, T. C. Who Needs a Contractile Actomyosin Ring? The Plethora of Alternative Ways to Divide a Protozoan Parasite. **Frontiers In Cellular And Infection Microbiology**, [s.l.], v. 9, p.1-30, 21 nov. 2019. Frontiers Media SA. http://dx.doi.org/10.3389/fcimb.2019.00397.

HAYNES, P. A.; CROSS, G. A. M. Differential glycosylatin of epitope-tagged glycoprotein Gp72 during the *Trypanosoma cruzi* life cycle. **Molecular and Biochemical Parasitology**, v. 83, p. 253–256, 1996.

HERBIG-SANDREUTER, A. Further studies on *Trypanosoma rangeli* Tejera 1920. **Acta Trop**, v. 14, n. 3, p. 193-207, 1957.

HU, H. et al. The trypanosome-specific proteins FPRC and CIF4 regulate cytokinesis initiation by recruiting CIF1 to the cytokinesis initiation site. **Journal Of Biological Chemistry**, [s.l.], v. 294, n. 45, p.16672-16683, 20 set. 2019. American Society for Biochemistry & Molecular Biology (ASBMB). http://dx.doi.org/10.1074/jbc.ra119.010538.

JENSEN, R. Orthologs and paralogs - we need to get it right. **Genome Biology**, [s.l.], v. 2, n. 8, p.1-3, ago. 2001. Springer Science and Business Media LLC. http://dx.doi.org/10.1186/gb-2001-2-8-interactions1002.

KAUFER, A. et al. The evolution of trypanosomatid taxonomy. **Parasites & Vectors**, [s.l.], v. 10, n. 1, p.1-17, 8 jun. 2017. Springer Science and Business Media LLC. http://dx.doi.org/10.1186/s13071-017-2204-7.

KENNEDY, P; G. E. Update on human African trypanosomiasis (sleeping sickness). **Journal Of Neurology**, [s.l.], v. 266, n. 9, p.2334-2337, 17 jun. 2019. Springer Science and Business Media LLC. http://dx.doi.org/10.1007/s00415-019-09425-7.

KOERICH, L. B. et al. Differentiation of *Trypanosoma rangeli*: high production of infective Trypomastigote forms in vitro. **Parasitol Res**, v. 88, n. 1, p. 21-5, 2002.

KOHL, L.; ROBINSON, D.; BASTIN, P. Novel roles for the flagellum in cell morphogenesis and cytokinesis of trypanosomes. **The Embo Journal**, [s.l.], v. 22, n. 20, p.5336-5346, 15 out. 2003. Wiley. http://dx.doi.org/10.1093/emboj/cdg518.

KURASAWA, Y. et al. The trypanosome-specific protein CIF3 cooperates with the CIF1 protein to promote cytokinesis in *Trypanosoma brucei*. **Journal Of Biological Chemistry**, [s.l.], v. 293, n. 26, p.10275-10286, 15 maio 2018. American Society for Biochemistry & Molecular Biology (ASBMB). http://dx.doi.org/10.1074/jbc.ra118.003113.

LACOMBLE, S. et al. Three-dimensional cellular architecture of the flagellar pocket and associated cytoskeleton in trypanosomes revealed by electron microscope tomography. **Journal Of Cell Science**, [s.l.], v. 122, n. 8, p.1081-1090, 19 mar. 2009. The Company of Biologists. http://dx.doi.org/10.1242/jcs.045740.

LACOUNT, D. J.; BARRET, B.; DONELSON, J. E. *Trypanosoma brucei* FLA1 Is Required for Flagellum Attachment and Cytokinesis. **Journal of Biological Chemistry**, [s.l.], v. 277, n. 20, 17 mai. 2002. The American Society for Biochemistry and Molecular Biology. http://dx.doi.org/10.1074/jbc.M200873200.

LANDER, N.; CHIURILLO, M. A. State-of-the-art CRISPR /Cas9 Technology for Genome Editing in Trypanosomatids. **Journal Of Eukaryotic Microbiology**, [s.l.], v. 66, n. 6, p.981-991, 7 jul. 2019. Wiley. http://dx.doi.org/10.1111/jeu.12747.

LIDANI, K. C. F. et al. Chagas Disease: From Discovery to a Worldwide Health Problem. **Frontiers In Public Health**, [s.l.], v. 7, p.1-13, 2 jul. 2019. Frontiers Media SA. http://dx.doi.org/10.3389/fpubh.2019.00166.

LUKES, J. et al. Kinetoplast DNA Network: Evolution of an Improbable Structure: Evolution of an Improbable Structure. **Eukaryotic Cell**, [s.l.], v. 1, n. 4, p.495-502, ago. 2002. American Society for Microbiology. http://dx.doi.org/10.1128/ec.1.4.495-502.2002.

MCALLASTER, M. R. et al. Proteomic identification of novel cytoskeletal proteins associated with TbPLK, an essential regulator of cell morphogenesis in *Trypanosoma*

brucei. **Molecular Biology Of The Cell**, [s.l.], v. 26, n. 17, p.3013-3029, set. 2015. American Society for Cell Biology (ASCB). http://dx.doi.org/10.1091/mbc.e15-04-0219.

MOLYNEUX, D. Division of the human trypanosome, *Trypanosoma* (*Herpetosoma*) *rangeli*. **Ann Trop Med Parasitol**, v. 67, n. 3, p. 371-2, 1973.

MORAES, M. H. de et al. Different serological cross-reactivity of *Trypanosoma rangeli* forms in *Trypanosoma cruzi*-infected patients sera. **Parasites & Vectors**, [s.l.], v. 1, n. 1, p.1-20, 2008. Springer Science and Business Media LLC. http://dx.doi.org/10.1186/1756-3305-1-20.

MORALES, S. V. **Estudo da resposta inflamatória durante a infecção por *Trypanosoma rangeli***. Trabalho de Conclusão de Curso, Universidade Federal de Santa Catarina, 2012.

MORENO, S A.; NAVA, M. *Trypanosoma evansi* is alike to *Trypanosoma brucei brucei* in the subcellular localisation of glycolytic enzymes. **Memórias do Instituto Oswaldo Cruz**, [s.l.], v. 110, n. 4, p.468-475, 29 maio 2015. FapUNIFESP (SciELO). http://dx.doi.org/10.1590/0074-02760150024.

NOZAKI, T.; HAYNES, P. A.; CROSS, G. A. Characterization of the *Trypanosoma brucei* homologue of a *Trypanosoma cruzi* flagellum-adhesion glycoprotein. **Molecular and Biochemical Parasitology**, v. 82, n. 2, p. 245–255, 1996.

OSÓRIO, A. L. A. R. et al. *Trypanosoma* (Duttonella) *vivax*: its biology, epidemiology, pathogenesis, and introduction in the New World - a review. **Memórias do Instituto Oswaldo Cruz**, [s.l.], v. 103, n. 1, p.1-13, fev. 2008. FapUNIFESP (SciELO). http://dx.doi.org/10.1590/s0074-02762008000100001.

OSORIO, Y.; TRAVI, B. L.; PALMA, G. I.; SARAVIA, N. G. Infectivity of *Trypanosoma rangeli* in a promonocytic mammalian cell line. **J Parasitol**, v. 81, n. 5, p. 687-93, 1995.

PRESTES, E. B. et al. Messenger RNA levels of the Polo-like kinase gene (PLK) correlate with cytokinesis in the *Trypanosoma rangeli* cell cycle. **Experimental Parasitology**, [s.l.], v. 204, p.1-9, set. 2019. Elsevier BV. http://dx.doi.org/10.1016/j.exppara.2019.107727.

RADWANSKA, M. et al. Salivarian Trypanosomosis: A Review of Parasites Involved, Their Global Distribution and Their Interaction With the Innate and Adaptive Mammalian Host Immune System. **Frontiers In Immunology**, [s.l.], v. 9, p.1-20, 2 out. 2018. Frontiers Media SA. http://dx.doi.org/10.3389/fimmu.2018.02253.

ROBINSON, D. R. et al. Microtubule polarity and dynamics in the control of organelle positioning, segregation, and cytokinesis in the trypanosome cell cycle. **The Journal Of Cell Biology**, [s.l.], v. 128, n. 6, p.1163-1172, 15 mar. 1995. Rockefeller University Press. http://dx.doi.org/10.1083/jcb.128.6.1163.

ROCHA, G. M. et al. The flagellar attachment zone of *Trypanosoma cruzi* epimastigote forms. **Journal Of Structural Biology**, [s.l.], v. 154, n. 1, p.89-99, abr. 2006. Elsevier BV. http://dx.doi.org/10.1016/j.jsb.2005.11.008.

SAMBROOK, J.; RUSSELL, D. W. **Molecular Cloning: A Laboratory Manual.** New York: Cold Spring Harbor, 2001.

SCHÖNENBERGER, B. R. Cultivation and in vitro cloning or procyclic culture forms of *Trypanosoma brucei* in a semi-defined medium. Short communication. Acta Trop., 36 (3), 289-92, 1979.

SKALICKÝ, T. et al. Extensive flagellar remodeling during the complex life cycle of *Paratrypanosoma*, an early-branching trypanosomatid. **Proceedings Of The National Academy Of Sciences**, [s.l.], v. 114, n. 44, p.11757-11762, 16 out. 2017. Proceedings of the National Academy of Sciences. http://dx.doi.org/10.1073/pnas.1712311114.

SILVA, L. H. P; NUSSENZWEIG, V. Sôbre uma cêpa de *T. cruzi* altamente virulenta para o camundongo branco. Folia Clin. Biol. (São Paulo), 20:191-208, 1953.

SIMPSON, A. G. B. et al. Early Evolution within Kinetoplastids (Euglenozoa), and the Late Emergence of Trypanosomatids. **Protist**, [s.l.], v. 155, n. 4, p.407-422, 1 dez. 2004. Elsevier BV. http://dx.doi.org/10.1078/1434461042650389.

SNARY, D. et al. Cell surface antigens of *Trypanosoma cruzi*: use of monoclonal antibodies to identify and isolate an epimastigote specific glycoprotein. **Molecular and Biochemical Parasitology**, v. 3, n. 6, p. 343–356, 1981.

STOCO, P. et al. Other Major Trypanosomiasis, in Arthropod Borne Diseases, pp 299-324, 2016, Ed. Springer, Carlos Brisola Marcondes (Editor). (DOI 10.1007/978-3-319-13884-8_19).

SUN, S. Y. et al. An intracellular membrane junction consisting of flagellum adhesion glycoproteins links flagellum biogenesis to cell morphogenesis in *Trypanosoma brucei*. **Journal of Cell Science**, v. 126, n. 2, p. 520–531, 2013.

SUNTER, J. D.; GULL, K. The Flagellum Attachment Zone: 'The Cellular Ruler' of Trypanosome Morphology. **Trends In Parasitology**, [s.l.], v. 32, n. 4, p.309-324, abr. 2016. Elsevier BV. http://dx.doi.org/10.1016/j.pt.2015.12.010.

TANOURA, K.; YANAGI, T.; DE GARCIA, V. M.; KANBARA, H. *Trypanosoma rangeli*--in vitro metacyclogenesis and fate of metacyclic trypomastigotes after infection to mice and fibroblast cultures. **J Eukaryot Microbiol**, v. 46, n. 1, p. 43-8, 1999.

TEKAIA, F. Inferring Orthologs: Open Questions and Perspectives. **Genomics Insights**, [s.l.], v. 9, n. 1, p.17-28, jan. 2016. SAGE Publications. http://dx.doi.org/10.4137/gei.s37925.

PAREDES, C. H.; PAREDES, R. Un caso de infección humana por *Trypanosoma rangeli*. **Rev Fac Med Bog**, v., n. 18, p. 343-75, 1949.

PÉREZ-MOLINA, J. A.; MOLINA, I. Chagas disease. **The Lancet**, [s.l.], v. 391, n. 10115, p.82-94, jan. 2018. Elsevier BV. http://dx.doi.org/10.1016/s0140-6736(17)31612-4.

STEINDEL, M. **Caracterização de cepas de *Trypanosoma rangeli* e *Trypanosoma cruzi* isoladas de reservatórios e vetores silvestres em Santa Catarina**. Tese de Doutorado, Universidade Federal de Minas Gerais, 1993.

URDANETA-MORALES, S.; TEJERO, F. *Trypanosoma* (*Herpetosoma*) *rangeli* Tejera, 1920: mouse model for high, sustained parasitemia. **J Parasitol**, v. 71, n. 4, p. 409-14, 1985.

URDANETA-MORALES, S.; TEJERO, F. *Trypanosoma* (*Herpetosoma*) *rangeli* Tejera, 1920. Intracellular amastigote stages of reproduction in white mice. **Rev Inst Med Trop Sao Paulo**, v. 28, n. 3, p. 166-9, 1986.

WAGNER, G. et al. The *Trypanosoma rangeli* trypomastigote surfaceome reveals novel proteins and targets for specific diagnosis. **Journal of Proteomics**, v. 82, p. 52–63, 2013.

WHEELER, R. J.; GLUENZ, E.; GULL, K. The Limits on Trypanosomatid Morphological Diversity. **Plos One**, [s.l.], v. 8, n. 11, p.1-18, 19 nov. 2013. Public Library of Science (PLoS). http://dx.doi.org/10.1371/journal.pone.0079581.

WHEELER, R. J.; GULL, K.; SUNTER, J. D. Coordination of the Cell Cycle in Trypanosomes. **Annual Review Of Microbiology**, [s.l.], v. 73, n. 1, p.133-154, 8 set. 2019. Annual Reviews. http://dx.doi.org/10.1146/annurev-micro-020518-115617.

WOODS, K. et al. Identification and characterization of a ttage specific membrane protein involved in flagellar attachment in *Trypanosoma brucei*. **PLoS ONE**, v. 8, n. 1, 2013.

ZELEDÓN, R. Trypanosomiasis rangeli. **Rev Biol Trop**, v. 2, n. 2, p. 231-68, 1954.

ZHOU, Q. et al. A coiled-coil- and C2-domain-containing protein is required for FAZ assembly and cell morphology in *Trypanosoma brucei*. **Journal Of Cell Science**, [s.l.], v. 124, n. 22, p.3848-3858, 15 nov. 2011. The Company of Biologists. http://dx.doi.org/10.1242/jcs.087676.

ZHOU, Q. et al. Two distinct cytokinesis pathways drive trypanosome cell division initiation from opposite cell ends. **Proceedings Of The National Academy Of Sciences**, [s.l.], v. 113, n. 12, p.3287-3292, 29 fev. 2016. Proceedings of the National Academy of Sciences. http://dx.doi.org/10.1073/pnas.1601596113.

ZHOU, Q.; LI, Z. A backup cytokinesis pathway in *Trypanosoma brucei*. **Cell Cycle**, [s.l.], v. 15, n. 18, p.2379-2380, 25 abr. 2016. Informa UK Limited. http://dx.doi.org/10.1080/15384101.2016.1181882.

ZHOU, Q. et al. The CIF1 protein is a master orchestrator of trypanosome cytokinesis that recruits several cytokinesis regulators to the cytokinesis initiation site. **Journal Of Biological Chemistry**, [s.l.], v. 293, n. 42, p.16177-16192, 31 ago. 2018. American Society for Biochemistry & Molecular Biology (ASBMB). http://dx.doi.org/10.1074/jbc.ra118.004888.

ZUÑIGA, C. et al. Characterization of a *Trypanosoma rangeli* strain of Colombian origin. **Mem Inst Oswaldo Cruz**, v. 92, n. 4, p. 523-30, 1997.

SUPPLEMENTARY MATERIAL A – List of CIF1 and CIF1-interacting proteins from *Trypanosoma brucei*.

Gene ID (Tritrypdb 4.2)	Name	Nº aa	Domains	Reference
Tb927.11.15800	CIF1/TOEFAZ1	793	2 X coiled coil, zinc-finger	McAllaster et al., 2015
Tb927.9.14290	CIF2	468	EF-hand	Zhou, Hu, Li, 2016
Tb927.10.13100	CIF3	438	3 X coiled-coil	Kurasawa et al., 2018
Tb927.10.8240	CIF4	374	6 X coiled-coil	Hu et al., 2019
Tb927.11.9290	FAZ20	763	Kinase, coiled-coil	Zhou, Hu, Li, 2016
Tb927.5.4380	KPP1	636	Plus3, phosphatase catalytic domain	Zhou, Hong, Li, 2018
Tb927.9.9960	KAT80	538	WD40-repeat, katanin p80 subunit	Casanova et al., 2009
Tb927.8.4950	KLIF	1456	Kinesin, tropomyosin	Hilton et al., 2018
Tb927.10.870	FRW1	1351	5 X coiled-coil	Zhou et al., 2019
Tb927.10.6360	FPRC	487	2 X coiled-coil	Zhou et al., 2019

SUPPLEMENTARY MATERIAL B – List of genes upstream and downstream FLA1BP from *Trypanosoma brucei*.

Gene ID (Tritrypdb 4.2)	Name	Nº aa
Tb927.8.4000	ABC1 family	398
Tb927.8.4010	FLA1	546
Tb927.8.4020	ZC3H24	242
Tb927.8.4030	CITFA-5a	212
Tb927.8.4040	endonuclease G	506
Tb927.8.4050	FLA1BP-2	750
Tb927.8.4060	FLA2	590
Tb927.8.4070	ZC3H25	242
Tb927.8.4080	hypothetical protein	212
Tb927.8.4090	endonuclease G	506
Tb927.8.4100	FLA1BP-1	750
Tb927.8.4110	FLA3	590
Tb927.8.4120	ZC3H26	242

SUPPLEMENTARY MATERIAL C – List of genes upstream and downstream FLA1BP from *Trypanosoma cruzi*.

T. brucei	***T. cruzi* ortholog**		
Gene ID (Tritrypdb 4.2)	**Gene ID (Tritrypdb 4.2)**	**Nº aa**	**Location**
Tb927.8.4000	C4B63_21g111	674	PRFA01000021:244,899..246,923(+)
Tb927.8.4010	C4B63_21g104	578	PRFA01000021:227,489..229,225(+)
Tb927.8.4020	C4B63_21g102	272	PRFA01000021:223,339..224,157(+)
Tb927.8.4030	C4B63_21g101	276	PRFA01000021:235,535..236,902(+)
Tb927.8.4040	C4B63_21g107	455	PRFA01000021:235,535..236,902(+)
Tb927.8.4050	C4B63_21g106	712	PRFA01000021:231,213..233,351(+)
Tb927.8.4060	C4B63_21g104	578	PRFA01000021:227,489..229,225(+)
Tb927.8.4070	C4B63_21g102	272	PRFA01000021:223,339..224,157(+)
Tb927.8.4080	C4B63_21g101	276	PRFA01000021:235,535..236,902(+)
Tb927.8.4090	C4B63_21g107	455	PRFA01000021:235,535..236,902(+)
Tb927.8.4100	C4B63_21g106	712	PRFA01000021:231,213..233,351(+)
Tb927.8.4110	C4B63_21g104	578	PRFA01000021:227,489..229,225(+)
Tb927.8.4120	C4B63_21g102	272	PRFA01000021:223,339..224,157(+)

SUPPLEMENTARY MATERIAL D – List of genes upstream and downstream FLA1BP from *Trypanosoma rangeli*.

T. brucei	***T. rangeli* ortholog**			
Gene ID (Tritrypdb 4.2)	**Nº aa**	**Scaffold**	**Starting position**	**Ending position**
Tb927.8.4000	271	3	637204	638017
Tb927.8.4010	622	3	621338	623203
Tb927.8.4020	295	3	618341	619225
Tb927.8.4030	295	3	617168	618052
Tb927.8.4040	467	3	628747	630147
Tb927.8.4050	730	3	624580	626769
Tb927.8.4060	622	3	621338	623203
Tb927.8.4070	295	3	618341	619225
Tb927.8.4080	295	3	617168	618052
Tb927.8.4090	467	3	628747	630147
Tb927.8.4100	730	3	624580	626769
Tb927.8.4110	622	3	621338	623203
Tb927.8.4120	295	3	618341	619225

SUPPLEMENTARY MATERIAL E – Alignment of FLA1BP from *Trypanosoma brucei*, *Trypanosoma cruzi* and *Trypanosoma rangeli*. Red = Highly conserved sequence between Trypanosomatids.

```
TbFla1BP      MCFIFGVEMSNLAKRPMSLRKLPQLLLLIMIGIAFVAVECIGAPVKLPRRVDTVAGQFGV   60
TcFla1BP      ------------------MSRFQRLLFALFAGFLFSFTASVVVAMPLRYMVETVSGITGS   42
TrFla1BP      ----------------MRISLLQALL--IVTSVLIAATLEMAAAMPLRYMVETVSGVSGV   42
                                  :  :  **  :. .. :  .  : . : *   *:**:*  *

TbFla1BP      EGETNGYPNTTRLTEPYALCRGRTNDEILVGSSNSFRNYSRKTKETGTYLRYNVGDSV--   118
TcFla1BP      IGHVNGGPGTSLLTRPSAICQGRNEDELLFGTQGYFRNFSRSTKMTGILLGDGTVQILDG   102
TrFla1BP      IGAVDGGRGKSLLTRPLALCQGRNEDEILIGMEGFFRTYSRSTQMTGTLLGNGTAADVDG   102
               * .:*  ..: **.* *:*:**.:**:*.* .. **.:**.*: **  *  ..   :

TbFla1BP      ISGSSTINKPRSCVRRGSGNHTIIYFVDDQKDIKYIVGDDVSSFSVPTSGSSLNAVAVHEG   178
TcFla1BP      TWSQARIDGPRGCVRGIFNQKMIVYFVEGQSSLRYFTSNYVHTVTISINLSFTDVKLYEG   162
TrFla1BP      LWANARVDKPAGCVSTLRNNMMFVYFVESQNRLRYITNHSILSIQLEKGASFTDVALYGD   162
                ..: :: * .**    .:  ::***:.*. ::*:... : :. :  . *:. * :: .

TbFla1BP      TLYVTDQNNKSVWKCGLGGAGKPQSCEEKKFTSVTLDAKPEGIAVTSKGIFVTARDSSNK   238
TcFla1BP      KLYITEQTKDEVWGCDIDADGAPVSCALKTGFKCD-YGKYHGITVTKLGVFVVGE-SAA-   219
TrFla1BP      RLYMTEQNKDNVWSCEIGMDGTPTHCAEENDFKCE-YTKYNGIAVNELGVFVVGGSSQT-   220
               **:*:*.:..** * :.  * *  *  :.  .     * .**:*.. *:**..  *

TbFla1BP      GALLWLDMSGGNRKGNVSGGFVDVFSTESGVLYAATEKELYTVTATDTSLSVTSFAGKNT   298
TcFla1BP      -GICHFDM-HGNKISVLGGNYIDVFSLPSDELYIMSYTELLHLRVIGSAMVVEKFAGRSD   277
TrFla1BP      -GICHFDS-RGTNISHLPGGYSDVFSVPSGVLYAMSQQQLYHLHVAGSSMTVDLFAGNRS   278
               .:  :*   *.. . : *.: ****  *. **  :  :*  : . .::: *  ***.

TbFla1BP      SQCYFPTNGEDIVLCDNSRLLVIEEYEMYVTSKAKHTMRALTLPPVNLTAIFRGRPAPVG   358
TcFla1BP      ATCPPLIDGYDFTLCKNLRLFVIEQSEMYLATT-LNTVRSVTLPPAIVWIELPPPPLPIG   336
TrFla1BP      LTCPPVVDGYAFTMCSNRRLFVLAENEMYLSDW-LSTVRAVTLPPAIVPAQLPPSPLPLG   337
                *    :*  :.:*.* **:*: : ***::     *:*::****. :   :   * *:*

TbFla1BP      YPNTT-IMEQFVASLTEDVNKALGTNDSYVDPDSVRVDPDTWETNFTVFVQQTRFDNTTE   417
TcFla1BP      YPNDNEVMKKIIQLMNEELNKHLGTNGTYVSQETMHVDANTWATKFAVMVQQQDFENATT   396
TrFla1BP      YPDAQKVMPEIVALMNKALNKRLGTKSTYAPQNDMHVNDSTWVTDFVVLVQQADFVNVTT   397
              **:   :* :::  :.: :** ***:.:*.  : ::*: .** *.*.*:***  * *.*

TbFla1BP      -EKLRSLTYTQTDKTVDEYYGLTDEYVYIDTVLVPFCDDASLVTIQRALAREAGRALNFS   476
TcFla1BP      PGEVLTTHFARTKQFVKDYYDRVNEVLYMDTSIMPFCNDTMLNAVMHRLVTVVREVLSFP   456
TrFla1BP      PGEVATTNFAAVQRAVTAYYDRIDEALYMDTSIFPFCNATMMNAVMHELVSVVRKVLEFP   457
                :: :  :: ..: *  **.  :* :*:** :.***: : : :: : *.  . ..*.*

TbFla1BP      LVYADKPITFGSDVAENVTAVKLLMPHSFKNATTPKQLSAANLTDFAHNLVKDLRASDTR   536
TcFla1BP      LIYANPPEVRKEFDFENITTMKLLMPASFNNDTTREALMDADMDAALLQILRELYGPEHV   516
TrFla1BP      LIYANPPMRVTINGVANITRMKLLMPEPFSNETTHEIMAELNANTALQDILRVEYGAANV   517
              *:**: *          *:* :*****  *.* ** : :   :      ::::   .

TbFla1BP      VDITFPDPPFNFSAVVPEREQEVRWFVHGKVMKQLEICERLGSQGDAAVIAAAADATARG   596
TcFla1BP      VTLVFPMPQYDFSKLTDEQLVEVRWFILDLVRARLEECAVLSVDGVGA------------   564
TrFla1BP      VQLVFPFPKFDFSKLMPVQDMEVRWFIQNMVNAQLETCKSIAFGGNIAAGGNIA------   571
              * :.** * ::** :   :  *****: . *  :** *  :.  *  *

TbFla1BP      KANVTLNTSGVKANDTGVGPNTTNTAGGANTTANVAANGTANVIVNPSTNATPTGTTNAS   656
TcFla1BP      ------------------------------------------------------------   564
TrFla1BP      -------------------------AGG----NIAAGGDIA-----------AG-----   585


TbFla1BP      VTNTTERAVPVVAPTQPSNGYAECRSAITNRTETQNMEPPYDRKHRYEVFLPKKYDFNVS   716
TcFla1BP      ---------------SVSSHSSVCEAVITNRTETVVSHPPFNIQSEYEVFVPSRYKFNAS   609
TrFla1BP      -----------RDIAAGGDGNSTCEAVITNRTQTVVTRPPFNVQNEYEVFVPHKYNFNVS   634
                        ..  : *.:.*****:*   .**:: : .****:* :*.**.*

TbFla1BP      WCVDIIDWRDLDEMLNNRTDEVVEKSLSWCGHGCIIAFAVVGSLIAACLVVLAVVLTSKR   776
TcFla1BP      LCLDGIDWTVLEELIKNYTEENKPRHKSACDRSCIIGLAVLAALVLTALIAVMVVLTSKR   669
TrFla1BP      RCLEGIDWDPLEYLLNNYSAANTTRHNPACNRGCIIGVAVVAAVVLTALIAIVVVLTSKR   694
               *:: ***  *: :::* :     :    *.:.***..**:.::: :.*:.: *******

TbFla1BP      RRLAAVVAPPRPKFVSTVEDDDEDRVSNIGVPLTDGKGTTAP-818
TcFla1BP      RRLAAVVAPVHPKFKSTLDEDEEEMETTNPLEVKDEQRA----708
```

```
TrFla1BP        KRLAAVVAPVPPKFKSTLDDDDEEMETSNPLEANNEEHALDRY 737
                :********  *** **:::*:*:  :.  :  .: : :
```